UNIVERSIDADE FEDERAL DO RIO GRANDE DO SUL
FACULDADE DE FARMÁCIA
PROGRAMA DE PÓS-GRADUAÇÃO EM CIÊNCIAS FARMACÊUTICAS

Desenvolvimento de nanocápsulas mucoadesivas contendo sinvastatina para o tratamento do glioblastoma pela via nasal

FRANCIELE ALINE BRUINSMANN

PORTO ALEGRE, 2021

UNIVERSIDADE FEDERAL DO RIO GRANDE DO SUL
FACULDADE DE FARMÁCIA
PROGRAMA DE PÓS-GRADUAÇÃO EM CIÊNCIAS FARMACÊUTICAS

Desenvolvimento de nanocápsulas mucoadesivas contendo sinvastatina para o tratamento do glioblastoma pela via nasal

Tese apresentada por **Franciele Aline Bruinsmann** para obtenção do TÍTULO DE DOUTORA em Ciências Farmacêuticas

Orientador: Profa. Dra. Sílvia Stanisçuaski Guterres

PORTO ALEGRE, 2021

Tese apresentada ao Programa de Pós-Graduação em Ciências Farmacêuticas, em nível de Doutorado da Faculdade de Farmácia da Universidade Federal do Rio Grande do Sul e aprovada em 12 de março de 2021, pela Banca Examinadora constituída por:

Prof. Dr. Bruno Sarmento
Universidade do Porto

Profa. Dra. Jade de Oliveira
Universidade Federal do Rio Grande do Sul

Profa. Dra. Simone Cristina Baggio Gnoatto
Universidade Federal do Rio Grande do Sul

Bruinsmann, Franciele Aline
Desenvolvimento de nanocápsulas mucoadesivas contendo sinvastatina para o tratamento do glioblastoma pela via nasal / Franciele Aline Bruinsmann. -- 2021.
174 f.
Orientadora: Sílvia Stanisçuaski Guterres.

Tese (Doutorado) -- Universidade Federal do Rio Grande do Sul, Faculdade de Farmácia, Programa de Pós-Graduação em Ciências Farmacêuticas, Porto Alegre, BR-RS, 2021.

1. Nanocápsulas. 2. Sinvastatina. 3. Glioblastoma. 4. Administração intranasal. 5. Mucoadesão. I. Stanisçuaski Guterres, Sílvia, orient. II. Título.

Este trabalho foi desenvolvido no Laboratório 405 do Departamento de Produção e Controle de Medicamentos da Faculdade de Farmácia da UFRGS, na Università di Parma/Itália e no Laboratório de Imunobioquímica do Câncer do Departamento de Bioquímica da UFRGS. Agradecimentos ao CNPq e a CAPES que financiaram as bolsas de estudo.

AGRADECIMENTOS

À Profa. Sílvia Guterres pela confiança em mim depositada e oportunidade concedida de trabalhar ao seu lado durante os anos de iniciação científica, mestrado e doutorado. Pela orientação, incentivo e sobretudo pelos ensinamentos compartilhados ao longo destes anos.

Ao Prof. Fábio Sonvico pela orientação e oportunidades disponibilizadas durante a realização do doutorado sanduíche na Universidade de Parma (Itália).

À Profa. Adriana Pohlmann pelo conhecimento transmitido e entusiasmo pela pesquisa.

Ao Prof. Fabrício Figueiró e a mestranda Amanda de Fraga Dias do laboratório 22 do Departamento de Bioquímica pela oportunidade de colaboração e suporte nos experimentos.

Aos colegas do laboratório 405 e K204. Em especial, as amigas que participaram de forma mais direta neste trabalho e/ou me permitiram participar dos seus projetos – Aline Alves, Aline Cardoso, Gabriele Souto, Lali Zancan e Cristina Venturini. A Stefania Pigana da Università di Parma pela amizade e apoio.

À UFRGS, a Faculdade de Farmácia e ao PPGCF pela oportunidade de realizar toda minha formação acadêmica.

À CAPES e ao CNPq pelo pela concessão das bolsas de estudos no Brasil e na Itália.

Ao Marcelo pelo companheirismo, incentivo, paciência e ajuda.

Aos meus pais, Zélia e Sílvio, pela formação que me propiciaram, suporte e incentivo.

APRESENTAÇÃO

A presente tese encontra-se estruturada na forma de capítulos, com encarte de publicações, de acordo com as normas vigentes no Regimento do Programa de Pós-Graduação em Ciências Farmacêuticas da Universidade Federal do Rio Grande do Sul. Sendo assim, este exemplar encontra-se dividido da seguinte forma:

- Introdução;
- Objetivo, geral e específicos;
- Capítulo 1 - Artigo científico de revisão: *Nasal Drug Delivery of Anticancer Drugs for the Treatment of Glioblastoma: Preclinical and Clinical Trials*.
- Capítulo 2 - Artigo científico original: *Chitosan-Coated Nanoparticles: Effect of Chitosan Molecular Weight on Nasal Transmucosal Delivery*.
- Capítulo 3 - Artigo científico original: *Nose-to-brain delivery of Simvastatin Mediated by Chitosan-coated lipid-core Nanocapsules for the Treatment of Glioblastoma.*
- Discussão geral;
- Conclusões;
- Referências.

RESUMO

A entrega de fármacos ao cérebro representa um desafio, especialmente na terapia de malignidades do sistema nervoso central (SNC). O glioblastoma é o mais comum e mais letal tumor cerebral. Recentemente, a sinvastatina (SVT) tem demonstrado propriedades antitumorais promissoras. No entanto, a SVT apresenta baixa biodisponibilidade sistêmica devido ao seu extenso metabolismo de primeira passagem hepático. A via nasal e a utilização da nanotecnologia são estratégias que podem promover o aumento da distribuição cerebral de fármacos. Neste contexto, o objetivo foi desenvolver nanocápsulas de núcleo lipídico revestidas por quitosana contendo SVT ($LNC_{SVT\text{-}chit}$) para administração intranasal visando o tratamento do glioblastoma. As formulações foram revestidas com quitosana utilizando a técnica inovadora de revestimento *one pot*. Os resultados mostram que as formulações apresentaram tamanhos de partícula adequados (<220 nm), distribuição de tamanho estreita, carga de superfície positiva e alta eficiência de encapsulação. As nanocápsulas apresentaram liberação controlada da SVT e propriedades mucoadesivas devido a presença da quitosana no seu revestimento. Os resultados da permeação pelo sistema *Transwell*® utilizando a linhagem celular nasal RPMI 2650 como monocamada evidenciaram que o nanoformulação aumentou a permeação da SVT. Estes resultados foram confirmados pelo estudo de permeação *ex vivo* em mucosa nasal de coelho. A citotoxicidade *in vitro* da $LNC_{SVT\text{-}chit}$ foi comparável à SVT livre na linhagem de glioma de rato C6, já na linhagem de glioma humano U-138 MG o tratamento com $LNC_{SVT\text{-}chit}$ foi mais citotóxico após 72 h de tratamento. Em estudos realizados em ratos, a administração intranasal da $LNC_{SVT\text{-}chit}$ aumentou significativamente (2,4 vezes) a quantidade de SVT no tecido cerebral de ratos em comparação com a SVT livre. O tratamento com $LNC_{SVT\text{-}chit}$ promoveu uma diminuição significativa no crescimento e malignidade do tumor em ratos portadores de glioma em comparação com os grupos controles e SVT livre. Além disso, o tratamento com $LNC_{SVT\text{-}chit}$ não causou nenhuma característica evidente de toxicidade. Portanto, os resultados sugerem que a administração intranasal de $LNC_{SVT\text{-}chit}$ representa uma nova estratégia promissora para o tratamento do glioblastoma.

Palavras-chave: Nanocápsulas; Sinvastatina; Administração intranasal; Glioblastoma; Mucoadesão.

ABSTRACT

Drug delivery to the brain represents a challenge, especially in the treatment of malignancies of the central nervous system (CNS). Glioblastoma is the most common and lethal brain tumor. Recently, simvastatin (SVT) has shown promising antitumor properties. However, SVT has low systemic bioavailability due to an extensive hepatic first-pass metabolism. The nasal route and the use of nanotechnology are strategies that can promote increased cerebral distribution of drugs. In this context, the objective of this work was to develop simvastatin-loaded lipid-core nanocapsules coated with chitosan ($LNC_{SVT\text{-}chit}$) for intranasal administration in the treatment of glioblastoma. The formulations were coated with chitosan using the innovative one-pot technique. Results show that the formulations presented adequate particle sizes (<220 nm), narrow size distribution, positive surface charge and high encapsulation efficiency. The nanocapsules presented controlled release drug and mucoadhesive properties due to the presence of chitosan in its coating. The results of the permeation by the Transwell® system using the nasal cell line RPMI 2650 as monolayer showed that the nanoformulation increased the permeation of SVT. These results were confirmed by the *ex vivo* permeation study across rabbit nasal mucosa. *In vitro* cytotoxicity of $LNC_{SVT\text{-}chit}$ was comparable to non-encapsulated SVT in C6 rat glioma cells, whereas $LNC_{SVT\text{-}chit}$ were more cytotoxic than non-encapsulated SVT after 72 h of incubation against U-138 MG human glioblastoma cell line. In studies carried out in rats, $LNC_{SVT\text{-}chit}$ enhanced significantly the amount of drug in rat brain tissue after intranasal administration (2.4-fold) compared with free SVT. In addition, $LNC_{SVT\text{-}chit}$ did not cause any characteristics of toxicity in treated rats. Considered overall, the results suggest that the nose-to-brain administration of $LNC_{SVT\text{-}chit}$ represents a novel potential strategy for glioblastoma treatment.

Keywords: Nanocapsules; Simvastatin; Intranasal administration; Glioblastoma; Mucoadhesion.

SUMÁRIO

LISTA DE FIGURAS

INTRODUÇÃO

CAPÍTULO 1

CAPÍTULO 2

CAPÍTULO 3

LISTA DE TABELAS

CAPÍTULO 1

CAPÍTULO 2

CAPÍTULO 3

INTRODUÇÃO

1. Câncer e tumores do Sistema Nervoso Central (SNC)

O câncer é definido pela Organização Mundial da Saúde (OMS), como um grupo de doenças caracterizadas por um crescimento desordenado de células anormais e com capacidade de invasão a tecidos adjacentes e/ou de se espalhar para outros órgãos. Esse processo de invasão a outros órgãos é chamado de metástase e é uma das principais causas de morte por câncer (WHO, 2020). O câncer é um importante problema de saúde pública, visto que é a segunda principal causa de morte no mundo (ZAORSKY *et al*., 2017; WHO, 2020). O impacto desta doença na economia é muito significativo. Em 2010, estimou-se o custo total de 1,16 trilhões de dólares (WHO, 2020).

No Brasil, surgiram 559371 novos casos e 243588 mortes relatados devido ao câncer em 2018 (GLOBOCAN/IARC, 2018). Segundo o Instituto Nacional do Câncer (INCA), a estimativa no Brasil para o ano de 2020 é a ocorrência de 625 mil novos casos, incluindo o câncer de pele não melanoma (INCA, 2019). Em 2025, a OMS projeta que os casos de câncer cresçam em até 50% no Brasil em decorrência do aumento e do envelhecimento da população (REZENDE *et al*., 2019).

Os tumores do SNC se referem a um grupo heterogêneo de neoplasias com mais de 100 tipos reconhecidos pela OMS, sendo classificados de acordo com as características histopatológicas, genéticas e grau de malignidade (HUTTNER, 2012; LIM e JACKSON 2018). Esses tumores são, geralmente, nomeados de acordo com o tipo de célula cerebral ou parte do cérebro em que se inicia o desenvolvimento. Os tumores podem ser benignos ou malignos, e incluem os meningiomas, meduloblastomas, craniofaringiomas, gangliogliomas e gliomas. O tumores no SNC podem ser causados pelo somatório de alterações adquiridas ao longo do tempo por predisposição genética ou por exposição. Exposição à radiação ionizante, ambientais (arsênio, chumbo e mercúrio) e ocupacionais (trabalhadores na indústria petroquímica, de borracha, plástico e gráfica), além de obesidade e deficiência do sistema imunológico são fatores de riscos conhecidos (AMERICAN CANCER SOCIETY, 2019; INCA, 2019).

No mundo, foram estimados 162 mil casos novos em homens e 134 mil em mulheres em 2018 (INCA, 2019). A estimativa para o Brasil, no triênio de 2020-2022, é de 5870 novos casos de câncer que afetam o SNC em homens e 5230 em mulheres

para cada ano. Esses valores correspondem a um risco estimado de 5,61 novos casos a cada 100 mil homens e 4,97 para cada 100 mil mulheres (INCA, 2019). Sem considerar os tumores de pele não melanoma, o câncer do SNC em homens ocupa a oitava posição na Regiões Sul (8,63/100 mil). Para as mulheres, é o sétimo mais frequente na Região Sul (7,64/100 mil). Segundo a Agência Internacional de Pesquisa em Câncer, os tumores do SNC foram responsáveis por 10711 óbitos em 2018 no Brasil (GLOBOCAN/IARC, 2018).

1. 1 Glioblastoma

Gliomas são os tumores cerebrais primários mais comuns em adultos, representando cerca de 80% de todos os tumores primários do SNC (OSTROM *et al*., 2018). A OMS classifica os gliomas em 4 graus (I a IV). Os gliomas de grau I são geralmente benignos, enquanto os gliomas de grau II a IV são malignos e se infiltram de maneira difusa no cérebro. O glioblastoma é classificado como grau IV, sendo o tumor cerebral primário mais comum e mais letal em adultos (LEECE *et al*., 2017).

O glioblastoma é dividido em dois subtipos: primário e secundário. O primário se manifesta majoritariamente em pacientes idosos, sendo altamente agressivo e invasivo. Usualmente, não há qualquer evidência clínica prévia da doença. Já o glioblastoma secundário se manifesta em pacientes mais jovens, que inicialmente apresentam astrocitomas difusos de baixo grau ou astrocitomas anaplásicos. Neste caso, o prognóstico é significativamente melhor. Histologicamente, o glioblastoma primário e secundário são indistinguíveis, mas diferem em seus perfis genéticos e epigenéticos (OHGAKI e KLEIHUES, 2013).

Estima-se que o glioblastoma afete 3,21 indivíduos em cada 100.000 da população e o tempo de sobrevida médio é de cerca de 12 meses após o diagnóstico (OSTROM *et al*., 2018). Além disso, a sobrevida relativa de cinco anos é inferior a 5% (THAKKAR *et al*., 2014). A sua etiologia é complexa e ainda não foi totalmente elucidada, porém fatores genéticos e ambientais são as causas mais prováveis da doença (SONG *et al.*, 2009).

O glioblastoma apresenta-se como uma malignidade muito difícil de ser tratada devido à sua natureza altamente invasiva, sendo caracterizados por uma grande

infiltração no tecido cerebral normal circundante e rápido crescimento. Ocorre a destruição de extensas áreas de tecido nervoso, causando edema e necrose. O edema causa um efeito de massa adicional e leva a distúrbios neurológicos (TATARANU *et al*., 2018).

Os tratamentos atuais consistem na ressecção cirúrgica máxima, seguido de radioterapia e quimioterapia adjuvante (HAN *et al*., 2015). Atualmente, a temozolomida (TMZ) é o tratamento quimioterápico padrão. A TMZ é um agente alquilante do DNA com administração oral. Esse fármaco possui administração simples e menos efeitos adversos quando comparado com outros agentes quimioterápicos como a doxorrubicina, carboplatina e o docetaxel (TAN *et al*., 2012; XU *et al*., 2017; CAGEL *et al*., 2017). No entanto, sua eficácia clínica permanece limitada, uma vez que os tumores apresentam uma resistência rápida ao tratamento (TIEK *et al*., 2018). Além disso, em vários casos, o tumor pode ser intrinsecamente resistente à TMZ antes do tratamento inicial.

Adicionalmente, o glioblastoma é um tumor altamente vascularizado, assim fármacos que inibem a angiogênese podem ser uma estratégia de tratamento. A angiogênese é definida como um processo de formação de novos vasos sanguíneos a partir de um endotélio vascular existente, sendo muito importante no crescimento e progressão tumoral (BAGRI *et al*., 2010). Neste contexto, o bevacizumabe (Avastin®), um anticorpo monoclonal recombinante humanizado, que se liga especificamente ao fator de crescimento endotelial vascular (do inglês, *vascular endothelial growth facto*r, VEGF), vem sendo utilizado. No entanto, em 2014, resultados de dois estudos clínicos de fase III sobre o uso de bevacizumabe como tratamento de primeira linha foram publicados e não mostraram aumento na sobrevida média quando a terapia padrão foi combinada com esse anticorpo (GILBERT *et al*., 2014; CHINOT *et a*l., 2014)

A completa ressecção cirúrgica do glioblastoma representa a maneira mais eficaz de aumentar a sobrevida dos pacientes (LI, *et al* 2016). No entanto, na maioria dos casos, menos de 90% do tumor pode ser removido (PIRZKALL *et al*., 2009). Esses tumores exibem alto grau de invasividade e estão, frequentemente, localizados em áreas eloquentes do cérebro, incluindo áreas que controlam a fala, função motora e os sentidos (DAVIS, 2016). Sendo assim, o glioblastoma apresenta uma taxa de recorrência de mais de 90% após o tratamento (MORSY e NG, 2016).

O glioblastoma também está localizado em uma área de difícil acesso para a terapia medicamentosa convencional devido à presença da barreira hematoencefálica (BHE), que limita a passagem dos agentes quimioterápicos para o SNC (HARDER *et al*., 2018). Além disso, mecanismos de resistência a multidrogas, por exemplo, a ação da glicoproteína-P, reduzem a passagem de fármaco pelas células endoteliais que compõe a BHE. Portanto, ocorre uma diminuição do acúmulo de fármaco dentro das células tumorais, devido ao efluxo para o meio extracelular, resultando em uma diminuição da eficácia terapêutica (SZAKACS *et al*., 2006).

Sumarizando, o glioblastoma apresenta um péssimo prognóstico para os pacientes e o arsenal terapêutico disponível atualmente é incapaz de alterar substancialmente esse prognóstico. Considerando esse cenário, o desenvolvimento de novas estratégias para o tratamento dessa doença é muito importante, sendo um dos maiores desafios da terapia do câncer.

2. Sinvastatina

As estatinas são fármacos que atuam primariamente no fígado inibindo a ação da enzima 3-hidróxi-3-metil-glutaril-coenzima A (HMG-CoA) redutase. Essa enzima catalisa a reação de produção do mevalonato, sendo esse o passo inicial da via biossintética de produção do colesterol. Portanto, são fármacos amplamente utilizados no tratamento de hipercolesterolemia e, assim, reduzem o risco de eventos cardiovasculares (CHIANG *et al*., 2015).

A inibição da HMG-CoA redutase não reduz apenas a síntese do colesterol, mas também a produção de isoprenoides, que são intermediários dessa via biossintética. Os isoprenoides dolicol, geranil pirofosfato (GPP) e farnesil pirofosfato (FPP) atuam como adjuvantes na prenilação, que é um processo de modificação pós-transcricional baseado na adição de um grupo fenil lipofílico às proteínas. Essa modificação permite a ligação de diversas proteínas na membrana celular. E, essas proteínas preniladas, ao aderirem na membrana celular, participam de diversos processos essenciais de sinalização celular (TANAKA *et al*., 2013). O GPP e FPP atuam na regulação do ciclo celular e são responsáveis pela isoprenilação das proteínas intracelulares Ras e Rho. Essas proteínas regulam o sinal de tradução de vários receptores de membrana, que são responsáveis

pela transcrição de genes envolvidos na proliferação, diferenciação e apoptose celular. Mutações do gene Ras e Rho são encontradas em uma ampla variedade de células tumorais (JAKOBISIAK e GOLAB, 2003; BIFULCO *et al*., 2008)

A sinvastatina (figura 1) é um fármaco análogo a mevastatina, que foi o primeiro inibidor de HMG-CoA redutase descoberto em 1976, originalmente isolado como produto metabólico de culturas de *Penicillium citrinium* (LIAO e ULRICH, 2005). Caracteriza-se por um sólido cristalino, solúvel em solventes orgânicos como clorofórmio, dimetilsulfóxido, metanol e etanol. Sua fórmula molecular é $C_{25}H_{38}O_5$, apresentando uma massa de 418,6 g/mol e logP de 4,68.

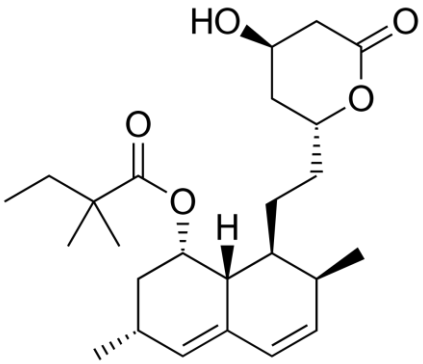

Figura 1. Estrutura química da sinvastatina.

A sinvastatina possui um sistema de anéis hexahidronaftaleno como núcleo e substituintes polares (Figura 1), que se ligam bem ao bolso de ligação de adenosina trifosfato (ATP) de proteínas quinases (LI *et al*., 2020). Essas proteínas estão envolvidas em inúmeras vias de sinalização na progressão do câncer (SHEN *et al*., 2015). Além disso, a sinvastatina é estruturalmente semelhante a muitos inibidores de quinase já disponíveis no mercado. Por exemplo, ela compartilha mais de 50% de similaridade química com o bosutinibe e o erlotinibe (LI *et al*., 2020).

A sinvastatina é administrada como pró-fármaco na forma de lactona, sendo hidrolisada enzimaticamente *in vivo* em seu correspondente β-hidroxiácido. Sua conversão ocorre pela ação das enzimas carboxiesterases presentes no fígado, intestino e plasma (LAIZURE *et al*., 2013). Além disso, essas enzimas também podem ser encontradas no cérebro, pulmão e coração (WANG *et al*., 2018).

Esse fármaco é bem absorvido pelo trato gastrointestinal, porém, devido à alta biotransformação no fígado, apresenta uma baixa biodisponibilidade sistêmica. Assim,

após a administração oral, a concentração plasmática da sinvastatina é inferior a 5% (TODD e GOA, 1990). A sua metabolização é mediada pelo citocromo P450, principalmente, CYP3A4 e CYP3A5. A excreção biliar representa a principal via de eliminação da sinvastatina e seus metabólitos (WILLRICH *et al*., 2009).

De forma geral, a sinvastatina é bem tolerada e seus efeitos adversos são dose-dependentes. A toxicidade muscular, incluindo miopatia e rabdomiólise, é rara quando administrada em doses normais (ARMITAGE *et al*., 2007). Além disso, esses efeitos estão associados à presença de condições coexistentes, incluindo insuficiência hepática, colestase ou doenças renais (BELLOSTA; PAOLETTI; CORSINI, 2004). As alterações nas enzimas hepáticas, como alanina e aspartato aminotransferase, são incomuns. Efeitos adversos como diarreia, náuseas e dor abdominal são mais pronunciados quando o fármaco é administrado em doses elevadas (ARMITAGE *et al*., 2007).

Nos últimos anos, a faixa de terapias com estatinas expandiu devido aos seus efeitos pleiotrópicos. Esses efeitos estão associados à redução dos níveis circulantes de isoprenoides (HÖGLUND e BLENNOW, 2007) e incluem a modulação da resposta imunológica, o aumento da função endotelial, a diminuição do estresse oxidativo e inflamação (LIAO e ULRICH, 2005; DAVIES *et al*., 2016). Essa gama de efeitos pleiotrópicos sugere que as estatinas podem ser empregadas no tratamento de diversas doenças, desde demência até o tratamento do câncer.

De acordo com a literatura, as estatinas apresentam efeito antitumoral em diversas linhagens de células tumorais como mama (CAMPBELL *et al*., 2006; KOTAMRAJU *et al*., 2007; YANG *et al*., 2016), melanoma (SHELLMAN *et al*., 2005; SAITO *et a*l., 2008), cólon (CHO *et al*., 2008), próstata (GOC *et al*., 2012, DENG *et al*., 2019), linfoma (QI *et al*., 2013) e pulmão (YU *et al*., 2013; ALIZADEH *et al*., 2017). No caso da sinvastatina, foi demonstrado que ela reduz a proteína antiapoptótica Bcl-2 e aumenta a expressão da proteína pró-apoptótica Bax (SPAMPANATO *et al*., 2012).

Em diferentes linhagens celulares de glioblastoma (C6, U-87 MG, U-138 MG, LN 405 e RG II), a sinvastatina também mostrou supressão da proliferação celular e a indução de apoptose (CHAN *et al*., 2003; KOYUTURK, ERSOZ, ALTIOK, 2004; WU *et al*., 2009; YANAE *et al*., 2011; MISIRKIC *et al*., 2012). Além disso, foi demonstrado

que ela pode inibir de forma dose dependente o fator de crescimento endotelial vascular (VEGF), impedindo assim o crescimento e progressão tumoral (SLEIJFER *et al*., 2005).

No entanto, quando a sinvastatina foi administrada por via oral (1 mg/Kg e 10 mg/Kg) e avaliada em um modelo ortotópico *in vivo* de glioma, não demonstrou inibição do crescimento tumoral (BABABEYGY *et al*., 2009). Um fator importante para o insucesso no tratamento de tumores do SNC tem sido atribuído à limitada permeabilidade dos seus metabólitos hidrofílicos pela BHE, visto que após a administração oral, a sinvastatina é extensamente metabolizada no fígado, gerando metabólitos hidrofílicos (ROMANA *et al*., 2014). Corroborando com esses resultados, Patel e colaboradores (2015) demonstraram, no seu estudo de microdiálise cerebral em ratos, que, após administração oral de 100 mg/kg, a sinvastatina não alcançou o cérebro em concentração suficiente para sugerir inibição do crescimento do tumor. A dose utilizada no estudo é equivalente à dose máxima tolerada em pacientes (7,5 mg/kg). Cabe ressaltar que, dentre as estatinas, a sinvastatina foi a selecionada para realização da microdiálise cerebral devido à sua potencial capacidade de atravessar a BHE, que foi determinada utilizando dois modelos *in silico.* Contudo, como mencionado, os resultados do experimento *in vivo* não confirmaram essa capacidade e os autores relataram que o estudo de eficácia pré-clínica não teve continuidade (PATEL *et al*., 2015).

Por outro lado, Ferris e colaboradores (2012) conduziram um estudo observacional com 517 pacientes, que avaliou a associação entre o uso de estatinas e o risco da ocorrência de glioma (FERRIS *et al*., 2012). Os pacientes selecionados faziam o tratamento há, no mínimo, 6 meses e, pelo menos, 2 vezes por semana. Os resultados mostraram uma associação inversa entre a incidência doença e o uso de sinvastatina e lovastatina. O resultado mais significativo foi associado à utilização dos fármacos por mais de 10 anos. As estatinas hidrofílicas (pravastatina e rosuvastatina) também foram incluídas no estudo, porém não apresentaram resultados significativos (FERRIS *et al*., 2012). Para outros tipos de tumores, o uso de estatinas por, pelo menos, cinco anos foi associado a um risco significativamente reduzido de câncer colorretal (POYNTER *et al*., 2005) e de câncer de próstata avançado (PLATZ *et al*., 2006).

Em outro estudo observacional conduzido na Dinamarca, 2656 casos e 18480 controles foram avaliados entre 2000 e 2009. Também foi demonstrado que o uso a longo prazo de estatinas (mais de 5 anos) foi associado a um risco reduzido de desenvolver a doença. Neste estudo, as estatinas hidrofílicas também não apresentaram efeito quimiopreventivo (GAIST *et al*., 2013).

3. Administração intranasal

A administração oral é um dos métodos mais desejáveis e convenientes de administração de fármacos. Entretanto, a administração oral de diversos fármacos é difícil ou muitas vezes impossível, por questões de solubilidade, absorção, estabilidade ou toxicidade. Entre as vias de administração de fármacos não convencionais, a administração intranasal tem recebido crescente interesse. Tradicionalmente, a administração de fármacos por essa via tem sido associada ao tratamento de doenças da cavidade nasal e seios paranasais, como congestão nasal, infecções nasais e rinossinusite alérgica ou crônica (DJUPESLAND, 2013).

A via nasal tem demonstrado ser um local de administração em que ocorre absorção rápida e eficiente de moléculas como, por exemplo, peptídeos e proteínas normalmente não adequadas para administração oral (PIRES *et al*., 2009; CHAPMAN *et al*., 2013). Além disso, essa via está emergindo como uma alternativa para entrega de fármacos diretamente ao SNC. As principais vantagens da entrega nasal são (COMFORT *et al*., 2015):

- Alta vascularização;
- Alta permeabilidade;
- Baixo conteúdo enzimático dos fluidos nasais;
- Relativamente alta superfície de absorção;
- Rápido início do efeito terapêutico;
- Evita o metabolismo de primeira passagem;
- Administração não invasiva, segura e indolor com melhor conveniência e complacência dos pacientes;

O reconhecimento do potencial da via de administração intranasal tem conduzido a um grande aumento nas pesquisas nesse campo. A lista de produtos no mercado ou nos diferentes estágios de desenvolvimento pré-clínico e clínico está em constante crescimento. Diversas aplicações já estão disponíveis, como, por exemplo, cessação do tabagismo (nicotina, Nicotrol® NS, Pfizer), vacinação contra a gripe (FluMist® Quadrivalent, Astra Zeneca), tratamento da dor (fentanil, Intstanyl®, Takeda), osteoporose pós-menopausa (calcitonina de salmão, Fortical®, Upsher-Smith), enxaqueca (zolmitriptano, Zomig®, AstraZeneca; sumatriptano, Imigram, GSK) e endometriose (nafarelina, Synarel®, Pfizer; buserelina, Suprecur®, Sanofi-Aventis) (SONVICO *et al.*, 2018).

Anatomicamente, a cavidade nasal humana é subdividida em três regiões, o vestíbulo nasal, a região respiratória e a região olfatória (ILLUM, 2000). Apresenta uma área total de cerca de 160 cm² e o volume total de cerca de 15 mL (GIZURARSON, 2012). O vestíbulo nasal corresponde ao segmento inicial da cavidade nasal, sendo constituído por epitélio estratificado pavimentoso e rico em pelos, que são responsáveis por filtrar o ar durante a inspiração.

A maior parte da cavidade nasal corresponde a região respiratória, que apresenta uma grande área superficial e vascularização, sendo, portanto, uma zona muito importante para a administração de fármacos. A parte anterior é coberta com epitélio escamoso, que se converte a epitélio pseudo-estratificado ou epitélio respiratório, consistindo de quatro tipos celulares dominantes: células colunares ciliadas, células colunares não ciliadas, células caliciformes e células basais. Aproximadamente de 15% a 20% das células respiratórias são cobertas por uma camada ciliar. A função dos cílios é mover o muco da superfície epitelial à faringe. Cada célula respiratória é também coberta por volta de 300 microvilosidades, aumentando a área superficial celular e promovendo o transporte de substâncias. As células caliciformes são responsáveis pela produção do muco, que aprisiona partículas inaladas e é deslocado pelo batimento dos cílios para a faringe, onde é deglutido ou expectorado (SUMAN, 2013).

O muco consiste em uma combinação de água, glicoproteínas de alto peso molecular (mucinas), lipídeos, íons, enzimas e proteínas. Trata-se de um hidrogel viscoelástico capaz de capturar agentes potencialmente nocivos, eliminando-os da

superfície epitelial através do movimento ciliar. Os fármacos com baixa solubilidade aquosa apresentam uma absorção e biodisponibilidade reduzidas como consequência de interações não específicas com glicoproteínas e lipídeos da camada de muco (SIGURDSSON *et al*., 2013). A superfície basal das células colunares ciliadas está em contato sináptico com fibras nervosas do nervo trigêmeo, sendo essa uma via de acesso direta de fármacos ao SNC, evitando assim a BHE (SELVARAJ, K.; GOWTHAMARAJAN, K.; KARRI, 2018).

O epitélio olfativo, que representa a região olfatória, tem uma área superficial pequena dedicada à detecção de odor. Esse epitélio é pseudoestratificado colunar, consistindo em três tipos de células: células olfatórias, células epiteliais de sustentação e células basais. As células olfatórias são neurônios bipolares localizados no estrato mediano do epitélio olfativo e intercalados entre as células sustenculares. Os axônios das células olfatórias são responsáveis pela formação do nervo olfatório, que é uma importante via de acesso ao SNC. Os fármacos podem acessar o SNC pelas ramificações do nervo olfatório com a vantagem de não sofrer a triagem da BHE (JONES, 2001; SUMAN, 2013).

Portanto, devido a ligação da cavidade nasal com o SNC, a partir nervo trigêmeo e nervo olfatório, a via nasal para entrega de fármacos diretamente ao SNC se apresenta como uma estratégia muito interessante (DHURIA *et al*., 2010). O acesso direto ao SNC, evitando a triagem da BHE, possibilita a utilização da via nasal como alternativa para a liberação no cérebro de agentes terapêuticos com baixa ou nenhuma absorção cerebral após administração sistêmica ou oral (SHAH; YADAV; AMIJI, 2013; BRUINSMANN *et al*., 2019). Além disso, um fármaco administrado pela via nasal pode atingir o SNC pela via vascular. Este é um mecanismo secundário e indireto de entrega, pelo qual o fármaco é primeiramente absorvido na circulação sistêmica e, subsequentemente, acessa o SNC após cruzar a BHE (SONVICO *et al*., 2018).

Entretanto, a administração intranasal apresenta algumas limitações, como a necessidade do fármaco atravessar a mucosa nasal, a rápida eliminação da formulação pelo mecanismo de depuração mucociliar, que pode remover rapidamente a formulação da cavidade nasal. Também algumas restrições são determinadas pela anatomia da cavidade nasal (pequeno volume de administração e área superficial limitada da mucosa

olfativa) (COMFORT *et al*., 2015). Por outro lado, o uso de sistemas de liberação de fármacos mucoadesivos podem promover a fixação e aumentar a absorção do fármaco pela mucosa nasal (CASETTARI e ILLUM, 2014).

4. Nanopartículas para a entrega no SNC

Diversas estratégias tem sido utilizadas para aumentar a entrada dos fármacos no SNC, como o uso de agentes (químicos ou físicos) que desestruturem momentaneamente a BHE, a administração do fármaco diretamente no líquido encéfalo-raquidiano ou no espaço parenquimatoso. Contudo, esses procedimentos são invasivos e conferem riscos aos pacientes, por exemplo, infecções intracranianas ou edema cerebral (ALAM *et al*., 2010; WOHLFART *et al*., 2012).

A nanotecnologia tem se mostrado promissora, visto que diversos estudos pré-clínicos demonstraram a passagem de fármacos pela BHE quando encapsulados em nanocarreadores, conferindo aumento da distribuição cerebral (ZARA *et al*., 2002; FROZZA *et al*., 2010). Além disso, o aumento do efeito farmacológico em modelos pré-clínicos, como de doença de Alzheimer (SADEGH *et al*., 2019; ZHANG *et al*., 2014), Parkinson (HU *et al*., 2011; LINDNER *et al*., 2015), depressão (HE *et al*., 2016) e glioblastoma multiforme (ZHAN *et al*., 2010; GANIPINENI *et al*., 2019).

Os sistemas poliméricos nanoestruturados têm atraído atenção em virtude da sua versatilidade, estabilidade nos fluidos biológicos, bem como biocompatibilidade e biodegradabilidade (POHLMANN *et al*., 2013). As nanopartículas poliméricas são sistemas carreadores de fármacos que apresentam diâmetro inferior a 1µm, perfil granulométrico homogêneo e monomodal (SCHAFFAZICK *et al*., 2003). Nesse contexto, as nanocápsulas poliméricas, merecem destaque, pois apresentam método de preparo relativamente simples, elevada capacidade de encapsulamento e liberação controlada dos fármacos (MORA-HUERTAS; FESSI; ELAISSARI, 2010).

As nanocápsulas poliméricas consistem em uma estrutura vesicular com um invólucro polimérico disposto ao redor de um núcleo oleoso (FESSI *et al*.,1989) ou lipídico (VENTURINI *et al*., 2011). Na ausência do núcleo oleoso, podem ser preparadas nanoesferas, que consistem em uma matriz polimérica (POHLMANN *et al*., 2007). As nanocápsulas de núcleo lipídico (LNCs, do inglês *lipid core nanocapsules*),

desenvolvidas por nosso grupo de pesquisa, são compostas por uma dispersão de monoestearato de sorbitano (lipídio sólido) e triglicerídeos de cadeia média (lipídio líquido) no núcleo, sendo circundadas por uma parede polimérica de poli (ε-caprolactona) (PCL), e micelas de polissorbato 80 como sistema estabilizante (JÄGER *et al*., 2007; JÄGER *et al*., 2009; VENTURINI *et al*., 2011; FIEL *et al*., 2013). Este núcleo lipídico confere propriedades de controle a liberação do fármaco e aumento da eficiência de encapsulação quando comparado ao núcleo das nanocápsulas convencionais contendo apenas lipídios líquidos (JAGER *et al*., 2009; FIEL *et al*., 2011).

As nanocápsulas de núcleo lipídico tem mostrado propriedades interessantes como aumento da eficácia farmacológica em modelos de inflamação (BERNARDI *et al*., 2009a), proteção de fármacos da degradação química (KULKAMP *et al.*, 2009) e fotoquímica (FONTANA *et al.*, 2010; OURIQUE *et al.*, 2011), entrega cerebral eficiente de fármacos como resveratrol (FROZZA *et al*., 2010) e curcumina (ZANOTTO-FILHO *et al*., 2013) quando administrados por via oral e intraperitoneal, bem como redução de efeitos adversos da olanzapina (DIMMER *et al*., 2014). Além disso, esses nanosistemas demonstraram melhora na eficácia antitumoral *in vitro* e *in vivo* da indometacina (BERNARDI *et al*., 2008; BERNARDI *et al*., 2009b), do resveratrol (FIGUEIRÓ *et al*, 2013), do metotrexato (FIGUEIRÓ *et al*., 2015) e do acetilenogenol (DREWES *et al*., 2016) quando comparados aos fármacos não encapsulados. As LNCs também demonstraram segurança *in vivo* em experimentos de toxicidade aguda e subcrônica (BULCÃO *et al*., 2012).

Bender e colaboradores (2012) desenvolveram um processo de duas etapas para obtenção de LNCs revestidas com quitosana. A quitosana é um biopolímero catiônico obtido pela desacetilação parcial da quitina sob condições alcalinas (MUXIKA *et al*., 2012). Esse biopolímero apresenta várias propriedades interessantes para aplicação farmacêutica, como biodegradabilidade, biocompatibilidade, atividade antibacteriana e controle na liberação de fármacos (KIM *et al*., 2008). Além disso, apresenta propriedades mucoadesivas e de melhoramento da permeabilidade de fármacos, que são particularmente desejáveis para a aplicação na liberação nasal (WAYS *et al*., 2018; ALI

et al., 2018). Essas ações são mediadas pela reorganização estrutural das *tight junctions* do epitélio nasal, aumentando o transporte paracelular (passivo) de fármacos.

Outro tipo de transporte envolvido na absorção pela mucosa nasal é o transporte transcelular (ativo). Dentre os fatores que influenciam esse tipo de transporte, destacam-se: o tamanho da partícula, uma que vez o transporte passivo é favorecido para partículas menores, enquanto partículas maiores sofrem transporte ativo; e a carga das partículas, onde partículas carregadas tendem a ser internalizadas pelo transporte ativo (ILLUM, 2006). Além disso, a quitosana aumenta o tempo de retenção da formulação na cavidade nasal, devido a sua capacidade mucoadesiva (BERNKOP-SCHNÜRCH *et al*., 2012). Essa ação se dá pela interação eletrostática dos grupamentos amino (carga positiva) da quitosana com os grupamentos de ácido siálico (carga negativa) presentes no muco da cavidade nasal (SINGH e RANA, 2013).

Considerando a necessidade de novas alternativas para o tratamento do glioblastoma, as vantagens da administração intranasal, aliadas ao uso de sistemas nanotecnológicos para a entrega de fármacos no cérebro, diversos estudos foram conduzidos nos últimos anos visando o tratamento dessa doença (BRUINSMANN *et al*., 2019). Deste modo, o presente trabalho de tese propõe a obtenção de nanocápsulas mucoadesivas contendo sinvastatina para administração intranasal visando uma nova estratégia de tratamento para o glioblastoma.

OBJETIVOS

1. Objetivo geral

Desenvolvimento, caracterização físico-química e biológica de nanocápsulas mucoadesivas contendo sinvastatina como nova estratégia para tratamento de glioblastoma pela via nasal.

2. Objetivos específicos

- Desenvolver e caracterizar as suspensões de nanocápsulas contendo sinvastatina e revestidas por dois tipos de quitosana pela técnica *one-pot*;
- Avaliar o perfil de liberação *in vitro* das formulações e sua capacidade mucoadesiva pela interação entre as nanocápsulas e a mucina;
- Avaliar o transporte *in vitro* da sinvastatina pelo modelo de monocamada celular de células nasais cultivadas em sistema *Transwell*®, bem como o seu transporte *ex vivo* em mucosa nasal de coelho;
- Investigar o efeito citototóxico da sinvastatina e da suspensão de nanocápsulas selecionada em duas linhagens celulares de glioma (C6 e U138-MG);
- Estimar a distribuição cerebral da sinvastatina após a administração intranasal da sinvastatina livre e nanoencapsulada em ratos Wistar;
- Avaliar do efeito do tratamento pela via intranasal da sinvastatina na sua forma livre e nanoencapsulada sobre o crescimento de glioma implantados em ratos Wistar.

Capítulo 1

Nasal Drug Delivery of Anticancer Drugs for the Treatment of Glioblastoma: Preclinical and Clinical Trials

Artigo publicado em 26/11/2019 na revista Molecules (JCR 2018=3.06)

molecules

MDPI

Review

Nasal Drug Delivery of Anticancer Drugs for the Treatment of Glioblastoma: Preclinical and Clinical Trials

Franciele Aline Bruinsmann [1,2,†], Gustavo Richter Vaz [2,3,†], Aline de Cristo Soares Alves [1], Tanira Aguirre [4], Adriana Raffin Pohlmann [1,5], Silvia Stanisçuaski Guterres [1] and Fabio Sonvico [2,*]

1 Programa de Pós-Graduação em Ciências Farmacêuticas, Universidade Federal do Rio Grande do Sul, Porto Alegre 90610-000, Brazil; fbruinsmann@gmail.com (F.A.B.); alves.alinecs@yahoo.com.br (A.d.C.S.A.); adriana.pohlmann@ufrgs.br (A.R.P.); silvia.guterres@ufrgs.br (S.S.G.)

2 Food and Drug Department, University of Parma, Parco Area delle Scienze 27/a, 43124 Parma, Italy; richtervaz@gmail.com

3 Laboratório de Nanotecnologia Aplicada à Saúde, Programa de Pós-Graduação em Ciências da Saúde, Universidade Federal do Rio Grande, Rio Grande, RS 96210-900, Brazil

4 Programa de Pós-Graduação em Biociências, Universidade Federal de Ciências da Saúde de Porto Alegre, Porto Alegre, RS 900500-170, Brazil; tanira@ufcspa.edu.br

5 Departamento de Química Orgânica, Instituto de Química, Universidade Federal do Rio Grande do Sul, Porto Alegre 91501-970, Brazil

* Correspondence: fabio.sonvico@unipr.it; Tel.: +39-0521-906-282

† These Authors contributed equally to this work.

Received: 25 October 2019; Accepted: 24 November 2019; Published: 26 November 2019

Abstract: Glioblastoma (GBM) is the most lethal form of brain tumor, being characterized by the rapid growth and invasion of the surrounding tissue. The current standard treatment for glioblastoma is surgery, followed by radiotherapy and concurrent chemotherapy, typically with temozolomide. Although extensive research has been carried out over the past years to develop a more effective therapeutic strategy for the treatment of GBM, efforts have not provided major improvements in terms of the overall survival of patients. Consequently, new therapeutic approaches are urgently needed. Overcoming the blood–brain barrier (BBB) is a major challenge in the development of therapies for central nervous system (CNS) disorders. In this context, the intranasal route of drug administration has been proposed as a non-invasive alternative route for directly targeting the CNS. This route of drug administration bypasses the BBB and reduces the systemic side effects. Recently, several formulations have been developed for further enhancing nose-to-brain transport, mainly with the use of nano-sized and nanostructured drug delivery systems. The focus of this review is to provide an overview of the strategies that have been developed for delivering anticancer compounds for the treatment of GBM while using nasal administration. In particular, the specific properties of nanomedicines proposed for nose-to-brain delivery will be critically evaluated. The preclinical and clinical data considered supporting the idea that nasal delivery of anticancer drugs may represent a breakthrough advancement in the fight against GBM.

Keywords: nasal delivery; glioblastoma multiforme; drug delivery; nanoparticles; nose-to-brain delivery; pre-clinical studies; clinical evaluation

1. Introduction

Malignant brain tumors are devastating diseases with high morbidity and mortality in adults. In children, they represent the second leading cause of cancer related deaths [1,2]. Glioblastoma

multiforme (GBM) is the most common and the most lethal malignant primary brain tumor in adults. Moreover, GBM shows a recurrence rate of higher than 90%, even after multimodal treatment that combines surgery and chemotherapy [3]. The World Health Organization (WHO) classifies GBM as Grade IV, which is the highest in CNS tumors classification, based on the level of malignancy. Indeed, GBM is the most invasive and aggressive type of glial tumors. Primary GBMs, i.e., which arise without a known precursor, are the most common form of GBM (~90%), and they tend to be more aggressive and generally affect older patients. Alternatively, secondary GBMs develop slowly through progression from a lower-grade astrocytic tumor (WHO Grade II or III). These tumors are more frequent in younger patients and they are characterized by a significantly more favorable prognosis. Histologically, primary and secondary GBMs are indistinguishable, but they differ in their genetic and epigenetic profiles [4,5]. It is estimated that GBM has an incidence of 3.21 cases per 100,000 persons in the United States [6], with median survival time of around 7–15 months from the time of diagnosis [7]. The incidence rates of glioblastoma increase with age, with the highest rates in individuals aged between 75 and 84 years [6]. Patient survival at five years form diagnosis is lower than 5% [8]. The etiology of GBM is complex and it has not been fully elucidated, but a mix of genetic and environmental factors is the most likely cause of the disease [9].

GBM is a tumor that is extremely challenging to treat due to its highly invasive nature. Current treatments are based on maximal surgical resection, followed by radiotherapy and adjuvant chemotherapy [10]. Temozolomide (TMZ) is the standard chemotherapeutic agent for the treatment of GBM. This second-generation imidazotetrazinone derivative exerts its anticancer effect through DNA methylation [11]. TMZ is, in fact, a prodrug, which is spontaneously hydrolyzed at physiological pH to its alkylating metabolite 3-methyl-(triazen-1-yl)-imidazole-4-carboxamide (MTIC) [11]. TMZ is orally administered and it leads to fewer side effects when compared with other chemotherapeutic agents parenterally administered [12]. Notwithstanding, its clinical effectiveness remains limited, since tumors rapidly develop resistance to the treatment [13]. In addition, several GBM cases are intrinsically resistant to TMZ, even during initial treatments. This inherent resistance is a consequence of various defense mechanisms, such as the expression of multi-drug resistance proteins and DNA repair systems impairment [14]. The extensive and complete surgical resection of GBM represents the most effective way to increase the survival of GBM patients [15]. However, the surgical intervention is difficult and, in most cases, less than 90% of the tumor can be removed [16]. In fact, these tumors exhibit a high degree of invasiveness and are often localized in important functional areas of the brain, including areas that are involved in the control of speech, motor functions, and senses [17]. Furthermore, the blood–brain barrier (BBB) limits the passage of molecules, including many anticancer drugs, from the bloodstream into the brain [18]. As a consequence of the restrictive nature of the BBB combined with the low brain permeability to most drugs, high doses have to be administered to obtain therapeutic concentrations in the brain. Although several strategies have been proposed to overcome these obstacles (e.g., oncolytic viruses, targeted therapies, immunotherapy, vaccines, etc.), brain delivery of therapeutic molecules against glioblastoma remains a challenge [19].

Nose-to-brain delivery has been proposed as a non-invasive approach to directly access the brain through bypassing the BBB. It is actively investigated as an alternative administration route for the delivery of pharmaceutically active molecules that are potentially useful in a number of CNS disorders. In particular, the intranasal delivery route could represent a major breakthrough in the treatment of GBM, since it offers an effective drug delivery approach for a number of innovative therapeutic strategies (Figure 1).

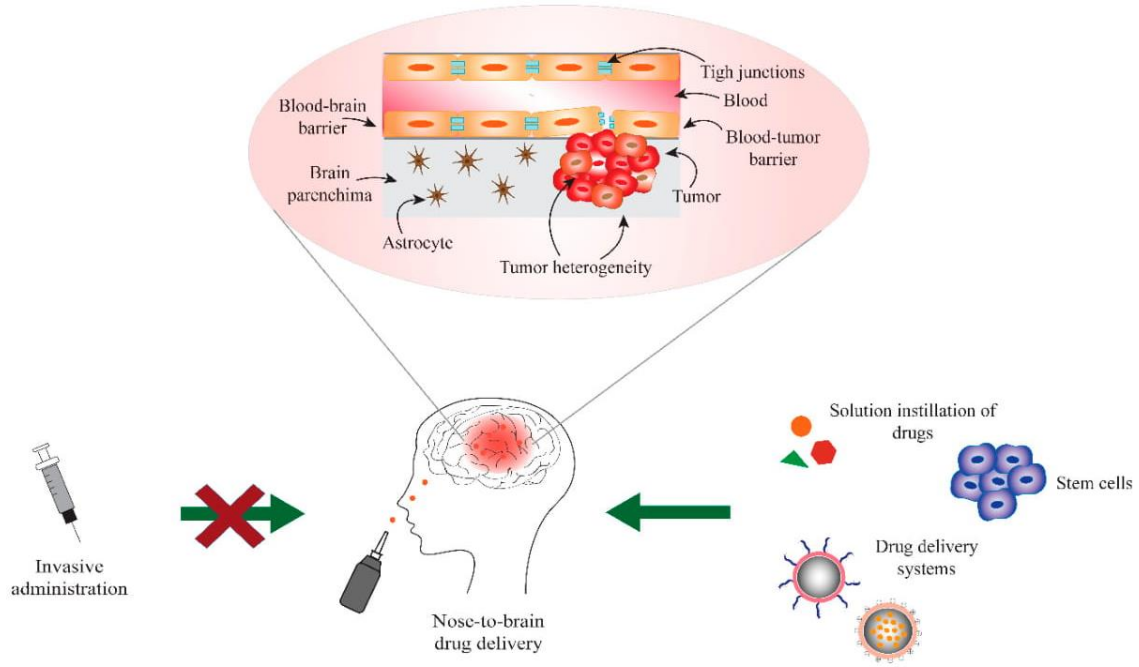

Figure 1. Obstacles and opportunities in the nose to brain drug delivery approaches for the treatment of glioblastoma multiforme (GBM).

2. Blood-Brain and Blood-Tumor Barriers (BBB/BTB)

The BBB protects the CNS by exhibiting a highly selective permeability to substances that are present in blood in order to preserve brain homeostasis and ensure the correct neuronal functioning of the brain. The BBB is a cellular barrier and its properties are mainly due to the presence of tight junctions (TJ) between the endothelial cells of brain capillaries and the involvement of surrounding cells, i.e., adjoining pericytes, astrocytes, and microglia [20,21]. The BBB selectively ensures the supply of essential nutrients and oxygen into the CNS, while also preventing the passage of macromolecules as well as of undesirable toxic or infectious agents, thus providing an adequate brain homeostasis [22,23]. Along with these defensive functions, the BBB also prevents the entry of xenobiotic drugs from the blood into the brain. The BBB is only normally permeable to small and lipophilic molecules, with a molecular weight (Mw) lower than 400–500 Da [24]. In addition, the LogP that is required for an efficient transport across the BBB is estimated to be in the range of 1.5 and 2.7 [25]. Low hydrogen-bonding potential is another important drug characteristic to ensure access to the CNS [26].

In brain tumors, the microenviroment differs from that of the healthy brain, since the morphology, function, and organization of BBB are affected. The result of this alteration is the formation of the so-called blood-tumor barrier (BTB) [27–29]. In high-grade gliomas, as in glioblastoma, the BTB is made from existing and newly formed blood vessels that contribute to the delivery of nutrients and oxygen to the tumor and facilitate glioma cell migration to other parts of the brain [27,30]. The tumor expansion creates hypoxic areas that trigger the overexpression of vascular endothelial growth factor (VEGF) and, consequently, the promotion of neoangiogenesis [31]. The neovascularization process commonly leads to the formation of abnormal vessels that are then able to sustain the high metabolic activity of the tumor cells. The increased fenestration or loss of tight junctions between endothelial cells characterizes these vessels. Furthermore, these new vascular endothelial cells are overexpressing caveolae, have increased pinocytotic activity, and are rich in mitochondria [31–33]. Nevertheless, the BTB presents continuous fenestrated vessels with a defined pore size, which precludes the entrance of hydrophilic compounds and large molecules to the brain tumor [30,34]. As a consequence, most of the antitumor agents are not delivered to the brain tumors due to the presence of BTB [30,34]. The permeability of the BTB can increase as the brain tumor progresses to the late development stages, since an impairment of

the BBB/BTB often occurs along with an intensification of the enhanced permeability and retention (EPR) effect, which results in a tendency of large molecules and particles in the nanoscale to accumulate at the brain tumor site [32,34].

3. Nose-to-Brain Drug Delivery

The choice of the treatment and, ultimately, average patient survival, depend on the glioma type, size, location, and grade [35,36]. In some cases, the median survival can be extended by the addition of adjuvant chemotherapy (TMZ) to the radiotherapy (RT) [37,38]. Stupp et al. found that the median survival of patients receiving TMZ in addition to RT was 14.6 months when compared with 12.1 months among those who were assigned to RT alone [39]. However, despite the benefits, treatment with TMZ can entail some severe side effects, such as nausea, vomiting, lymphopenia, neutropenia, thrombocytopenia, fatigue, disturbed sleep, and depression [40–42]. Furthermore, the risk of neurocognitive impairment is increased when RT is administered to the whole brain and even more when the chemotherapy is associated to RT [43–45].

Approaches to overcome the physiological barriers and limitations to access the human CNS include the exploitation of ways that are suitable for the direct administration of the drug to the brain. This can be done by intraventricular, intrathecal, or nasal administration [46]. The intrathecal administration requires some risky surgical procedures and the drugs administered can present limited distribution throughout the brain parenchyma and cerebrospinal fluid (CSF). A better distribution into the CSF can be obtained by intraventricular administration, but this type of administration requires the implant of drug release controlling reservoirs. Furthermore, some severe side effects can occur when drugs are intrathecally and intraventricularly administrated, including meningitis, arachnoiditis, and focal neurologic injury. Moreover, these approaches will result in the potential increase of drug-related toxicities because of the restricted volume of distribution if CSF flow abnormalities are present [47,48]. As a consequence, these invasive brain administration approaches appear to only be applicable to a limited number of selected patients.

The intranasal route of administration is able to bypass the BBB and it appears to be an alternative route for the delivery of drugs to the CNS. In fact, several evidences have been provided in the scientific literature supporting the claim that drugs can reach the CNS after administration into the nasal cavity [49–51]. It is essential to understand the mechanisms of transport of the compounds, the anatomy of the nervous system, and the pathophysiology of the disease, as well as several experimental parameters, in order to design a formulation that allows access to the CNS through the intranasal route efficiently [52]. In the next paragraphs, the anatomical organization of the nasal cavity will be briefly discussed, focusing on the structures that are necessary for understanding nose-to-brain transport, since excellent descriptions can be found in many review papers and textbooks [53].

Anatomically, the nose presents two cavities limited by a septal and a lateral wall dominated by the turbinates, structures that are responsible for the temperature regulation and humidification of the inspired air [54]. The innervation of the human nasal cavity can be divided into sensory and olfactory nerves. The sensory innervation consists of the first and second divisions of the trigeminal nerve (ophthalmic nerve and maxillary nerve), while the olfactory innervation is ascribed to the olfactory nerve [55,56]. The nasal cavity can be divided into three regions: the vestibular region, the respiratory region, and the olfactory region. The vestibular region, which is located in the frontal part of the nasal cavity, is followed by the respiratory region that presents approximately 130 cm^2 of area, and it is characterized by the sensory/trigeminal innervation. In humans, this is the largest region and it can reach up to 80–90% of the nasal cavity [57]. The respiratory epithelium is responsible for covering the nasal conchae, i.e., bone projections of the lateral walls of the nasal cavity and also the paranasal sinuses, i.e., cavities in the facial bones that communicate with the nasal cavity [58]. The last region of the nasal cavity is the olfactory region, which, in humans, represents approximately 10% of the nasal cavity surface area. This region is located in the upper part of the nasal fossa, below the lamina cribrosa (or cribriform plate) of the ethmoid bone and it is innervated by the olfactory nerve [54,59,60]. Olfactory

cells are bipolar unmyelinated neurons that present dendrites with terminations protruding above the surface of the nasal mucosa interspaced between the supporting cells and an axon extending through the connective tissue towards the olfactory bulb located in the CNS [61]. The constant replacement of olfactory receptor neurons makes the olfactory mucosa relatively "leaky", allowing for the nose-to-brain transport [62]. The molecular weight and the hydrophilic/lipophilic nature of the drug directly influence the absorption of the drugs through the nasal route. Poor bioavailability after nasal administration is generally observed for drugs with a molecular weight greater than 1 kDa [63]. Lipophilic compounds presenting a molecular weight lower than 1 kDa in some cases present bioavailability close to 100%, i.e., similar to drug exposure obtained after intravenous administration [64].

Mucociliary clearance takes place after the administration into the nasal cavity of a formulation, generally starting from the vestibular region [65]. The formulation is then moved to the posterior region of the nasal cavity in the direction of the respiratory and olfactory regions. The transport to the brain of the drug or of the formulation itself can happen via five different pathways: the olfactory nerve, the trigeminal nerve, the lymphatic, the CSF, and the vascular pathway. The nose-to-brain transport can occur via a single route or through a combination of pathways mentioned above, depending of the nature of the drug, the characteristics of the formulation and the physiological conditions [66]. The substances can then move towards lamina propria and the brain by two different mechanisms, the intracellular and the extracellular transport mechanisms. Once at the lamina propria, the substances follow the perineural channels that are created by a glial cell type, the olfactory ensheathing cells, which cover the non-myelinated axons, cross the cribriform plate, and enter into the CSF and olfactory bulb (Figure 2).

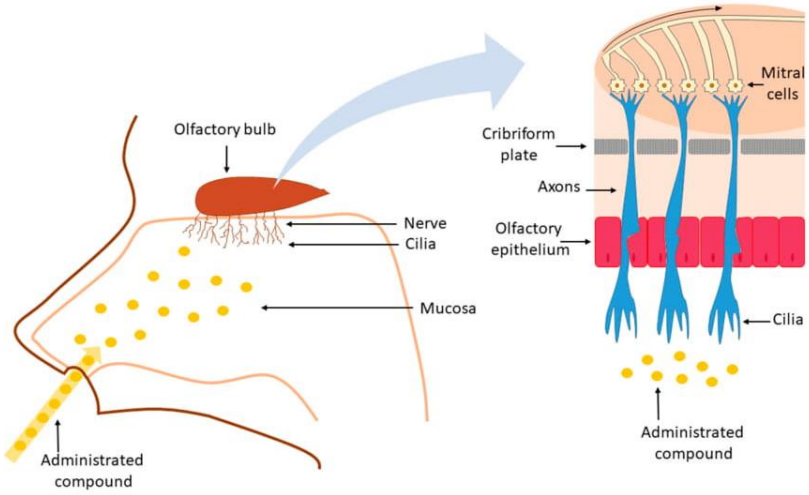

Figure 2. Structures involved in nose-to-brain transport by the olfactory pathway.

From the CSF, the substances are then distributed throughout the brain via bulk flow after being mixed with the interstitial fluid. They are also rapidly distributed throughout the CNS via perivascular transport [52,67].

The olfactory nerve pathway exploits the unique position of olfactory receptor neurons located in the olfactory mucosa, being a direct connection between CNS and the external environment [23,68]. The permeation of the compounds to the CNS occurs along or within the neurons present at the olfactory epithelium through the olfactory pathway [69]. In the case of intraneuronal axonal transport, the compounds are internalized in the olfactory epithelial neurons and then conveyed to the olfactory bulb, thus enabling the compounds to be further distributed to the rest of the brain [70]. In the intracellular form of transport, generally preferred by substances with a hydrodynamic radius above 20 nm, permeation can happen through endocytosis by sensory olfactory neurons and subsequent intraneuronal transport to the olfactory bulb, or through transcellular transport to the cells of the lamina

propria [49,71]. However, the intraneuronal axonal transport is usually quite slow, with the times of delivery to the CNS ranging from hours to several days. The paracellular transport involves the absorption of the compounds across the nasal epithelium and the extracellular diffusion associated with bundles of nerves with consequent migration to the cranial compartment [72]. In fact, the perineural spaces of the cranial nerves, as in the case of the olfactory and trigeminal nerves, seem to allow for communication with the CSF of the subarachnoid space, which allows a rapid access route for the molecules absorbed across the nasal mucosa to reach the CNS [70]. The direct nose-to-brain transport can also occur by the trigeminal nerve, which innervates the respiratory and olfactory epithelia of the nasal cavity and allows the access of compounds to the caudal and rostral sections of the brain after intranasal administration [73,74]. However, it is important to point out that it is not generally possible to determine a specific/exclusive way that molecules/peptides access the CNS after the nasal administration, because this access can occur simultaneously by multiple pathways [66]. In fact, in conjunction with these pathways, other mechanisms can also provide access to the CNS from the nasal cavity, such as the nasal and the brain lymphatic systems that connect to the CSF and CNS interstitial spaces drainage by bulk flow mechanisms through perivascular channels surrounding blood vessels [66,75]. Another mode for the penetration of compounds into the CNS from the nasal respiratory region is through an indirect way via the vascular pathway. In fact, nasal blood vessels present continuous but fenestrated endothelia that enable the small molecule passage and the delivery to the brain by distribution across the BBB [74,76].

Despite the numerous advantages, nose-to-brain drug delivery can be limited as a result of some aspects that are related to the intranasal administration, such as low bioavailability of peptides and proteins due to enzymatic degradation, high clearance from the nasal cavity due to mucociliary transport, and other restrictions determined by the anatomy of the nasal cavity, such as small administration volume, limited surface area of the olfactory mucosa, mucus barrier, etc. In terms of enzymatic degradation, it can occur in the lumen of the nasal cavity or during transit across the epithelial barriers due to the presence of exo-peptidases, such as mono- and diaminopeptidases, which can cleave peptides at their N and C terminal and endo-peptidases that can attack internal peptide bonds [77]. The mucus present in the upper respiratory region acts as a physical and chemical barrier that entraps particles and molecules. The mucus is then drained from the nasal cavity into the pharynx through ciliary movement to be swallowed or expectorated [58]. Despite these limitations, Quintana and collaborators [78] reported results from a clinical trial that investigated the intranasal delivery of oxytocin (OT) to 16 male health adults. The treatment groups were divided in: two different doses of intranasal OT, i.e., eight and 24 IU; one IU intravenous OT and placebo with a period of at least six days between treatments to prevent potential carryover and/or administration-related effects. The blood samples were collected to determine the peripheral levels of OT, cross-reactive vasopressin (AVP), and cortisol. All of the treatments produced similar plasma OT increases when compared with placebo. However, the behavioral data that were obtained by emotional expression evaluation suggested that OT delivered intranasally while using a Breath Powered bi-directional device (Optinose, Oslo, Norway) reached the brain and influenced social cognition, whereas IV administered OT, which similarly increased plasma OT concentration, did not. The data from this study supported a direct nose-to-brain effect, independent of blood absorption, for low-dose (8 IU) OT [78].

4. Drugs for GBM Treatment Administered Intranasally

Several studies have been conducted to determine the best treatment of GBM via the intranasal approach, while using monotherapy or drug combinations, including natural and/or synthetic compounds. The studies that were conducted with this purpose of developing an effective way to treat this aggressive brain tumor are summarized below.

Natural compounds, such as curcumin (CC), a polyphenolic extracted from the rhizomes of the *Curcuma longa* that presents anti-oxidant and anti-inflammatory characteristics, are interesting in the treatment of cancer and neurodegenerative disorders and they have been proposed for the treatment of GBM. The anticancer activity of CC has been attributed to the ability of the compound to reduce the expression of E3 ubiquitin ligase NEDD4, a neuronal precursor that is responsible for substrate recognition implicated in cancer development, and the inhibition of Notch1 and pAKT cancer cells signaling pathways, leading to glioma cell growth inhibition, apoptosis, and the suppression of migration and invasion [79,80]. Mukherjee and collaborators [81] used the intranasal route to deliver CC coupled to a glioblastoma specific antibody (CD68 Ab). The targeted CC-CD68 Ab conjugate was intranasally administered to mice in which glioma GL261 cells were implanted in the brain. Ten days after GL261 cells implantation, male adults C57BL/6 mice had CC-CD68 Ab solution in PBS intranasally administered every 72 h, while another group of animals received a solution of a commercially available lipid-complexed form of CC, i.e., Curcumin Phytosome (CCP), by intraperitoneal injection every 72 h. The intranasal delivery of CC-CD68 Ab conjugate and the intraperitoneal injection of CCP both caused GL261 brain tumor remission in 50% of mice, which confirmed that the CD68 Ab could be delivered to the brain via the intranasal route and confirming that CD68 Ab presented a targeted therapeutic effect after intranasal delivery. Furthermore, 70% of the animals that received CC-CD68 Ab intranasal and 60% of those treated intraperitoneal with CCP were still alive at day 90, while all of the control group animals, i.e., vehicle-treated mice, were already dead at that time. In the same study, a marked induction and activation of microglial NF-kB and STAT1 transcription factors were also observed. The transcription factors function together to cause the induction of nitric oxide synthase (iNOS) and, consequently, tumor regression. Therefore, the findings in this study indicate that intranasally delivered CC targeted conjugates can directly kill GBM cells and also repolarize tumor-associated microglial cells (TAMs) to the tumoricidal state [81].

Another natural compound, anthranoid 4,5-dihydroxyanthraquinone-2-carboxylic acid, which is also known as rhein, exhibits anti-inflammatory, anti-oxidant, anti-fibrosis, neuroprotective, and anti-tumor activities [82,83]. The anti-tumor activity of rhein is attributed to the inhibition of MAPK, PI3K-AKT, and HIF-1 signaling pathways and the down-regulation of VEGF signaling pathway [83,84]. Blacher and colleagues [85], aiming at demonstrating that the inhibition of the ectoenzyme CD38 in tumor microenvironment can attenuate glioma progression, conducted a study while using a syngeneic mouse glioma progression model. The animals, C57BL/6J wild-type (WT) and CD38-deficient C57BL/6J (CD38-/-) mice, were pretreated with vehicle or rhein by nasal administration. After 24 h, the glioma cells (GL261) were intracranially injected into the brains of the mice and the administration of vehicle or rhein was carried three times per week over 22 days. The researchers found that the rhein is capable of inhibiting the CD38 enzymatic activity, which reduces the microglia activation that support the progression of the tumor. In fact, the intranasal administration of rhein to WT mice significantly inhibited glioma progression, suggesting that CD38 is a therapeutic target in the tumor microenvironment and that small-molecule inhibitors of CD38 may serve as a useful approach for treating glioma. Furthermore, computed tomography (CT) images of the mice brains showed that the WT and Cd38-/- mice treated intranasally with rhein had the volume of the tumor reduced. However, this effect was significantly higher in WT mice when compared to Cd38-/- (reduction of 74 and 19% on day 22, respectively), demonstrating that rhein inhibits glioma progression and that this effect is mainly CD38 dependent. With this study, it was possible to conclude that the intranasal administration is an effective drug delivery route to the CNS and that the rhein has therapeutic potential for treating glioblastoma [85]. These data additionally support the possibility of brain access from the nasal cavity and demonstrate that the compounds can be directed to the CNS to be effective in the treatment of GBM, even in monotherapy.

Nevertheless, other studies explored the use of compounds in combination. The study that was performed by Shingaki and coworkers evaluated the direct brain uptake from the nasal cavity of a model drug, 5-fluorouracil (5-FU), and whether the inhibition of CSF secretion by choroid plexus could lead to increased drug concentration in the brain [86]. 5-FU is a fluoropyrimidine that is widely used in the treatment of malignant tumors, such as breast, skin, colorectal, and neck [87]. This uracil pyrimidine analog is an antimetabolite drug that can inhibit the thymidylate synthase enzyme and perform a mis-incorporation of fluoronucleotides into RNA and DNA, which leads to cytotoxicity and cell death [88–90]. In this study, 5-FU was intravenously infused or nasally perfused in the presence and absence of intravenous administration of acetazolamide (AZA) in male Wistar rats. In groups of co-treatment, AZA (25 mg/kg) was injected 15 min. before starting the nasal perfusion of 5-FU. AZA is an inhibitor of the secretion of CSF by choroid plexus epithelial cells. In these cells, the CSF secretion is linked to the active transport of Na^+ ions and AZA significantly decreases the activity of the Na/K ATPase [91]. The study demonstrated that the intravenous administration of AZA was able to enhance the CSF concentration of nasally administered 5-FU by 200–300% when compared to that obtained by 5-FU nasal perfusion without pre-treatment with AZA. AZA enhancement of nose-to-brain drug transport was obtained by decreasing the CSF secretion from the choroid plexus and, thus, sustaining the concentration of the nasally applied drug in the CSF [86]. These results demonstrated that 5-FU is capable of accessing the brain through nasal administration. It was concluded that the co-administration of active compounds to treat neurological diseases with drugs that can decrease CSF secretion from the choroid plexus could be an interesting alternative to the treatment of diseases into the brain, like GBM, since an enhancement of the concentrations of the active compounds in the brain is obtained.

In another study, the same group reported a similar effect on the nasal administration of methotrexate (MTX) in male Wistar rats [92]. MTX is a folic acid antagonist that inhibits enzyme dihydrofolate reductase, having a therapeutic effect on a wide range of cancer types [93]. MTX presents a low penetration across the BBB, which limits its therapeutic use for GBM treatment by the oral route [94]. In the study, MTX was nasally administrated while using sodium carboxymethyl cellulose (CMC) to enhance the nasal residence time of the formulation, and AZA was orally administrated 30 min. before the nasal administration of MTX as a co-therapy. The brain uptakes of tritium labelled MTX after intranasal administration of a formulation containing CMC and after intraperitoneal administration were evaluated by blood samples and analysis of the cerebral cortex. MTX was administered for five days with the interval of two days between each treatment to evaluate the results after repeated administrations. The results showed that the amount of MTX quantified in CSF was higher than in the plasma 15 min. after intranasal administration, which indicated significant direct transport of MTX from the nasal cavity to the CSF. In contrast, a higher concentration was obtained in plasma when compared to those obtained in the CSF after intraperitoneal administration. At the same time, the effect of oral administration of AZA 30 min. before the nasal administration of MTX was evaluated and it was found that the co-treatment increased the concentration of MTX in CSF by 195% [92]. The study demonstrated that the intranasal administration is a promising route of the administration of drugs directed towards brain diseases and that AZA can enhance the amount of MTX in the CSF, which is in agreement with the results that were obtained with 5-FU [86,92].

In another study, MTX was loaded in chitosan microspheres that were designed for nasal administration. The microspheres were produced by spray-drying technique while using chitosan with different molecular weights to promote the nose-to-brain delivery of the MTX. The animals received MTX by the intravenous injection or MTX was intranasally administered while using a drug solution or MTX-loaded chitosan microspheres. The study demonstrated a higher concentration of MTX in rat brain tissues after intranasal administration of the MTX-loaded chitosan microspheres when compared to the MTX solution, while MTX could not be detected in rat brain sections after the intravenous administration. The fact that MTX-loaded chitosan microspheres showed a higher nose-to-brain transport, when compared to MTX aqueous solution after nasal administration, was attributed to the

presence of chitosan. Indeed, chitosan is considered to be a safe mucoadhesive polymer that could effectively improve the nose-to-brain transport of a hydrophilic drug, like MTX, through intranasal administration [95].

Another study proposed the nasal delivery of temozolomide (TMZ) [96]. TMZ is efficiently absorbed after oral administration and it is available in capsules. Additionally, TMZ has shown good penetration across the BBB and a tolerable toxicity profile [97]. However, the increase in survival for the multimodal treatment with TMZ and radiotherapy is only 2.5 months when compared with radiotherapy alone and existing studies suggest that 60–75% of patients with GBM present no clinical benefit from treatment with TMZ [98]. Based on these data, a rat model bearing orthotopic C6 glioma xenografts was used to study the therapeutic effect of the intranasal administration of TMZ to exploit the brain-targeting properties of this delivery route. In fact, the intranasal administration of TMZ was proposed to limit the systemic exposure to the drug and thus reduce the toxic effects on healthy organs. The animals were treated with saline solution or with TMZ by three different administration routes, intravenous, oral, or intranasal, and the tumor size, rat survival time, and pathological changes were observed during the 40 days of the experiment. Magnetic resonance imaging showed a significant reduction in the volume of glioma xenografts in the intranasal TMZ group when compared to all of the other groups, including controls ($p < 0.05$). Analysis of proliferating cell nuclear antigen (PCNA) and tumor cell apoptosis that were obtained by immunohistochemistry and terminal deoxynucleotidyl transferase dUTP nick end labelling (TUNEL) assay demonstrated that the animals that were treated by the intranasal route presented the lowest expression of PCNA and the highest tumor cell apoptosis rate. The median survival time of the C6 glioma-bearing rats was also significantly longer in the intranasal TMZ group when compared to the other three groups. The control animals that were treated with saline solution survived 20 days, the animals treated with TMZ orally administered survived 21.5 days, animals receiving TMZ intravenously survived 19 days, while animals that were treated with TMZ intranasally survived 31 days [96]. The results presented in this study suggest that the intranasal TMZ administration can suppress the growth of C6 glioma in vivo and it might serve as an effective strategy for glioma treatment.

Intranasal administration in nude mice xenograft models carrying human glioblastoma tumors generated from the human glioma stem cell lines TG16, TG1N, and TG20 by Pineda and co-authors also tested a solution of TMZ in dimethyl sulfoxide (DMSO) [99]. The human glioma cell lines TG16, TG1N, and TG20 were administered by intrastriatal injection to ten-week-old female Swiss nu/nu mice. One month after the graft, the anesthetized mice intranasally received 10 µL of TMZ or vehicle; this procedure was repeated three times a week for two weeks. The TMZ administered intranasally delayed tumor growth and significantly extended the lifespan of the mice engrafted with TG16 and TG1N cells, but presented no effects on the tumors generated by TG20 cells that are resistant to TMZ in vitro. The presented results demonstrated that the intranasal route should be further considered as an option for TMZ delivery into the brain to treat intrastriatal brain tumors [99].

The studies that are reviewed above collectively demonstrate that the intranasal administration of anticancer drugs can induce benefits in the treatment of GBM and the intranasal route of administration might allow for direct access of the drugs to the brain serving as an effective strategy for glioblastoma treatment. However, meaningful comparative studies between intranasal and other administration routes (oral or parenteral) should be always duly conducted to conclusively highlight the potential clinical benefits of using the nose-to-brain delivery over more traditional but well-established administration routes.

Clinical Trials on the Use of Intranasal Perillyl Alcohol for Glioblastoma Treatment

Perillyl alcohol (POH) is a natural compound that belongs to the group of hydroxylated monoterpenes found in many essential oils (peppermint, spearmint, cherries, and others) [100]. The amphipathic character of POH makes it readily soluble in biological membranes and it has been found to be capable of interacting with the lipid bilayers of gliomas cells, leading to effective POH

delivery into these cells [101]. A post translational Ras inhibition effect has been suggested by some studies as the main mechanism of anticancer action of POH but not observed in others. Thus, the action of POH is often described as pleiotropic, affecting multiple cell growth regulation processes [102].

Thirteen clinical studies were conducted while using orally delivered POH to cancer patients (ovarian, prostate, breast, colorectal, and pancreatic cancers) to establish the safety and efficacy of this molecule [103]. POH was dosed in capsules along with soybean oil, and the dose regimen included dozens of capsules per day per patient. However, no significant therapeutic response was observed, and the trials were halted before reaching Phase 3 clinical trials. In subsequent studies, the focus was shifted to the use of the intranasal route for the delivery for POH. Here we will briefly summarize the results of the clinical trials that were conducted on GBM patients, although an excellent review has been recently published on this specific topic [102].

To date, POH is the only therapeutic agent that is intended for cancer treatment employing the intranasal route that reached clinical trials Phases 1 and 2. It should be noted that these studies use an inhalation protocol, which might not solely involve the nose-to-brain delivery mechanism. Clinical trials have consistently showed the safety and tolerability of POH administered by the nasal route for up to eight years in addition to positive therapeutic responses in some cases [102,104,105]. The first clinical trial that was carried out in Brazil enrolled 37 patients with recurrent malignant glioma, including 29 with glioblastoma aging from 38 to 62 years old. POH was administered by inhalation four times a day at a concentration of 0.3% *v*/*v* to deliver a total daily dose of 220 mg. After six months, 14 patients with GBM showed partial response (one patient) or stable disease parameters (13 patients), suggesting some antitumor activity for POH [106]. A following study included 141 patients with recurrent glioblastoma divided into a treatment group, which included 83 patients with recurrent primary GBM and six with secondary GBM receiving POH and a control group with 52 patients receiving supportive care. The treatment consisted of the inhalation of POH four times per day to reach a total daily dose of 440 mg. The results showed a significant increase in survival between the POH treated groups over control group, between patients with secondary GBM over patients with primary GBM and between patients with tumor with deeper localization (thalamus, basal ganglia) over those with tumor at the lobar region. Subsequently, a four-year study with a cohort of 198 patients with recurrent malignant glioma (151 with primary GBM and 38 with secondary GBM) was conducted while again using a protocol of inhalation of POH four times a day, but adopting a higher dosing compared to previous studies (533.6 mg/day). Patients with secondary GBM had a significant increase in survival time when compared to patients with primary GBM, confirming the results of the previous studies, but, most importantly, 19% of patients that were enrolled in this trial remained in clinical remission after four years under exclusive POH inhalation treatment [104]. Santos and colleagues recently reported a study that combined the inhalation of POH (55 mg four times per day) with a ketogenic diet (KD) for three months. In the context of cancer therapy, some authors argue that the KD is viewed as a metabolic therapy and it consists of a high-fat, low-carbohydrate with adequate amounts of protein, promoting a specific metabolic state that is characterized by increased ketone body levels and low glucose levels in the blood [102]. The data showed that the 88% of patients that followed this treatment showed partial responses and stable disease parameters at the end of the study [107].

Encouraged by the positive results that were observed in the clinical trials performed in Brazil, a synthetic GMP grade POH (NEO100) is now under Phase 1/2A clinical trials in the U.S.A. sponsored by Neonc Technologies, Inc. (NCT02704858) [103]. These studies started in 2016 and are still recruiting patients with recurrent glioblastoma. The treatment protocol will follow that adopted in previous trials, with a regimen of POH being inhaled four times a day over a period of six months. Four dosing levels will be studied: 96 mg, 144 mg, 192 mg, and 288 mg per inhalation in order to determine the maximum tolerated dose (MTD). A total of 25 patients will be treated at the MTD and pharmacokinetic studies will be conducted during Phase 1 at the first dosing and after the first dose of the third cycle [103]. The study is expected to be concluded in October 2020 and no partial results were made available to date.

5. Drug Delivery Systems for Nose-to-Brain Delivery in Glioblastoma Therapy

Several therapies that apply novel drug delivery systems are under investigation for the treatment of GBM. Recently, nanoparticles (NP) have received significant attention due to the several advantages that they offer over conventional therapy, such as, for example, their ability in some cases to carry drugs across the BBB [34,108]. Furthermore, these systems offer controlled drug release, which potentially allow for a decrease in the frequency of administrations [109]. Moreover, nanoparticles are expected to improve the drug physicochemical stability and increase the biological availability [110,111].

The application of NP for the direct enhancement of drug delivery from the nasal cavity to the brain demonstrates great potential. The encapsulation of drugs into NP can overcome some of the problems related to intranasal administration (e.g., the poor capacity of penetration through the nasal mucosa, the rapid mucociliary clearance, and the enzymatic degradation), and thus enhance nose-to-brain drug delivery [112]. The small diameter of the NP also allows for them to be more effectively transcellularly transported to the brain [61]. Besides, NP may offer improved drug delivery to the brain, since they can prevent extracellular transport by P-glycoprotein (P-gp) efflux proteins localized in the olfactory epithelium and the endothelial cells that surround the olfactory bulb [113,114]. Additionally, the nanocarriers may also have their surface functionalized with specific ligands to transport agents even more effectively through the BBB [115]. Chitosan nanoparticles, polymeric nanoparticles, liposomes, solid lipid nanoparticles, nanoemulsions, micelles, and nanoplexes, among others, are the NP that have been mainly studied for nose-to-brain delivery. Table 1 summarizes the main features of the NP specifically designed for GBM therapy by the intranasal route in recent years and under pre-clinical stages of development.

Table 1. Characteristics and pre-clinical findings in the last 10 years using nanocarriers administered by the intranasal route for GBM therapy.

Drug	Type of Nanocarrier	Surface Modification	Preparation Method	Size (nm)	Zeta Potential (mV)	In Vivo Model	Ref.
Bevacizumab	Polymeric NPs(PLGA)	-	Emulsification-evaporation	185.0 ± 3.0	~−2	U-87-luc mice	[116]
Ecto-5′-nucleotidase (CD73)	Nanoemulsion	-	Microfluidization	262.7 ± 12.8	+3.5 ± 3.0	C6 rat glioma	[117]
Teriflunomide	Microemulsion	-	Progressive aqueous phase titration	22.81 ± 0.48	−22.62 ± 1.1	-	[118]
Melatonin	Polymeric NPs(PCL)	-	Nanoprecipitation	166.7 ± 6.3	−34.0 ± 5.2	-	[119]
Temozolomide	Polymeric NPs(PLGA)	Anti-EPHA3	Emulsion-solvent evaporation	125 to 146	−21 to + 23	C6 rat glioma	[120]
Kaempferol	Nanoemulsion	Chitosan	High-pressure homogenization	180.53 ± 4.90 (coated) 145.07 ± 4.91 (uncoated)	+26.09 ± 2.67 (coated) −18.10 ± 2.55 (uncoated)	-	[121]
Temozolomide	Nanoemulsion	-	High-pressure homogenization	134 nm	−13.11	-	[122]
Farnesylthiosalicylic acid	Hybrid nanoparticles	-	Emulsion sonication	164.3 ± 10.3	−12.0 ± 1.3	RG2 rat glioma	[123]
Curcumin	Microemulsion	-	Oil titration method	<20	~+10	-	[124]
Curcumin	Nanostructured Lipid Carriers	-	High pressure homogenization	146.8	−21.4 ± 1.87	-	[125]
siRNA	Chitosan nanoparticles	-	Ionic gelation	141 ± 5	+32	GL261 tumor bearing mice	[126]
siRNA siRNA + TMZ or immunotherapy	Chitosan nanoparticles	-	Ionic gelation	141	+32	GL261 tumor bearing mice	[127]
Methotrexate	Polymeric nanodispersion(PLA)	-	Emulsion/Solvent evaporation	351 ± 13.4	+25.1 ± 1.2	-	[128]
Carboplatin	Polymericnanoparticles(PCL)	-	Double emulsion/solvent evaporation	311.6 ± 4.7	−16.3 ± 3.7	-	[129]
BMP4 plasmid DNA	Polymeric nanoparticles(PBAE)	-	Self-assembly	218 ± 7	+17 ± 1	U87 rat glioma	[130]
Camptothecin	Polymer micelles(MPEG-PCL)	Tat	Self-assembly	88.5 ± 20.2	+10.4 ± 2.84	C6 rat glioma	[131]
siRaf-1/Camptothecin	Polymer micelles(MPEG-PCL)	Tat	Self-assembly	60 to 200	−2.86 to 15.9	C6 rat glioma	[132]

Abbreviations: PLGA, Poly(lactic-co-glycolic acid); PCL, Poly(ε-caprolactone); PLA, Poly(lactic acid); PBAE, Poly(beta-amino ester); MPEG-PCL, Methoxy[poly(ethylene glycol)]-b-[poly(ε-caprolactone)] amphiphilic block copolymers.

5.1. Polymer-based NP

Polymeric NP are an extremely versatile formulation approach and have demonstrated great potential in drug delivery. Recently, some authors proposed melatonin-loaded poly(ε-caprolactone) (PCL) nanoparticles (MLT-NP) for intranasal administration in the treatment of GBM [119]. Melatonin (MLT) is an indolic hormone that is synthesized and secreted by the pineal gland, acting in the regulation of the circadian cycle [133]. Synthetic MLT is marketed as a dietary supplement. Therefore, MLT is not officially approved by the FDA for any specific therapeutic indication. However, there are several studies that show its action as antioxidant, antitumor, immune system modulator, and neuroprotective agent [134,135]. However, its short half-life, low oral bioavailability, poor solubility, and extensive first-pass metabolism that limit the drug's ability to reach therapeutic concentrations limit its therapeutic use [136]. MLT-NP were characterized by an average size of 166.7 ± 6.3 nm and 51% encapsulation efficiency (EE), and showed a controlled release of MLT (71.2% release in 48 h). The formulation demonstrated strong activity against the U-87 MG glioblastoma cell line, which resulted in an IC_{50} ~2500-fold lower than that of the free MLT. Moreover, selective cytotoxicity effects of MLT-NP towards the tumor cell line were demonstrated, since, at low doses of MLT-NP, no cytotoxic effect was observed against MRC-5 human pulmonary fibroblasts. Fluorescence tomography images evidenced a rapid and direct translocation of the NP from the nasal cavity to the brain after the nasal administration of MLT-NP to rats. The in vivo pharmacokinetic study was conducted on male Wistar rat and the result showed a significant increase in the brain uptake of the MLT when MLT-NP were administered. Moreover, 0.5 h after administration, the percentage of administered MLT-NP in the brain was ~9- and ~18-fold higher than that of obtained using an MLT suspension administered intranasally and orally, respectively [119].

In a similar study, another group developed a polymeric NP formulation of carboplatin while using the biodegradable polymer poly(ε-caprolactone) [129]. Carboplatin (CPt) is an antineoplastic drug that belongs to the class of platinum-based alkylating agents and is approved for the treatment of various forms of cancer. However, the development of resistance, systemic toxicity, and rapid blood clearance are common problems that are related to CPt use in clinical practice [137]. CPt is available as a solution (Paraplatin®, Bristol-Meyers Squibb) for intravenous administration. Polyvinyl alcohol (PVA) was selected as the emulsifying agent for the production of the polymeric NP, as it provides the nanocarriers with lower particle size and enhances the maximal EE, while at the same time reducing particle aggregation. The in vitro drug release studies showed that the drug was released from the NP with a biphasic pattern characterized by an initial burst, followed by a prolonged sustained release due to a non-Fickian diffusion. Permeation studies across sheep nasal mucosa provided data similar to the in vitro release studies. In vitro cytotoxicity towards LN229 human GBM cells showed enhanced cytotoxicity by CPt-loaded NP only for long incubation times (96 h). In situ nasal perfusion studies that were conducted in Wistar rats with two CPt-loaded PCL NP containing different amounts of PVA demonstrated that both of the formulations showed progressive nasal absorption of CPt over time. Indeed, nanoencapsulated CPt showed better nasal absorption when compared to the free drug, as indicated by the smaller amount of CPt detected in the perfusate after intranasal administration [129].

GBM is characterized as a highly vascularized tumor as a consequence of the overexpression of endothelial growth factor (VEGF) [138]. Bevacizumab (BCZ; Avastin®, Roche), an anti-VEGF monoclonal antibody, was approved by the FDA (2009) to be used as a single agent in the treatment of patients with recurrent GBM [139]. However, BCZ failed to improve overall patient survival rates in some clinical studies [140,141]. Sousa and collaborators developed BCZ-loaded PLGA NP with the objective of improving BCZ bioavailability and targeting the drug efficiently to the brain [116]. BCZ-loaded PLGA NP (185.0 ± 3.0 nm with slightly negative charge) and control (Avastin®) were intranasally administered to CD-1 mice for seven days. The in vivo pharmacokinetic study demonstrated a significant increase of BCZ concentration in the brain, with 5400 ± 2313 ng/g brain tissues and 1346 ± 391 ng/g brain tissues for PLGA NP and control, respectively. The amount of BCZ that was found in blood and off-target organs (lung and liver) was insignificant in the case of

PLGA NP formulation. On the other hand, BCZ was found in the blood, lung, and liver after intranasal administration of Avastin® control. Thus, the improvement offered by nose-to-brain delivery might be an alternative for decreasing the systemic side effects of BCZ. The authors examined the efficacy of the nanoformulation in a nude mice orthotopic GBM model while using bioluminescence and VEGF quantification. Upon nasal administration once a week for 14 days, the BCZ-loaded PLGA NP showed a significantly higher anti-angiogenic effect as compared to Avastin® intranasally administered. However, in terms of tumor growth, no statistical difference was observed between the treatments. The authors attributed these results to the previously reported slow release profile of BCZ from PLGA NP [142]. They also suggested that another in vivo model should be used to increase the number of administrations and evaluate tumor growth for a longer time [116].

Another group worked on lipid-PEG-PLGA hybrid nanoparticles (HNP) for intranasal delivery of farnesylthiosalicylic acid (FTA) with the aim of increasing the brain-targeting efficacy [123]. FTA, which is also known as salirasib, is a synthetic derivative of salicylic acid. FTA is a potent and specific inhibitor of Ras proteins, which are found in most malignant tumors [143]. However, FTA presents poor oral bioavailability and it is not able to cross the BBB at effective concentrations [144]. HNP were produced by the emulsion sonication method and it showed a particle size of around 160 nm and negative surface charge (−12 mV). The in vitro cytotoxicity after 24 h showed that the hybrid nanocarriers significantly decreased rat glioma-2 (RG2) cells viability of ~60%, as compared to only ~13% obtained while using free FTA treatment. Furthermore, cytotoxicity studies towards healthy cells evaluated using L929 mouse fibroblasts evidenced a significant toxic effect for free drug treatment, whereas FTA-loaded HNP did not show significant toxicity. For the in vivo studies, the RG2 cells were unilaterally implanted into the right *striatum* of female Wistar rats. After 10 days, glioma bearing rats received a single dose intravenous treatment or five repeated doses intranasally of FTA-loaded HNP (500 μM/20 μL). Free FTA and blank HNP were used as controls. The data obtained by magnetic resonance imaging (MRI) showed that tumor area decreased by 57.3% and 31.0% when compared to the controls for the single intravenous and repeated intranasal doses of HNP, respectively. In fact, intravenous and intranasal administrations of free drug and blank nanocarriers both had no significant effect in vivo. After a treatment period of five days, the intranasal administration of the nanocarrier achieved a significant decrease of 55.7% in tumor area, which was similar to that observed by intravenous administration of the same formulation (Figure 3A). This result was corroborated by the in vivo distribution studies that indicated that the percentage of the FTA dose reaching the brain was similar after intranasal and intravenous administration of HNP (Figure 3B). However, the highest accumulation of NP was detected in the olfactory bulb after intranasal administration, whereas following intravenous administration the nanocarrier caused a high accumulation of FTA in the spleen and liver (Figure 3B) [123].

Recently, several researchers have proposed the inclusion of nanoformulations within mucoadhesive gelling systems for nasal administration to enhance the nasal residence time and reduce the mucociliary clearance [145,146]. For example, Jain and collaborators developed an innovative MTX formulation for GBM by encapsulating the drug into polymeric PLA NP (MTX-NP) and including poloxamer 188 in combination with Carbopol 934 in the formulation to obtain a thermosensitive hydrogel [128]. It was demonstrated that the MTX-NP formulation mucoadhesion correlates with the amount of Carbopol 934 included while using a mucoadhesiveness testing apparatus. In vivo studies that were carried out using male Wistar rats indicated that the combination of the in situ gelling system and NP resulted in an increase of MTX in the brain when compared to data that were obtained with the MTX solution. The pharmacokinetic parameters demonstrated an increase in area under the plasma concentration–time curve (AUC) for the drug when administered through the nasal route when compared to the administration through the intravenous route. Moreover, PLA MTX-NP enhanced the maximum drug concentration (C_{max}) and AUC 1.5 times as compared to the control MTX solution that was administered by the nasal route [128].

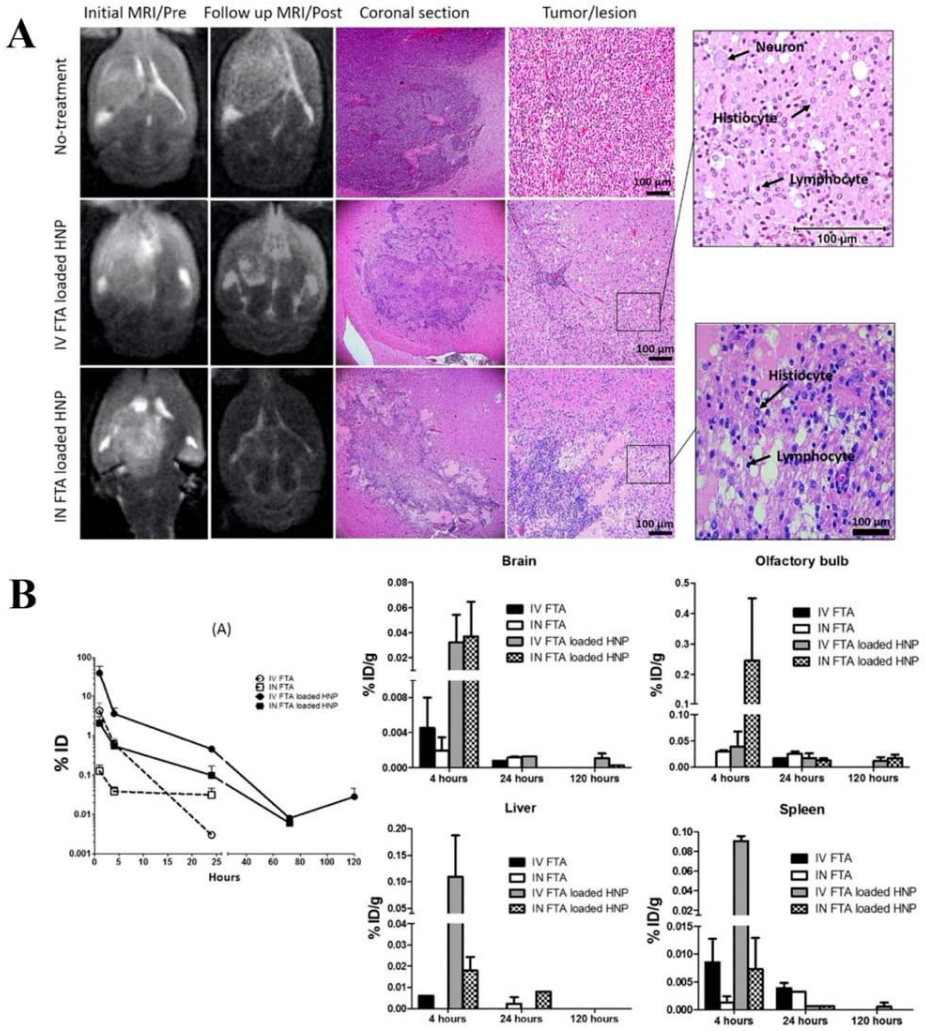

Figure 3. Initial/pre-treatment and follow up/post-treatment MRI images of rat brains from non-treated animals or after treatments with IV or IN farnesylthiosalicylic acid (FTA)-loaded hybrid nanoparticles (HNP) formulations and their corresponding coronal brain sections stained with hematoxylin and eosin (Panel A). In the coronal brain sections, the upper panels show a dense tumor area in the right *striatum* of non-treated rats, whereas the middle and lower panels show cellular re-organization of tumor cells after treatment with IV or IN administered FTA-loaded HNP, respectively. Presence of inflammatory response is shown by the abundant presence of histiocytes and lymphocytes. Biodistribution study of the formulations in healthy rats (Panel B). (**A**) Plasma FTA concentration *versus* time profile for the four treatment formulations. (**B**) Distribution of FTA in brain, olfactory bulb, liverm and spleen of healthy rats after 4, 24, and 120 h post-administration (reproduced with permission from [123]).

5.2. Lipid-Based NP

The encapsulation of drugs into nanocarriers has enhanced the therapeutic potential of a wide variety of molecules in view of the treatment of GBM. Among several bioactive compounds, many researchers have shown interest in the nanoencapsulation of curcumin. In fact, NP are able to overcome a number of limitations that are related to this natural compound, such as low solubility, low oral bioavailability, and low capacity to cross the BBB [147,148].

In this context, Madane and Mahajan developed a nanostructured lipid carrier (NLC) system for curcumin (CC) while using hot high-pressure homogenization [124]. CC showed a biphasic release pattern from NLC formulations, initially showing a burst release of approximately 25%, followed by a sustained release up to 24 h. Moreover, an ex vivo permeability study that was carried out using

Franz diffusion cells showed greater drug permeability across sheep nasal mucosa of CC that were formulated in the NLC system when compared to the free drug suspension. The in vitro cytotoxicity studies using the human astrocytoma-glioblastoma cell line U-373 MG showed IC_{50} values of 9.8 ng/mL for the nanoformulation and 13.6 ng/mL for the positive control (adrenomycin), demonstrating the potential effectiveness of CC-NLCs against glioblastoma. Biodistribution studies in Wistar rats showed a higher drug concentration in the animal brain after intranasal administration of CC-NLCs than free drug suspension (C_{max} was 5.4321 ± 2.098 ng/g with t_{max} 180 min. and 8.6201 ± 8.182 ng/g with t_{max} 120 min. for the free drug and for CC-loaded NLC, respectively) [124].

In another study, Shinde et al. investigated the brain bioavailability and efficacy in vitro of CC-loaded microemulsions (ME) after nasal and intravenous administration in rats [125]. The proposed drug delivery system consisted of microemulsion formulated with CC and docosahexaenoic acid (DHA), which, in addition to improving the CC bioavailability, also has antitumor effects of its own. In fact, the results of in vitro cytotoxicity studies showed a synergistic effect of CC with DHA that was formulated in a ME against the human U-87 MG glioblastoma cell line. Indeed, the IC_{50} value was 3.7 ± 0.2 ng/mL for CC-loaded DHA-ME, 502.7 ± 24.6 ng/mL for CC-ME, while it was 747.8 ± 53.0 ng/mL for a simple CC solution, thus confirming the synergistic anticancer effect of CC and DHA in the ME. It was suggested by the authors that the anticancer activity of DHA could be due to its natural affinity to the neuronal cells and DHA capacity to induce lipid peroxidation. Moreover, the combination of CC with DHA and its subsequent encapsulation in ME increased the distribution to the brain after intravenous and intranasal administration in healthy rats. CC brain concentrations following intranasal administration were strikingly higher when compared to intravenous administration, especially in the case of the MEs. In particular, the brain targeting efficiency (DTE) and direct transport percentage (DTP) that were calculated for the CC-loaded DHA-ME were 1,615% and 97%, respectively [125].

On a similar note, Gadhave and his team worked on ME and mucoadhesive hydrogel (MME) for the intranasal delivery of teriflunomide (TFM) with the aim of increasing the brain delivery of TFM [118]. TFM is a selective and reversible inhibitor of the mitochondrial enzyme dihydroorotate dehydrogenase that is necessary for the de novo synthesis of pyrimidine nucleotides [149]. The FDA approved the TFM in September 2012 for the treatment of adults with multiple sclerosis and it is available as a tablet for oral administration (Aubagio®, Sanofi-Aventis). However, it has been reported that the oral administration of TFM should be performed with caution due to the high risk of severe liver injury [150]. Recent studies have demonstrated the potential of TFM as an antitumor agent in breast cancer [151], prostate cancer [152], and lung cancer [153]. The development and optimization of TFM-MME were performed while using a Box-Behnken design of experiments. The optimized formulations were formulated by using the mixture of mucoadhesive agents HPMC K4M (0.3%) and Poloxamer 407 (17%). In the cytotoxicity assay that was carried out in the human U-87 MG glioblastoma cell line, the authors used carmustine as positive control. After 48 h of treatment, the cell viability was reduced to 38.5% and 37.8% at 160 µg/mL for carmustine and TFM-MME, respectively, which indicated that the cytotoxicity profiles against glioma cells were comparable. The in vivo biodistribution study in Swiss Albino mice was assessed by gamma scintigraphy via ^{99m}Tc labeling of the particles. The TFM-MME formulation showed enhanced brain accumulation (C_{max} 0.62% RA/g) with a DTPof 99.2% and a DTE of 359% when compared with the intravenous administration of TFM-ME. However, the in vitro and in vivo studies did not include the free TFM controls as comparators with the proposed ME. The in vivo safety of TFM-ME and TFM-MME was evaluated in toxicological studies that were carried out while using male Wistar rats receiving daily administrations of the two formulations for 28 days. TFM-MME formulation did not reflect any changes in liver or kidney biomarkers, hematology, and histopathological examination at low and medium doses. The study still needs more robust in vitro and in vivo investigations to demonstrate the efficacy of the TFM-ME and TFM-MME for treatment of GBM, although these formulations were demonstrated to be safe for nasal administration [118].

Colombo and collaborators investigated the brain biodistribution and antitumor efficacy of nanoemulsions containing kaempferol (KPF) that were prepared by high-pressure homogenization

with and without chitosan [121]. KPF is a natural flavonol that is found in several species of edible plants (berries, broccoli, apples, grapes, cabbage, and beans) and medicinal plants (*Ginkgo biloba*, *Rosmarinus officinalis*, *Aloe vera*, *Centella asiatica*, and *Hypericum perforatum*) [154]. This compound has shown antioxidant, anti-inflammatory, and anti-tumor activities [155]. Despite its excellent properties, it is a substance with low aqueous solubility and low oral bioavailability [156]. As a consequence, the FDA does not approve KPF and there are no pharmaceutical formulations that are available in the market containing this natural compound. However, when formulated in a nanoemulsion coated with chitosan, the amount of KPF permeating across pig nasal mucosa in ex vivo diffusion studies while using Franz diffusion cells significantly increased. Furthermore, during in vitro experiments, the formulation that was coated with chitosan reduced C6 glioma cell viability through the induction of apoptosis to a greater extent than either unencapsulated KPF or a chitosan-free nanoemulsion loaded with KPF. The IC_{50} values of the formulation that was coated with chitosan was about 20-fold smaller than free KPF. In vivo studies in Wistar rats indicated a significant increase in brain uptake after intranasal administration in comparison to the control KPF solution. The formulation that was coated with chitosan significantly enhanced the amount of drug reaching the brain. The KPF brain concentration that was detected after nasal administration of chitosan coated KPF-loaded nanoemulsion was, in fact, 5- and 4.5-fold higher than that obtained using the free drug solution and KPF-loaded nanoemulsion without chitosan, respectively. The increased KPF concentration in the brain was not only attributed to the intranasal administration, but also to the mucoadhesive properties and efficient permeation enhancement provided by chitosan [157,158].

Khan and collaborators proposed another approach based on lipid nanostructures [122], who developed nano-lipid chitosan hydrogel formulations for the nose-to-brain delivery of TMZ. The formulations were prepared by high-pressure homogenization while using vitamin E, as the lipid and Gelucire® 44/14, polysorbate 80, and Transcutol® as surfactants. Afterwards, the nano-lipid formulations were dispersed in chitosan (1.0% *w/v*) and converted to a hydrogel. The optimized formulation (size 134 nm, −13.11 mV, EE% 88.45) was able to control the TMZ release (60% release in 24 h) and increase the TMZ permeability of the TMZ by 2.5 times across nasal mucosa. Along with this, the formulation increased the in vitro cytotoxicity of TMZ towards the C6 glioma cell line. In vivo studies in Wistar rats showed an increased DTE of 326% and a DTP of 93% after intranasal administration of chitosan gel formulation containing the TMZ-loaded nano-lipids in comparison to the intranasal administration of nano-lipid formulation as a control (DTE, 113.36% and DTP, 71.74%) [122].

Recently, Azambuja and co-workers developed cationic nanoemulsions (NE) to deliver CD73 small interfering RNA (siRNA CD73) for GBM treatment through the intranasal route [117]. Ecto-5′-nucleotidase (CD73) regulates the extracellular adenosine monophosphate (AMP) and adenosine levels, which have been described as proliferation and drug resistance factors [159,160]. Moreover, CD73 is overexpressed in GBM cells and its inhibition impairs tumor progression [161]. The cationic nanoemulsions were manufactured by microfluidization while using lecithin, medium chain triglycerides, and 1,2-dioleoyl-sn-glycero-3-trimethylammonium propane (DOTAP). The NE-siRNA CD73 were prepared by the adsorption of siRNA to blank formulations (ζ-potential +32 mV) while using different theoretical ratios of cationic lipids to siRNA. In vitro studies using rat C6 glioma cells demonstrated that the NE-siRNA CD73 efficiently decrease cell viability after 48 h of treatment. On the other hand, NE-siRNA scramble that was used as control did not induce any alteration in C6 glioma cell viability. Additionally, cytotoxicity studies showed that the formulation was safe and it did not produce any toxicity in rat primary astrocyte cultures. Interestingly, it was demonstrated that tumor cells took up NE-siRNA CD73, both in vitro and in vivo, which resulted in CD73 knockdown. The in vivo results in glioblastoma-bearing rats demonstrated that NE-siRNA CD73 treatment by intranasal administration significantly decreased the glioma growth by 60% when compared to the control groups (untreated and NE-siRNA scramble). Furthermore, neither NE-siRNA CD73 nor NE-siRNA scramble treatment induced systemic toxicities to glioblastoma-implanted rats [117].

5.3. Polysaccharide NP

Galectin 1 (Gal-1) is a protein that is over-expressed in GBM and is highly associated with tumor progression [162]. The knockdown of Gal-1 using siRNA administration has shown promising results in GBM. Van Woensel and collaborators recently developed chitosan nanoparticles that were loaded with a Gal-1 siRNA for nasal delivery to treat GBM [126]. Gal-1 siRNA loaded chitosan NPs were spontaneously formed by direct complexation due the electric interaction of positively charged chitosan and negatively charged siRNA, which resulted in the successful encapsulation of the siRNA in the nanoparticles and protecting them from ribonucleases (RNases). The NP strongly adhered to the nasal mucosa and the siRNAs were detectable up to 8 h after administration, while the free siRNA only showed weak mucoadhesion. This was attributed to the mucoadhesive properties of chitosan that allowed the nanoparticles to overcome mucociliary clearance and improve the retention time in the nasal cavity [158]. In addition, the encapsulated siRNAs were effectively delivered to the glioma cells from the nasal cavity, since a strong reduction in Gal-1 expression was observed. There was also a reduction in the vascular diameter of the tumor microenvironment in the GL261mice brain tumor model [126].

In a subsequent study, the same group showed that Gal-1 knockdown obtained through nasal administration of chitosan nanoparticles that were loaded with a Gal-1 siRNA displays synergistic effects with TMZ oral treatment and immunotherapy with dendritic cell (DC) vaccination or programmed cell death protein-1 (PD-1) blockade via intraperitoneal administration, suggesting the possibility of combination therapy. The intranasal delivery of Gal-1 siRNA induced a remarkable switch in the tumor micro-environment cellular composition, which reduced macrophage polarization from M1 (pro-inflammatory) to M2 (anti-inflammatory) and inhibited the recruitment of monocytic myeloid derived suppressor cells during GBM progression. Furthermore, the results demonstrated that the median survival increased from 32 days in TMZ treated mice, to 53 days in mice that were orally and nasally treated with TMZ with chitosan nanoparticles loaded with a Gal-1 siRNA. The prophylactic vaccination model showed that the combining DC vaccine with chitosan nanoparticles that were loaded with a Gal-1 siRNA intranasally administered also increased the median survival to 53 days. Similarly, the concomitant intranasal administration of chitosan nanoparticles loaded with a Gal-1 siRNA improved the therapeutic effect of anti-PD-1 antibodies, and increased the median survival to 51.5 days when compared to the control groups (17.5 and 30 days for untreated mice and anti-PD-1 antibodies alone, respectively) [127].

5.4. Targeted NP

The functionalization of the surface of nanocarriers with targeting moieties is one strategy for improving brain tumor accumulation of drug delivery systems. Ephrin type-A receptor 3 (EPHA3) is a membrane-associated receptor that is overexpressed in the stroma and vasculature of gliomas [163]. Chu and co-authors developed PLGA NP functionalized with anti-EPHA3 antibodies for direct nose-to-brain delivery of temozolomide butyl ester (TBE) [120]. Nanoparticles that were loaded with TMZ were prepared by emulsion-solvent evaporation method and subsequently coated with N-trimethylated chitosan (TMC) and their surface functionalized with anti-EPHA3 antibodies. The drug release studies showed a sustained release of TMZ from the nanoparticles by up to 48 h. The results of a cytotoxicity assay on the C6 cells and of nanoparticles cellular uptake demonstrated that anti-EPHA3 functionalization could enhance GBM targeting increasing the cytotoxic effect of the drug. Furthermore, the fluorescence distribution and anti-glioma efficacy in glioma-bearing rats confirmed that the enhanced antitumoral effects were attributed to the nanoparticles surface modification. Anti-EPHA3 functionalized nanoparticles increased the median animal survival by 1.37-folds when compared to the non-targeted nanoparticles. Overall, the author concluded that anti-EPHA3 modified PLGA NP might potentially serve as a nose-to-brain drug carrier for the treatment of GBM [120].

Kanazawa et al. performed a comparative study between methoxy[poly(ethylene glycol)]-*b*-[poly(ε-caprolactone)] (MPEG-PCL) polymer micelles and the trans-activator of transcription (TAT) peptide-modified MPEG-PCL micelles [164]. TAT is a cell-penetrating peptide (CPP) that is derived from human immunodeficiency virus type 1 (HIV-1) containing a protein transduction domain that can induce endocytosis [165]. Polymer micelles were prepared by self-assembly exploiting the amphiphilic properties of the block copolymer. The use of micelles that were modified with TAT and loaded with a model drug, i.e., coumarin, showed an enhancement of direct intranasal brain delivery. Furthermore, the effect of particle size (100, 200, 300, and 600 nm) was investigated on brain distribution after the intranasal administration to glioma C6 cells-bearing rats. The coumarin concentrations in the brain administered with 100 nm micelles were significantly higher than in rat brain that was administered with 600 nm. Interestingly, the drug concentrations in the left side of the brain were higher than those in the right non-inoculated side [164].

Camptothecin (CPT) was encapsulated in TAT-modified micelles and administered by the intranasal route in rats in a later study from the same group. CPT, a quinolone alkaloid, is an inhibitor of the nuclear enzyme DNA-topoisomerase I, which relieves the DNA torsional strain by inducing reversible single-stranded breaks. This naturally occurring alkaloid is extracted from the bark of the Chinese tree, *Camptotheca acuminata* [166]. Even though CPT has shown interesting antitumor activity, its clinical use is limited by extremely low solubility, poor stability, and systemic toxicity. In fact, CPT was discontinued during Phase II trials in 1972 although the initial clinical trials had shown strong antitumor activity. CPT caused severe and unpredictable adverse effects, including myelosuppression, vomiting, diarrhea, and severe hemorrhagic cystic disease [167]. An in vitro cytotoxicity study in rat C6 glioma cells indicated that the CPT-loaded MPEG-PCL-TAT micelles showed higher cytotoxicity than CPT-loaded MPEG-PCL micelles. In vivo, when compared to unmodified micelles, TAT-modified micelles significantly increased the median survival time of rats bearing intracranial glioma tumors. Furthermore, body weight was significantly reduced when compared to untreated rats after seven days of nasal treatment with a simple CPT solution, which indicated severe systemic toxicity. In contrast, CPT-loaded MPEG-PCL or CPT-loaded MPEG-PCL-TAT did not cause significant changes in total body weight, which suggested that micellar formulations were effective in reducing the systemic toxicity of the drug [131].

This approach has also been studied to improve the co-administration of anticancer drugs and siRNA to the brain [132]. MPEG-PCL-TAT micelles were loaded with anti-rat Raf-1 siRNA (siRaf-1) and CPT and then evaluated for their brain uptake efficiency on a C6 glioma model (Figure 4A). When compared to intravenous delivery, intranasal delivered MPEG-PCL-TAT loaded with siRaf-1 significantly enhanced the nucleic acid concentration in rats brain (Figure 4C). As shown in Figure 4B and D, significant inhibition of tumor growth in vitro and in vivo was demonstrated. This was attributed to the combined effects of the CPT and the Raf-1 gene silencing of siRaf-1 in glioma tissues [132].

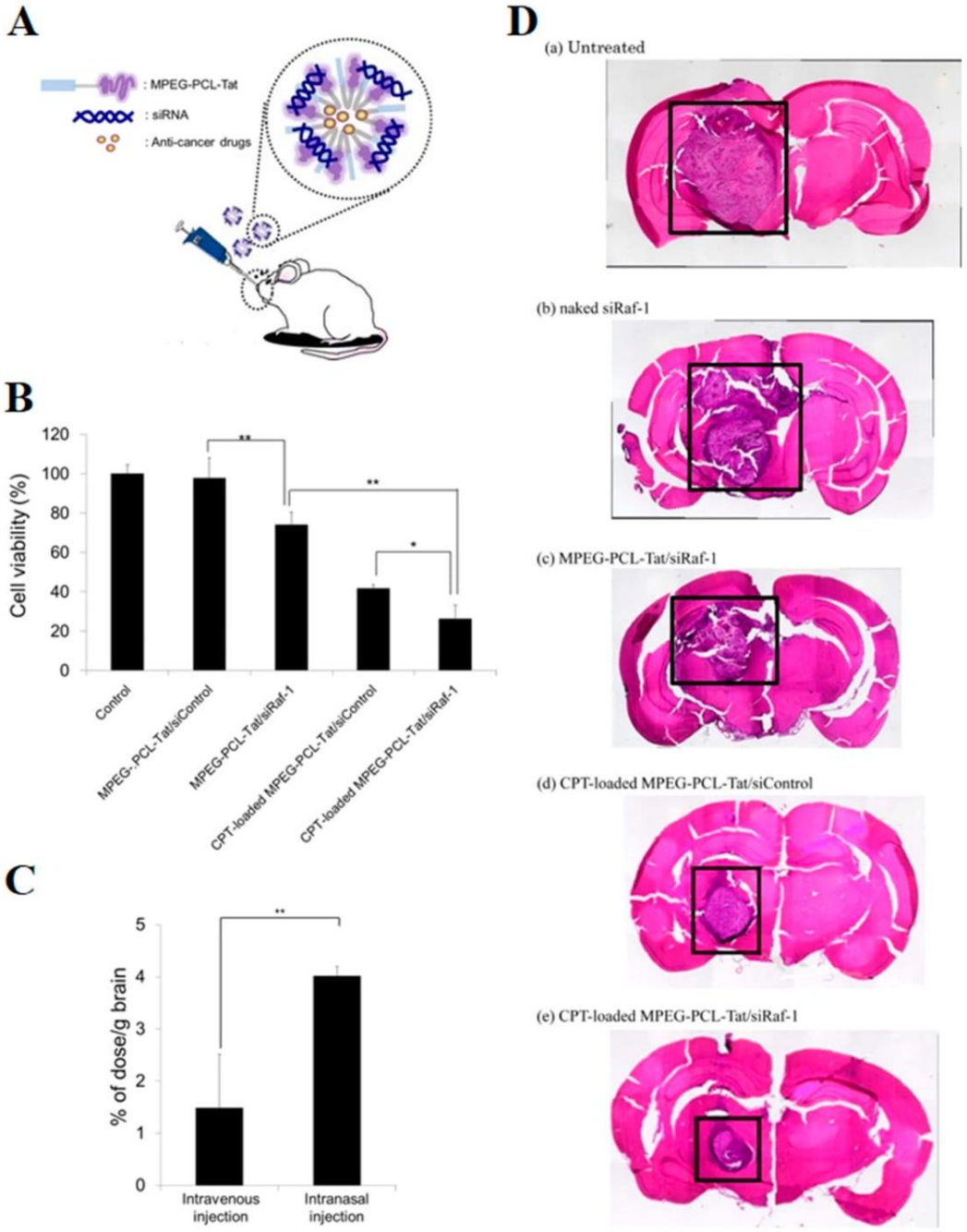

Figure 4. In vitro and in vivo efficacy of cell-penetrating peptide-modified micelles. (**A**) Illustrative model for camptothecin (CPT)-loaded MPEG-PCL-Tat/siRaf-1. (**B**) In vitro cytotoxicity (WST-8 assay) in C6 glioma cells transfected with CPT-loaded MPEG-PCL-Tat/siRaf-1 complexes. (**C**) Distribution of siRNA in brain tissue after intravenous or intranasal administration of MPEG-PCL-Tat/siRNA complex. Rats were killed after the administration of siRNA/MPEG-PCL-Tat complex (20 μg as siRNA), and each brain was enucleated. (**D**) Images of HE-stained brain tissue in intracranial C6 glioma-bearing rats after intranasal administration of siRaf-1 complexed with camptothecin-loaded micelles. After 2 weeks, tissues were taken from untreated rats (**a**) and rats treated with naked siRaf-1 (**b**), MPEG-PCL-Tat/siRaf-1 complex (**c**), CPT-loaded MPEG-PCL-Tat/siControl (**d**), and CPT-loaded MPEG-PCL-Tat/siRaf-1 (**e**) (* $p < 0.05$, ** $p < 0.01$) (adapted with permission from [132]. Copyright 2014 American Chemical Society).

6. Stem Cells for Treatment of GBM

Stem cells have been proposed in recent years for glioma therapy [168–171]. These cells have a tropism for brain tumoral tissue, a minimum tropism for normal neural cells, and the capability to cross the BBB [172–176]. Stem cells can be derived from multipotent stem cells, such as mesenchymal stem cells (MSCs) and neuronal stem cells (NSCs) [176]. MSCs are hematopoietic stem cells and they can be isolated from different tissue sources, making them easier to isolate than NSCs [177,178]. MSCs have the ability to self-renewal, to differentiate in specific functional cellular and immune-compatible nature [176]. MSCs established from adipose tissue [179], human dermis [180], and human umbilical cordon [181] can inhibit tumor cells proliferation through the secretion of a tumor suppressor soluble molecule, the dickkopf-1 (DKK-1). The authors observed an antitumoral effect through the inhibition of glioma cells migration, invasion, proliferation, and survival in a study with normal rat embryonic NSCs. Interestingly, the levels of mutant p53, serine/threonine kinase AKT phosphorylation, and extracellular signal-regulated protein kinases (ERK1/2), all of the pathways related to GBM uncontrolled growth, evasion of apoptosis, and enhanced tumor invasion were decreased [182].

The intranasal route is considered to be an interesting approach to administer stem cells. A study of Reitz and co-workers focused on the nasal delivery of neural stem/progenitor cells (NSPCs) to target brain tumors [183]. Intracerebral human (U87 and NCE-G55T2) and murine (syngenic Gl261) glioma cell-based glioblastoma models were used to evaluate the specific accumulation in mice brain of the NSPCs. The NSPCs intranasal administration was initiated ten days after glioma cells injection. The histological analysis performed five days after the start of the treatment demonstrated the presence of NSPCs in peritumoral and intratumoral areas of brain. The absence of NSPCs in the brains of animals belonging to the control group confirmed the NSPCs tropism for the tumor. The distribution study showed that the cells entered in the brain tumor area 6 h post-administration. The migration initially occurred (within 24 h) via the olfactory pathway, while the cells migrated later via the microvasculature of nasal mucosa [183]. In a different study, it was demonstrated that the nose-to-brain migration of MSCs that were delivered into the nasal cavity occurred via the olfactory and trigeminal pathways [184].

Stem cells have also been proposed as carriers to deliver cytotoxic agents with the intent to exploit their tropism towards brain tumors. Dey and co-workers evaluated the ability of NSCs to carry the oncolytic virus (OV) CRAd-S-pK7 by intranasal administration [185]. CRAd-S-pK7 virus selectively infects tumor cells [186] and the stem cells were able to efficiently deliver OV in various models of glioma [187–189]. In this study, NSCs were genetically modified without changes in their phenotype to improve their tropism towards tumor signaling. In two mice models of malignant glioma (GBM43 and GBM6 intracranial xenografts), the administration of NSCs by intranasal route extended the survival of CRAd-S-pK7 viruses in glioma tissue. This result was attributed to an efficient migration of modified NSCs to the brain tissue and the successful delivery of CRAd-S-pK7 to the tumor site. In addition, the authors were able to verify an extension of animal survival when treated with NSCs carrying the OV in association with radiotherapy (median survival benefit of five days) [185].

In another study, Balyasnikova and co-workers demonstrated that MSCs expressing TNF-related apoptosis-inducing ligand (TRAIL) were able to reach the tumoral tissue and improve the median survival of the irradiated mice with intracranial U87 glioma xenografts in comparison to the non-irradiated and irradiated control mice [190]. TRAIL is an anticancer protein that is expressed and secreted by several stem cells. Additionally, it selectively promotes apoptosis in glioma cells with minimal effects on healthy cells [177]. The authors also verified the rapid MSCs delivery via the nasal cavity, with the detection of MSCs in the animal brains already within 2 h after administration and their subsequent infiltration in the intracranial tumors.

The stem cells approach for GBM treatment has also been combined with nanotechnology. Mangraviti and co-workers developed a system that combined polymeric nanoparticles and human adipose tissue derived MSCs to deliver bone morphogenetic protein 4 (BMP4) and evaluated the antitumor effect in a primary malignant glioma model [130]. Polymeric NP of poly(beta-amino ester)s (PBAE) were determined to be a good option for the transfection of MSCs due to their favorable

physicochemical characteristics: hydrodynamic diameter next to 220 nm, polydispersity index lower than 0.2, and positive zeta potential. Thus, MSCs were transfected with polymeric nanoparticles to express BMP4 and subsequently administered via an intranasal route in rats. The treatment with BMP4 expressing MSCs significantly improved the survival of tumor bearing animals: 60% of treated rats survived up to 16 days after treatment with a 21.4% increase in median survival time over the control group animals [130].

7. Conclusions

GBM is a devastating brain disease with an extremely poor prognosis. Usually, the oral route of administration is considered to be the most convenient for patients. However, for the pharmacological treatment of GBM, it is essential for drugs to reach the brain in their bioactive form. Yet, the therapeutic agent has to overcome several biological barriers when orally administered, such as enzymatic degradation, first-pass metabolism, and BBB. At the moment, TMZ is the chemotherapy agent most used clinically in the treatment of GBM and it is orally administered. In the treatment of GBM, the intranasal route of administration and, more specifically, nose-to brain delivery, potentially presents several advantages over the oral and parenteral route for administering anticancer drugs. In this review, we reported that different therapeutic agents (small organic molecules, biotech compounds, stem cells) are under investigation for GBM treatment exploiting intranasal delivery. In terms of delivery systems, drugs that are entrapped into nanostructured carriers (nanoemulsions, microemulsions, and polymeric and lipid nanoparticles) have been designed and investigated to enhance nose-to-brain delivery. Some of these innovative formulations present surface modified nanocarriers that are able to target receptors and proteins overexpressed in GBM cells facilitating the specific drug delivery to the tumor cells. Nevertheless, most studies are currently only in a pre-clinical phase of development, where promising results remain based on animal models. Overall, the data that were obtained in pre-clinical models suggested a better biodistribution and an improved therapeutic effect of anticancer compounds after intranasal delivery. In addition, long-term clinical studies that were carried in humans with POH demonstrated patient compliance and promising results in selected GBM patients while using this route of delivery. Although there are still a restricted number of studies specifically focused on the intranasal delivery of anticancer compounds to treat GBM, this strategy has the potential to be clinically used for both innovative new drugs and drugs already in use, and may lead to new therapeutic options for GBM patients in the near future.

Funding: Franciele Aline Bruinsmann, Adriana Raffin Pohlmann, Silvia Stanisçuaski Guterres and Fabio Sonvico, would like to acknowledge the Brazilian government as recipients of CNPq grants in the programs "Ciências sem Fronteiras" (BOLSA PESQUISADOR VISITANTE ESPECIAL-PVE 401196/2014-3) and "Produtividade em Pesquisa". Gustavo Richter Vaz would like to acknowledge the Brazilian government as recipients of CAPES—Brazilian Federal Agency for Support and Evaluation of Graduate Education within the Ministry of Education of Brazil in the program "Programa Doutorado-Sanduíche no Exterior" (PDSE-88881.189309/2018-01). This study was financed in part by the Coordenação de Aperfeiçoamento de Pessoal de Nível Superior-Brasil (CAPES)-Finance Code 001, the INCT-NANOFARMA (FAPESP, Brazil) Grant #2014/50928-2, and (CNPq, Brazil) Grant # 465687/2014-8, and the PRONEX FAPERGS/CNPq 12/2014- Grant 16/2551-0000467-6.

Conflicts of Interest: The authors declare no conflict of interest.

References

1. Leece, R.; Xu, J.; Ostrom, Q.T.; Chen, Y.; Kruchko, C.; Barnholtz-Sloan, J.S. Global incidence of malignant brain and other central nervous system tumors by histology, 2003–2007. *Neuro Oncol.* **2017**, *19*, 1553–1564. [CrossRef] [PubMed]
2. Izycka-Swieszewska, E.; Bien, E.; Stefanowicz, J.; Szurowska, E.; Szutowicz-Zielinska, E.; Koczkowska, M.; Sigorski, D.; Kloc, W.; Rogowski, W.; Adamkiewicz-Drozynska, E. Malignant gliomas as second neoplasms in pediatric cancer survivors: Neuropathological study. *BioMed Res. Int.* **2018**, *2018*, 4596812. [CrossRef] [PubMed]

3. Morsy, A.A.; Ng, W.H. Re-do craniotomy for recurrent glioblastoma. *CNS Oncol.* **2015**, *4*, 55–57. [CrossRef] [PubMed]
4. Ohgaki, H.; Kleihues, P. The definition of primary and secondary glioblastoma. *Clin. Cancer Res.* **2013**, *19*, 764–772. [CrossRef] [PubMed]
5. Wilson, T.A.; Karajannis, M.A.; Harter, D.H. Glioblastoma multiforme: State of the art and future therapeutics. *Surg. Neurol. Int.* **2014**, *5*, 64. [PubMed]
6. Ostrom, Q.T.; Gittleman, H.; Truitt, G.; Boscia, A.; Kruchko, C.; Barnholtz-Sloan, J.S. CBTRUS Statistical Report: Primary Brain and Other Central Nervous System Tumors Diagnosed in the United States in 2011–2015. *Neuro Oncol.* **2018**, *20*, iv1–iv86. [CrossRef]
7. Ozdemir-Kaynak, E.; Qutub, A.A.; Yesil-Celiktas, O. Advances in glioblastoma multiforme treatment: New models for nanoparticle therapy. *Front. Physiol.* **2018**, *19*, 170. [CrossRef]
8. Thakkar, J.P.; Dolecek, T.A.; Horbinski, C.; Ostrom, Q.T.; Lightner, D.D.; Barnholtz-Sloan, J.S.; Villano, J.L. Epidemiologic and molecular prognostic review of glioblastoma. *Cancer Epidemiol. Prev. Biomark.* **2014**, *23*, 1985–1996. [CrossRef]
9. Song, W.; Ruder, A.M.; Hu, L.; Li, Y.; Ni, R.; Shao, W.; Kaslow, R.A.; Butler, M.; Tang, J. Genetic epidemiology of glioblastoma multiforme: Confirmatory and new findings from analyses of human leukocyte antigen alleles and motifs. *PLoS ONE* **2009**, *4*, e7157. [CrossRef]
10. Han, S.J.; Englot, D.J.; Birk, H.; Molinaro, A.M.; Chang, S.M.; Clarke, J.L.; Prados, M.D.; Taylor, J.W.; Berger, M.S.; Butowski, N.A. Incidence rates of glioblastoma increase, with rates highest in individuals age 75 to 84 years. *Neurosurgery* **2015**, *62*, 160–165. [CrossRef]
11. Wang, H.; Cai, S.; Ernstberger, A.; Bailey, B.J.; Wang, M.Z.; Cai, W.; Goebel, W.S.; Czader, M.B.; Crean, C.; Suvannasankha, A.; et al. Temozolomide-mediated DNA methylation in human myeloid precursor cells: Differential involvement of intrinsic and extrinsic apoptotic pathways. *Clin. Cancer Res.* **2013**, *19*, 2699–2709. [CrossRef] [PubMed]
12. Xu, W.; Li, T.; Gao, L.; Zheng, J.; Shao, A.; Zhang, J. Efficacy and safety of long-term therapy for high-grade glioma with temozolomide: A meta-analysis. *Oncotarget* **2017**, *8*, 51758–51765. [CrossRef] [PubMed]
13. Tiek, D.M.; Rone, J.D.; Graham, G.T.; Pannkuk, E.L.; Haddad, B.R.; Riggins, R.B. Alterations in cell motility, proliferation, and metabolism in novel models of acquired temozolomide resistant glioblastoma. *Sci. Rep.* **2018**, *8*, 7222. [CrossRef] [PubMed]
14. Syro, L.V.; Rotondo, F.; Camargo, M.; Ortiz, L.D.; Serna, C.A.; Kovacs, K. Temozolomide and pituitary tumors: Current understanding, unresolved issues, and future directions. *Front. Endocrinol.* **2018**, *9*, 318. [CrossRef] [PubMed]
15. Li, Y.M.; Suki, D.; Hess, K.; Sawaya, R. The influence of maximum safe resection of glioblastoma on survival in 1229 patients: Can we do better than gross-total resection? *J. Neurosurg.* **2016**, *124*, 977–988. [CrossRef] [PubMed]
16. Pirzkall, A.; McGue, C.; Saraswathy, S.; Cha, S.; Liu, R.; Vandenberg, S.; Lamborn, K.R.; Berger, M.S.; Chang, S.M.; Nelson, S.J. Tumor regrowth between surgery and initiation of adjuvant therapy in patients with newly diagnosed glioblastoma. *Neuro Oncol.* **2009**, *11*, 842–852. [CrossRef] [PubMed]
17. Davis, M.E. Glioblastoma: Overview of disease and treatment. *Clin. J. Oncol. Nurs.* **2016**, *20*, S2–S8. [CrossRef]
18. Harder, B.G.; Blomquist, M.R.; Wang, J.; Kim, A.J.; Woodworth, G.F.; Winkles, J.A.; Loftus, J.C.; Tran, N.L. Developments in blood-brain barrier penetrance and drug repurposing for improved treatment of glioblastoma. *Front. Oncol.* **2018**, *8*, 462. [CrossRef]
19. Paolillo, M.; Boselli, C.; Schinelli, S. Glioblastoma under siege: An overview of current therapeutic strategies. *Brain Sci.* **2018**, *8*, 15. [CrossRef]
20. Guo, J.; Schlich, M.; Cryan, J.F.; O'Driscoll, C.M. Targeted drug delivery via folate receptors for the treatment of brain cancer: Can the promise deliver? *J. Pharm. Sci.* **2017**, *106*, 3413–3420. [CrossRef]
21. Greene, C.; Campbell, M. Tight junction modulation of the blood brain barrier: CNS delivery of small molecules. *Tissue Barriers* **2016**, *4*, e1138017. [CrossRef] [PubMed]
22. Burgo, L.S.; Hernández, R.M.; Orive, G.; Pedraz, J.L. Nanotherapeutic approaches for brain cancer management. *Nanomedicine* **2014**, *10*, 905–919. [CrossRef] [PubMed]
23. Illum, L. Transport of drugs from the nasal cavity to the central nervous system. *Eur. J. Pharm. Sci.* **2000**, *11*, 1–18. [CrossRef]

24. Mc Carthy, D.J.; Malhotra, M.; O'Mahony, A.M.; Cryan, J.F.; O'Driscoll, C.M. Nanoparticles and the blood-brain barrier: Advancing from in-vitro models towards therapeutic significance. *Pharm. Res.* **2015**, *32*, 1161–1185. [CrossRef]
25. Pajouhesh, H.; Lenz, G.R. Medicinal chemical properties of successful central nervous system drugs. *NeuroRx* **2005**, *2*, 541–553. [CrossRef]
26. Warren, K.E. Beyond the blood:brain barrier: The importance of central nervous system (CNS) pharmacokinetics for the treatment of CNS tumors, including diffuse intrinsic pontine glioma. *Front. Oncol.* **2018**, *8*, 239. [CrossRef]
27. Van Tellingen, O.; Yetkin-Arik, B.; de Gooijer, M.C.; Wesseling, P.; Wurdinger, T.; de Vries, H.E. Overcoming the blood-brain tumor barrier for effective glioblastoma treatment. *Drug Resist Updates* **2015**, *19*, 1–12. [CrossRef]
28. Li, M.; Deng, H.; Peng, H.; Wang, Q. Functional nanoparticles in targeting glioma diagnosis and therapies. *J. Nanosci. Nanotechnol.* **2014**, *14*, 415–432. [CrossRef]
29. Chacko, A.M.; Li, C.; Pryma, D.A.; Brem, S.; Coukos, G.; Muzykantov, V. Targeted delivery of antibody-based therapeutic and imaging agents to CNS tumors: Crossing the blood-brain barrier divide. *Expert Opin. Drug Deliv.* **2013**, *10*, 907–926. [CrossRef]
30. Meng, J.; Agrahari, V.; Youm, I. Advances in targeted drug delivery approaches for the central nervous system tumors: The inspiration of nanobiotechnology. *J. Neuroimmune Pharmacol.* **2017**, *12*, 84–98. [CrossRef]
31. Ganipineni, L.P.; Danhier, F.; Préat, V. Drug delivery challenges and future of chemotherapeutic nanomedicine for glioblastoma treatment. *J. Control. Release* **2018**, *281*, 42–57. [CrossRef] [PubMed]
32. Li, M.; Luo, Z.; Xia, Z.; Shen, X.; Cai, K. Time-sequenced drug delivery approaches towards effective chemotherapeutic treatment of glioma. *Mater. Horiz.* **2017**, *4*, 977. [CrossRef]
33. Lyday, R.W.; Etters, A.M.; Kim, C.; Magana, F.; Pontipiedra, G.M.; Singh, N.K.M.; Kadavakollu, S. PDE5 inhibitors offer novel mechanisms in combination and solo cancer therapy. *Curr. Cancer Ther. Rev.* **2017**, *13*, 107–119. [CrossRef]
34. Liu, Y.; Lu, W. Recent advances in brain tumor-targeted nano-drug delivery systems. *Expert Opin. Drug Deliv.* **2012**, *9*, 671–686. [CrossRef]
35. Larjavaara, S.; Mäntylä, R.; Salminen, T.; Haapasalo, H.; Raitanen, J.; Jääskeläinen, J.; Auvinen, A. Incidence of gliomas by anatomic location. *Neuro Oncol.* **2007**, *9*, 319–325. [CrossRef]
36. Hadziahmetovic, M.; Shirai, K.; Chakravarti, A. Recent advancements in multimodality treatment of gliomas. *Future Oncol.* **2011**, *7*, 1169–1183. [CrossRef]
37. Buckner, J.C.; Shaw, E.G.; Pugh, S.L.; Chakravarti, A.; Gilbert, M.R.; Barger, G.R.; Coons, S.; Ricci, P.; Bullard, D.; Brown, P.D.; et al. Radiation plus procarbazine, CCNU, and vincristine in low-grade glioma. *N. Engl. J. Med.* **2016**, *374*, 1344–1355. [CrossRef]
38. Cairncross, G.; Wang, M.; Shaw, E.; Jenkins, R.; Brachman, D.; Buckner, J.; Fink, K.; Souhami, L.; Laperriere, N.; Curran, W.; et al. Phase III trial of chemoradiotherapy for anaplastic oligodendroglioma: Long-term results of RTOG 9402. *J. Clin. Oncol.* **2013**, *31*, 337–343. [CrossRef]
39. Stupp, R.; Mason, W.P.; Van den Bent, M.J.; Weller, M.; Fisher, B.; Taphoorn, M.J.; Belanger, K.; Brandes, A.A.; Marosi, C.; Bogdahn, U.; et al. Radiotherapy plus concomitant and adjuvant temozolomide for glioblastoma. *N. Engl. J. Med.* **2005**, *352*, 987–996. [CrossRef]
40. Weller, M.; van den Bent, M.; Hopkins, K.; Tonn, J.C.; Stupp, R.; Falini, A.; Cohen-Jonathan-Moyal, E.; Frappaz, D.; Henriksson, R.; Balana, C.; et al. EANO guideline for the diagnosis and treatment of anaplastic gliomas and glioblastoma. *Lancet Oncol.* **2014**, *15*, e395–e403. [CrossRef]
41. Stupp, R.; Brada, M.; van den Bent, M.J.; Tonn, J.C.; Pentheroudakis, G.; ESMO Guidelines Working Group. High-grade glioma: ESMO Clinical Practice Guidelines for diagnosis, treatment and follow-up. *Ann. Oncol.* **2014**, *25* (Suppl. 3), 93–101. [CrossRef] [PubMed]
42. Armstrong, T.S.; Shade, M.Y.; Breton, G.; Gilbert, M.R.; Mahajan, A.; Scheurer, M.E.; Vera, E.; Berger, A.M. Sleep-wake disturbance in patients with brain tumors. *Neuro Oncol.* **2017**, *19*, 323–335. [CrossRef] [PubMed]
43. Taphoorn, M.J.; Heimans, J.J.; van der Veen, E.A.; Karim, A.B. Endocrine functions in long-term survivors of low-grade supratentorial glioma treated with radiation therapy. *J. Neurooncol.* **1995**, *2*, 97–102. [CrossRef] [PubMed]

44. Gregor, A.; Cull, A.; Traynor, E.; Stewart, M.; Lander, F.; Love, S. Neuropsychometric evaluation of long-term survivors of adult brain tumours: Relationship with tumour and treatment parameters. *Radiother. Oncol.* **1996**, *41*, 55–59. [CrossRef]
45. Surma-aho, O.; Niemela, M.; Vilkki, J.; Kouri, M.; Brander, A.; Salonen, O.; Paetau, A.; Kallio, M.; Pyykkönen, J.; Jääskeläinen, J. Adverse long-term effects of brain radiotherapy in adult low-grade glioma patients. *Neurology* **2001**, *56*, 1285–1290. [CrossRef] [PubMed]
46. Hersh, D.S.; Wadajkar, A.S.; Roberts, N.; Perez, J.G.; Connolly, N.P.; Frenkel, V.; Winkles, J.A.; Woodworth, G.F.; Kim, A.J. Evolving Drug Delivery Strategies to Overcome the Blood Brain Barrier. *Curr. Pharm. Des.* **2016**, *22*, 1177–1193. [CrossRef]
47. Grossman, S.A.; Trump, D.L.; Chen, D.C.; Thompson, G.; Camargo, E.E. Cerebrospinal fluid flow abnormalities in patients with neoplastic meningi tis. An evaluation using 111indium-DTPA ventriculography. *Am. J. Med.* **1982**, *73*, 641–647. [CrossRef]
48. Blakeley, J. Drug delivery to brain tumors. *Curr. Neurol. Neurosci. Rep.* **2008**, *8*, 235–241. [CrossRef]
49. Lochhead, J.J.; Thorne, R.G. Intranasal delivery of biologics to the central nervous system. *Adv. Drug Deliv. Rev.* **2012**, *64*, 614–628. [CrossRef]
50. Chapman, C.D.; Frey, W.H.; Craft, S.; Danielyan, L.; Hallschmid, M.; Schioth, H.B.; Benedict, C. Intranasal treatment of central nervous system dysfunction in humans. *Pharm. Res.* **2013**, *30*, 2475–2484. [CrossRef]
51. Chauhan, M.B.; Chauhan, N.B. Brain Uptake of Neurotherapeutics after Intranasal versus Intraperitoneal Delivery in Mice. *J. Neurol. Neurosurg.* **2015**, *2*, 9. [CrossRef]
52. Dhuria, S.V.; Hanson, L.R.; Frey, W.H., II. Intranasal Delivery to the Central Nervous System: Mechanisms and Experimental Considerations. *J. Pharm. Sci.* **2010**, *99*, 1654–1673. [CrossRef] [PubMed]
53. Lledo, P.M.; Gheusi, G.; Vincent, J.D. Information processing in the mammalian olfactory system. *Physiol. Rev.* **2005**, *85*, 281–317. [CrossRef] [PubMed]
54. Dahl, R.; Mygind, N. Anatomy, physiology and function of the nasal cavities in health and disease. *Adv. Drug Deliv. Rev.* **1998**, *29*, 3–12.
55. Geurkink, N. Nasal anatomy, physiology and function. *J. Allergy Clin. Immunol.* **1983**, *72*, 123–128. [CrossRef]
56. Watelet, J.B.; Van Cauwenberge, P. Applied anatomy and physiology of the nose and paranasal sinuses. *Allergy* **1999**, *57*, 14–25. [CrossRef]
57. Jafek, B.W. Ultrastructure of human nasal mucosa. *Laryngoscope* **1983**, *93*, 1576–1599. [CrossRef]
58. Junqueira, L.C.; Carneiro, J. *Biologia Celular e Molecular*, 9th ed.; Guanabara Koogan: Rio de Janeiro, Brazil, 2012; pp. 337–338.
59. Leopold, D.A. The relationship between nasal anatomy and human olfaction. *Laryngoscope* **1988**, *98*, 1232–1238. [CrossRef]
60. Gizurarson, S. Anatomical and histological factors affecting intranasal drug and vaccine delivery. *Curr. Drug Deliv.* **2012**, *9*, 566–582. [CrossRef]
61. Mistry, A.; Stolnik, S.; Illum, L. Nanoparticles for direct nose-to-brain delivery of drugs. *Int. J. Pharm.* **2009**, *379*, 146–157. [CrossRef]
62. Caggiano, M.; Kauer, J.S.; Hunter, D.D. Globose basal cells are neuronal progenitors in the olfactory epithelium: A lineage analysis using a replication-incompetent retrovirus. *Neuron* **1994**, *13*, 339–352. [CrossRef]
63. Arora, P.; Sharma, S.; Garg, S. Permeability issues in nasal drug delivery. *Drug Discov. Today* **2002**, *7*, 967–975. [CrossRef]
64. Pires, A.; Fortuna, A.; Alves, G.; Falcão, A. Intranasal Drug Delivery: How, Why and What for? *J. Pharm. Sci.* **2009**, *12*, 288–311. [CrossRef] [PubMed]
65. Vyas, T.K.; Babbar, A.K.; Sharma, R.K.; Singh, S.; Misra, A. Intranasal mucoadhesive microemulsions of clonazepam: Preliminary studies on brain targeting. *J. Pharm. Sci.* **2006**, *95*, 570–580. [CrossRef] [PubMed]
66. Gomez, D.; Martinez, J.A.; Hanson, L.R.; Frey, W.H., II; Toth, C.C. Intranasal treatment of neurodegenerative diseases and stroke. *Front. Biosci.* **2012**, *4*, 74–89. [CrossRef]
67. Einer-Jensen, N.; Hunter, R. Counter-current transfer in reproductive biology. *Reproduction* **2005**, *129*, 9–18. [CrossRef]
68. Charlton, S.; Jones, N.S.; Davis, S.S.; Illum, L. Distribution and clearance of bioadhesive formulations from the olfactory region in man: Effect of polymer type and nasal delivery device. *Eur. J. Pharm. Sci.* **2007**, *30*, 295–302. [CrossRef]

69. Crowe, T.P.; Greenlee, M.H.W.; Kanthasamy, A.G.; Hsu, W.H. Mechanism of intranasal drug delivery directly to the brain. *Life Sci.* **2018**, *195*, 44–52. [CrossRef]
70. Illum, L. Is nose-to-brain transport of drugs in man a reality? *J. Pharm. Pharmacol.* **2004**, *56*, 3–17. [CrossRef]
71. Conner, S.D.; Schmid, S.L. Regulated portals of entry into the cell. *Nature* **2003**, *422*, 37–44. [CrossRef]
72. Jansson, B.; Björk, E. Visualization of In Vivo Olfactory Uptake and Transfer Using Fluorescein Dextran. *J. Drug Target.* **2002**, *10*, 379–386. [CrossRef] [PubMed]
73. Schaefer, M.L.; Böttger, B.; Silver, W.L.; Finger, T.E. Trigeminal collaterals in the nasal epithelium and olfactory bulb: A potential route for direct modulation of olfactory information by trigeminal stimuli. *J. Comp. Neurol.* **2002**, *444*, 221–226. [CrossRef] [PubMed]
74. Lochhead, J.J.; Wolak, D.J.; Pizzo, M.E.; Thorne, R.G. Rapid transport within cerebral perivascular spaces underlies widespread tracer distribution in the brain after intranasal administration. *J. Cereb. Blood Flow Metab.* **2015**, *35*, 371–381. [CrossRef] [PubMed]
75. Groothuis, D.R.; Vavra, M.W.; Schlageter, K.E.; Kang, E.W.; Itskovich, A.C.; Hertzler, S.; Allen, C.V.; Lipton, H.L. Efflux of drugs and solutes from brain: The interactive roles of diffusional transcapillary transport, bulk flow and capillary transportes. *J. Cereb. Blood Flow Metab.* **2007**, *27*, 43–56. [CrossRef] [PubMed]
76. Grevers, G.; Herrmann, U. Fenestrated endothelia in vessels of the nasal mucosa. An electron-microscopic study in the rabbit. *Arch. Otorhinolaryngol.* **1987**, *244*, 55–60. [CrossRef] [PubMed]
77. Lee, V.H. Enzymatic barriers to peptide and protein absorption. *Crit. Rev. Ther. Drug Carr. Syst.* **1988**, *5*, 69–97. [CrossRef]
78. Quintana, D.S.; Westlye, L.T.; Rustan, Ø.G.; Tesli, N.; Poppy, C.L.; Smevik, H.; Tesli, M.; Røine, M.; Mahmoud, R.A.; Smerud, K.T.; et al. Low-dose oxytocin delivered intranasally with Breath Powered device affects social-cognitive behavior: A randomized four-way crossover trial with nasal cavity dimension assessment. *Transl. Psychiatry* **2015**, *5*, e602. [CrossRef]
79. Wang, X.; Deng, J.; Yuan, J.; Tang, X.; Wang, Y.; Chen, H.; Liu, Y.; Zhou, L. Curcumin exerts its tumor suppressive function via inhibition of NEDD4 oncoprotein in glioma cancer cells. *Int. J. Oncol.* **2017**, *51*, 467–477. [CrossRef]
80. Nasr, M. Development of an optimized hyaluronic acid-based lipidic nanoemulsion co-encapsulating two polyphenols for nose to brain delivery. *Drug Deliv.* **2016**, *23*, 1444–1452. [CrossRef]
81. Mukherjee, S.; Baidoo, J.; Fried, A.; Atwi, D.; Dolai, S.; Boockvar, J.; Symons, M.; Ruggieri, R.; Raja, K.; Banerjee, P. Curcumin changes the polarity of tumor-associated microglia and eliminates glioblastoma. *Int. J. Cancer* **2016**, *139*, 2838–2849. [CrossRef]
82. Zhou, Y.X.; Xia, W.; Yue, W.; Peng, C.; Rahman, K.; Zhang, H. Rhein: A Review of Pharmacological Activities. *Evid. Based Complement. Altern. Med.* **2015**, *2015*, 578107. [CrossRef] [PubMed]
83. Sun, H.; Luo, G.; Chen, D.; Xiang, Z.A. Comprehensive and System Review for the Pharmacological Mechanism of Action of Rhein, an Active Anthraquinone Ingredient. *Front. Pharmacol.* **2016**, *7*, 247. [CrossRef] [PubMed]
84. Cong, X.D.; Ding, M.J.; Dai, D.Z.; Wu, Y.; Zhang, Y.; Dai, Y. ER stress, P66shc, and P-Akt/Akt mediate adjuvant-induced inflammation, which is blunted by argirein, a supermolecule and rhein in rats. *Inflammation* **2012**, *35*, 1031–1040. [CrossRef] [PubMed]
85. Blacher, E.; Baruch, B.B.; Levy, A.; Geva, N.; Green, K.D.; Garneau-Tsodikova, S.; Fridman, M.; Stein, R. Inhibition of glioma progression by a newly discovered CD38 inhibitor. *Int. J. Cancer* **2015**, *136*, 1422–1433. [CrossRef] [PubMed]
86. Shingaki, T.; Hidalgo, I.J.; Furubayashi, T.; Katsumi, H.; Sakane, T.; Yamamoto, A.; Yamashita, S. The transnasal delivery of 5-fluorouracil to the rat brain is enhanced by acetazolamide (the inhibitor of the secretion of cerebrospinal fluid). *Int. J. Pharm.* **2009**, *377*, 85–91. [CrossRef]
87. Van Kuilenburg, A.B.P. Dihydropyrimidine dehydrogenase and the efficacy and toxicity of 5-fluorouracil. *Eur. J. Cancer* **2004**, *40*, 939–950. [CrossRef]
88. Diasio, R.B.; Harris, B.E. Clinical pharmacology of 5-fluorouracil. *Clin. Pharmacokinet.* **1989**, *16*, 215–237. [CrossRef]
89. Silva, P. *Farmacologia*, 8th ed.; Guanabara Koogan: Rio de Janeiro, Brazil, 2010; pp. 1064–1071.
90. Longley, D.B.; Harkin, D.P.; Johnston, P.G. 5-Flurouracil: Mechanisms of action and clinical strategies. *Nat. Rev. Cancer* **2003**, *3*, 330–338. [CrossRef]

91. Uldall, M.; Botfield, H.; Jansen-Olesen, I.; Sinclair, A.; Jensen, R. Acetazolamide lowers intracranial pressure and modulates the cerebrospinal fluid secretion pathway in healthy rats. *Neurosci. Lett.* **2017**, *645*, 33–39. [CrossRef]
92. Shingaki, T.; Inoue, D.; Furubayashi, T.; Sakane, T.; Katsumi, H.; Yamamoto, A.; Yamashita, S. Transnasal Delivery of Methotrexate to Brain Tumors in Rats: A New Strategy for Brain Tumor Chemotherapy. *Mol. Pharm.* **2010**, *7*, 1561–1568. [CrossRef]
93. Hagner, N.; Joerger, M. Cancer chemotherapy: Targeting folic acid synthesis. *Cancer Manag. Res.* **2010**, *2*, 293–301. [PubMed]
94. Abolmaali, S.S.; Tamaddon, A.M.; Dinarvand, R. A review of therapeutic challenges and achievements of methotrexate delivery systems for treatment of cancer and rheumatoid arthritis. *Cancer Chemother. Pharmacol.* **2013**, *71*, 1115–1130. [CrossRef] [PubMed]
95. Sun, Y.; Shi, K.; Wan, F.; Cui, F. Methotrexate-loaded microspheres for nose to brain delivery: In vitro/in vivo evaluation. *J. Drug Deliv. Sci. Technol.* **2012**, *22*, 167–174. [CrossRef]
96. Li, Y.; Gao, Y.; Liu, G.; Zhou, X.; Wang, Y.; Wang, Y.; Ma, L. Intranasal administration of temozolomide for brain-targeting delivery: Therapeutic effect on glioma in rats. *Nan Fang Yi Ke Da Xue Xue Bao* **2014**, *34*, 631–635.
97. Baker, S.D.; Wirth, M.; Statkevich, P. Absorption, metabolism and excretion of 14C-temozolomide following oral administration to patients with advanced cancer. *Clin. Cancer Res.* **1999**, *5*, 309–317.
98. Mrugala, M.M.; Chamberlain, M.C. Mechanisms of Disease: Temozolomide and glioblastoma-look to the future. *Nat. Clin. Pract. Oncol.* **2008**, *5*, 476–486. [CrossRef]
99. Pineda, J.R.; Jeitany, M.; Andrieux, A.; Junier, M.P.; Chneiweiss, H.; Boussin, F.D. Intranasal Administration of Temozolomide Delayed the Development of Brain Tumors Initiated by Human Glioma Stem-Like Cell in Nude Mice. *Cancer Sci. Ther.* **2017**, *9*, 374–378.
100. Chen, T.C.; Fonseca, C.O.; Schönthal, A.H. Preclinical development and clinical use of perillyl alcohol for chemoprevention and cancer therapy. *Am. J. Cancer Res.* **2015**, *5*, 1580–1593.
101. da Fonseca, C.O.; Khandelia, H.; Salazar, M.D.A.; Schönthal, A.H.; Meireles, O.C.; Quirico-Santos, T. Perillyl alcohol: Dynamic interactions with the lipid bilayer and implications for long-term inhalational chemotherapy for gliomas. *Surg. Neurol. Int.* **2016**, *7*, 1–11. [CrossRef]
102. Chen, T.C.; da Fonseca, C.O.; Schönthal, A.H. Intranasal Perillyl Alcohol for Glioma Therapy: Molecular Mechanisms and Clinical Development. *Int. J. Mol. Sci.* **2018**, *19*, 3905. [CrossRef]
103. ClinicalTrials.gov. Available online: https://clinicaltrials.gov/ct2/show/NCT02704858 (accessed on 22 September 2019).
104. da Fonseca, C.O.; Simão, M.; Lins, I.R.; Caetano, R.O.; Futuro, D.; Quirico-Santos, T. Efficacy of monoterpene perillyl alcohol upon survival rate of patients with recurrent glioblastoma. *J. Cancer. Res. Clin. Oncol.* **2011**, *137*, 287–293. [CrossRef] [PubMed]
105. da Fonseca, C.O.; Teixeira, R.M.; Silva, J.C.; De Saldanha, D.A.; Gama Fischer, J.; Meirelles, O.C.; Landeiro, J.A.; Quirico-Santos, T. Long-term outcome in patients with recurrent malignant glioma treated with Perillyl alcohol inhalation. *Anticancer Res.* **2013**, *33*, 5625–5631. [PubMed]
106. da Fonseca, C.O.; Schwartsmann, G.; Fischer, J.; Nagel, J.; Futuro, D.; Quirico-Santos, T.; Gattass, C.R. Preliminary results from a phase I/II study of perillyl alcohol intranasal administration in adults with recurrent malignant gliomas. *Surg. Neurol.* **2008**, *70*, 259–266. [CrossRef] [PubMed]
107. Santos, J.G.; Da Cruz, W.M.S.; Schönthal, A.H.; Salazar, M.D.; Fontes, C.A.P.; Quirico-Santos, T.; Da Fonseca, C.O. Efficacy of a ketogenic diet with concomitant intranasal perillyl alcohol as a novel strategy for the therapy of recurrent glioblastoma. *Oncol. Lett.* **2018**, *15*, 1263–1270. [CrossRef]
108. Bernardi, A.; Braganhol, E.; Jäger, E.; Figueiró, F.; Edelweiss, M.I.; Pohlmann, A.R.; Guterres, S.S.; Battastini, A.M. Indomethacin-loaded nanocapsules treatment reduces in vivo glioblastoma growth in a rat glioma model. *Cancer Lett.* **2009**, *281*, 53–63. [CrossRef]
109. Saludas, L.; Pascual-Gil, S.; Roli, F.; Garbayo, E.; Blanco-Prieto, M.J. Heart tissue repair and cardioprotection using drug delivery systems. *Maturitas* **2018**, *110*, 1–9. [CrossRef]
110. Pohlmann, A.R.; Fonseca, F.N.; Paese, K.; Detoni, C.B.; Coradini, K.; Beck, R.C.; Guterres, S.S. Poly(e-caprolactone) microcapsules and nanocapsules in drug delivery. *Expert Opin. Drug Deliv.* **2013**, *10*, 623–638. [CrossRef]

111. Frank, L.A.; Contri, R.V.; Beck, R.C.; Pohlmann, A.R.; Guterres, S.S. Improving drug biological effects by encapsulation into polymeric nanocapsules. *Wiley Interdiscip. Rev. Nanomed. Nanobiotechnol.* **2015**, *7*, 623–639. [CrossRef]
112. Comfort, C.; Garrastazu, G.; Pozzoli, M.; Sonvico, F. Opportunities and challenges for the nasal administration of nanoemulsions. *Curr. Top. Med. Chem.* **2015**, *15*, 356–368. [CrossRef]
113. Graff, C.L.; Pollack, G.M. Functional evidence for P-glycoprotein at the nose-brain barrier. *Pharm. Res.* **2005**, *22*, 86–93. [CrossRef]
114. Pires, P.C.; Santos, A.O. Nanosystems in nose-to-brain drug delivery: A review of non-clinical brain targeting studies. *J. Control. Release* **2018**, *270*, 89–100. [CrossRef] [PubMed]
115. Sonvico, F.; Clementino, A.; Buttini, F.; Colombo, G.; Pescina, S.; Guterres, S.S.; Pohlmann, A.R.; Nicoli, S. Surface-Modified Nanocarriers for Nose-to-Brain Delivery: From Bioadhesion to Targeting. *Pharmaceutics* **2018**, *10*, 34. [CrossRef] [PubMed]
116. Sousa, F.; Dhaliwal, H.K.; Gattacceca, F.; Sarmento, B.; Amiji, M.M. Enhanced anti-angiogenic effects of bevacizumab in glioblastoma treatment upon intranasal administration in polymeric nanoparticles. *J. Control. Release* **2019**, *309*, 37–47. [CrossRef] [PubMed]
117. Azambuja, J.; Schuh, R.S.; Michels, L.R.; Gelsleichter, N.E.; Beckenkamp, L.R.; Iser, I.C.; Lenz, G.S.; de Oliveira, F.H.; Venturin, G.; Greggio, S.; et al. Nasal Administration of Cationic Nanoemulsions as CD73-siRNA Delivery System for Glioblastoma Treatment: A New Therapeutical Approach. *Mol. Neurobiol.* **2019**, *56*, 1–15. [CrossRef]
118. Gadhavea, D.; Gorain, B.; Tagalpallewar, A.; Kokare, C. Intranasal teriflunomide microemulsion: An improved chemotherapeutic approach in glioblastoma. *J. Drug Deliv. Sci. Technol.* **2019**, *51*, 276–289. [CrossRef]
119. de Oliveira Junior, E.R.; Nascimento, T.L.; Salomão, M.A.; da Silva, A.C.G.; Valadares, M.C.; Lima, E.M. Increased Nose-to-Brain Delivery of Melatonin Mediated by Polycaprolactone Nanoparticles for the Treatment of Glioblastoma. *Pharm. Res.* **2019**, *36*, 131. [CrossRef]
120. Chu, L.; Aiping, W.; Ni, L.; Yan, X.; Song, Y.; Zhao, M.; Sun, K.; Mu, H.; Liu, S.; Wu, Z.; et al. Nose-to-brain delivery of temozolomide-loaded PLGA nanoparticles functionalized with anti-EPHA3 for glioblastoma targeting. *Drug Deliv.* **2018**, *25*, 1634–1641. [CrossRef]
121. Colombo, M.; Figueiró, F.; de Fraga Dias, A.; Teixeira, H.F.; Battastini, A.M.O.; Koester, L.S. Kaempferol-loaded mucoadhesive nanoemulsion for intranasal administration reduces glioma growth in vitro. *Int. J. Pharm.* **2018**, *543*, 214–223. [CrossRef]
122. Khan, A.; Aqil, M.; Imam, S.S.; Ahad, A.; Sultana, Y.; Ali, A.; Khan, K. Temozolomide loaded nano lipid based chitosan hydrogel for nose to brain delivery: Characterization, nasal absorption, histopathology and cell line study. *Int. J. Biol. Macromol.* **2018**, *116*, 1260–1267. [CrossRef]
123. Sekerdag, E.; Lüle, S.; Bozdağ Pehlivan, S.; Öztürk, N.; Kara, A.; Kaffashi, A.; Vural, I.; Işıkay, I.; Yavuz, B.; Oguz, K.K.; et al. A potential non-invasive glioblastoma treatment: Nose-to-brain delivery of farnesylthiosalicylic acid incorporated hybrid nanoparticles. *J. Control. Release* **2017**, *261*, 187–198. [CrossRef]
124. Shinde, R.L.; Devarajan, P.V. Docosahexaenoic acid-mediated, targeted and sustained brain delivery of curcumin microemulsion. *Drug Deliv.* **2017**, *24*, 152–161. [CrossRef] [PubMed]
125. Madane, R.G.; Mahajan, H.S. Curcumin-loaded nanostructured lipid carriers (NLCs) for nasal administration: Design, characterization, and in vivo study. *Drug Deliv.* **2016**, *23*, 1326–1334. [PubMed]
126. Van Woensel, M.; Wauthoz, N.; Rosière, R.; Mathieu, V.; Kiss, R.; Lefranc, F.; Steelant, B.; Dilissen, E.; Van Gool, S.W.; Mathivet, T.; et al. Development of siRNA-loaded chitosan nanoparticles targeting Galectin-1 for the treatment of glioblastoma multiforme via intranasal administration. *J. Control. Release* **2016**, *227*, 71–81. [CrossRef] [PubMed]
127. Van Woensel, M.; Mathivet, T.; Wauthoz, N.; Rosière, R.; Garg, A.D.; Agostinis, P.; Mathieu, V.; Kiss, R.; Lefranc, F.; Boon, L.; et al. Sensitization of glioblastoma tumor micro-environment to chemo- and immunotherapy by Galectin-1 intranasal knock-down strategy. *Sci. Rep.* **2017**, *7*, 1217. [CrossRef]
128. Jain, D.S.; Bajaj, A.N.; Athawale, R.B.; Shikhande, S.S.; Pandey, A.; Goel, P.N.; Gude, R.P.; Patil, S.; Raut, P. Thermosensitive PLA based nanodispersion for targeting brain tumor via intranasal route. *Mater. Sci. Eng. C Mater. Biol. Appl.* **2016**, *63*, 411–421. [CrossRef]
129. Alex, A.T.; Joseph, A.; Shavi, G.; Rao, J.V.; Udupa, N. Development and evaluation of carboplatin-loaded PCL nanoparticles for intranasal delivery. *Drug Deliv.* **2016**, *23*, 2144–2153. [CrossRef]

130. Mangraviti, A.; Tzeng, S.Y.; Gullotti, D.; Kozielski, K.L.; Kim, J.E.; Seng, M.; Abbadi, S.; Schiapparelli, P.; Sarabia-Estrada, R.; Vescovi, A.; et al. Non-virally engineered human adipose mesenchymal stem cells produce BMP4, target brain tumors, and extend survival. *Biomaterials* **2016**, *100*, 53–66. [CrossRef]
131. Taki, H.; Kanazawa, T.; Akiyama, F.; Takashima, Y.; Okada, H. Intranasal Delivery of Camptothecin-Loaded Tat-Modified Nanomicells for Treatment of Intracranial Brain Tumors. *Pharmaceuticals* **2012**, *5*, 1092–1102. [CrossRef]
132. Kanazawa, T.; Morisaki, K.; Suzuki, S.; Takashima, Y. Prolongation of life in rats with malignant glioma by intranasal siRNA/drug codelivery to the brain with cell-penetrating peptide-modified micelles. *Mol. Pharm.* **2014**, *11*, 1471–1478. [CrossRef]
133. Zawilska, J.; Skene, D.; Arendt, J. Physiology and pharmacology of melatonin in relation to biological rhythms. *Pharmacol. Rep.* **2009**, *61*, 383–410. [CrossRef]
134. Kostoglou-Athanassiou, I. Therapeutic applications of melatonin. *Ther. Adv. Endocrinol. Metab.* **2013**, *4*, 13–24. [CrossRef] [PubMed]
135. Menéndez-Menéndez, J.; Martínez-Campa, C. Melatonin: An Anti-Tumor Agent in Hormone-Dependent Cancers. *Int. J. Endocrinol.* **2018**, *2018*, 3271948. [CrossRef] [PubMed]
136. Yadav, S.K.; Srivastava, A.K.; Dev, A.; Kaundal, B.; Choudhury, S.R.; Karmakar, S. Nanomelatonin triggers superior anticancer functionality in a human malignant glioblastoma cell line. *Nanotechnology* **2017**, *28*, 365102. [CrossRef] [PubMed]
137. Hamelers, I.H.; Van Loenen, E.; Staffhorst, R.W.; De Kruijff, B.; de Kroon, A.I. Carboplatin nanocapsules: A highly cytotoxic, phospholipid-based formulation of carboplatin. *Mol. Cancer Ther.* **2006**, *5*, 2007–2012. [CrossRef] [PubMed]
138. Huang, W.J.; Chen, W.W.; Zhang, X. Glioblastoma multiforme: Effect of hypoxia and hypoxia inducible factors on therapeutic approaches. *Oncol. Lett.* **2016**, *12*, 2283–2288. [CrossRef] [PubMed]
139. Wick, W.; Weller, M.; Van den Bent, M.; Stupp, R. Bevacizumab and recurrent malignant gliomas: A European perspective. *J. Clin. Oncol.* **2010**, *28*, e188–e189. [CrossRef]
140. Chinot, O.L.; Wick, W.; Mason, W.; Henriksson, R.; Saran, F.; Nishikawa, R.; Carpentier, A.F.; Hoang-Xuan, K.; Kavan, P.; Cernea, D.; et al. Bevacizumab plus radiotherapy-temozolomide for newly diagnosed glioblastoma. *N. Engl. J. Med.* **2014**, *370*, 709–722. [CrossRef]
141. Gilbert, M.R.; Dignam, J.J.; Armstrong, T.S.; Wefel, J.S.; Blumenthal, D.T.; Vogelbaum, M.A.; Colman, H.; Chakravarti, A.; Pugh, S.; Won, M.; et al. A randomized trial of bevacizumab for newly diagnosed glioblastoma. *N. Engl. J. Med.* **2014**, *370*, 699–708. [CrossRef]
142. Sousa, F.; Cruz, A.; Fonte, P.; Pinto, I.M.; Neves-Petersen, M.T.; Sarmento, B. A new paradigm for Antiangiogenic therapy through controlled release of bevacizumab from PLGA nanoparticles. *Sci. Rep.* **2017**, *7*, 3736. [CrossRef]
143. Rotblat, B.; Ehrlich, M.; Haklai, R.; Kloog, Y. The Ras inhibitor farnesylthiosalicylic acid (Salirasib) disrupts the spatiotemporal localization of active Ras: A potential treatment for cancer. *Methods Enzymol.* **2008**, *439*, 467–489.
144. Goldberg, L.; Haklai, R.; Bauer, V.; Heiss, A.; Kloog, Y. New derivatives of farnesylthiosalicylic acid (salirasib) for cancer treatment: Farnesylthiosalicylamide inhibits tumor growth in nude mice models. *J. Med. Chem.* **2009**, *52*, 197–205. [CrossRef] [PubMed]
145. Ugwoke, M.I.; Verbeke, N.; Kinget, R. The biopharmaceutical aspects of nasal mucoadhesive drug delivery. *J. Pharm. Pharmacol.* **2001**, *53*, 3–21. [CrossRef] [PubMed]
146. Kaur, P.; Garg, T.; Rath, G.; Goyal, A.K. In situ nasal gel drug delivery: A novel approach for brain targeting through the mucosal membrane. *Artif. Cells Nanomed. Biotechnol.* **2016**, *44*, 1167–1176. [CrossRef] [PubMed]
147. Liu, W.; Zhai, Y.; Heng, X.; Che, F.Y.; Chen, W.; Sun, D.; Zhai, G. Oral bioavailability of curcumin: Problems and advancements. *J. Drug Target.* **2016**, *24*, 694–702. [CrossRef] [PubMed]
148. Agrawal, M.; Saraf, S.; Saraf, S.; Antimisiaris, S.G.; Chougule, M.B.; Shoyele, S.A.; Alexander, A. Nose-to-brain drug delivery: An update on clinical challenges and progress towards approval of anti-Alzheimer drugs. *J. Control. Release* **2018**, *281*, 139–177. [CrossRef] [PubMed]
149. Bar-Or, A.; Pachner, A.; Menguy-Vacheron, F.; Kaplan, J.; Wiendl, H. Teriflunomide and its mechanism of action in multiple sclerosis. *Drugs* **2014**, *74*, 659–674. [CrossRef]
150. Xuan, J.; Ren, Z.; Qing, T.; Couch, L.; Shi, L.; Tolleson, W.H.; Guo, L. Mitochondrial dysfunction induced by leflunomide and its active metabolite. *Toxicology* **2018**, *396–397*, 33–45. [CrossRef]

151. Huang, O.; Zhang, W.; Zhi, Q.; Xue, X.; Liu, H.; Shen, D.; Geng, M.; Xie, Z.; Jiang, M. Teriflunomide, an immunomodulatory drug, exerts anticancer activity in triple negative breast cancer cells. *Exp. Biol. Med.* **2015**, *240*, 426–437. [CrossRef]
152. Hail, N., Jr.; Chen, P.; Bushman, L.R. Teriflunomide (Leflunomide) Promotes Cytostatic, Antioxidant, and Apoptotic Effects in Transformed Prostate Epithelial Cells: Evidence Supporting a Role for Teriflunomide in Prostate Cancer Chemoprevention. *Neoplasia* **2010**, *12*, 464–475. [CrossRef]
153. Jiang, L.; Zhang, W.; Li, W.; Ling, C.; Jiang, M. Anti-inflammatory drug, leflunomide and its metabolite teriflunomide inhibit NSCLC proliferation in vivo and in vitro. *Toxicol. Lett.* **2018**, *282*, 154–165. [CrossRef]
154. Calderón-Montaño, J.M.; Burgos-Morón, E.; Pérez-Guerrero, C.; López-Lázaro, M. A review on the dietary flavonoid kaempferol. *Mini Rev. Med. Chem.* **2011**, *11*, 298–340. [CrossRef] [PubMed]
155. Rajendran, P.; Rengarajan, T.; Nandakumar, N.; Palaniswami, R.; Nishigaki, Y.; Nishigaki, I. Kaempferol, a potential cytostatic and cure for inflammatory disorders. *Eur. J. Med. Chem.* **2014**, *86*, 103–112. [CrossRef] [PubMed]
156. Chen, Z.P.; Sun, J.; Chen, H.X.; Xiao, Y.Y.; Liu, D.; Chen, J.; Cai, H.; Cai, B.C. Comparative pharmacokinetics and bioavailability studies of quercetin, kaempferol and isorhamnetin after oral administration of Ginkgo biloba extracts, Ginkgo biloba extract phospholipid complexes and Ginkgo biloba extract solid dispersions in rats. *Fitoterapia* **2010**, *81*, 1045–1052. [CrossRef] [PubMed]
157. Vllasaliu, D.; Exposito-Harris, R.; Heras, A.; Casettari, L.; Garnett, M.; Illum, L.; Stolnik, S. Tight junction modulation by chitosan nanoparticles: Comparison with chitosan solution. *Int. J. Pharm.* **2010**, *400*, 183–193. [CrossRef]
158. Casettari, L.; Illum, L. Chitosan in nasal delivery systems for therapeutic drugs. *J. Control. Release* **2014**, *190*, 189–200. [CrossRef] [PubMed]
159. Ujházy, P.; Berleth, E.S.; Pietkiewicz, J.M.; Kitano, H.; Skaar, J.R.; Ehrke, M.J.; Mihich, E. Evidence for the involvement of ecto-5′-nucleotidase (CD73) in drug resistance. *Int. J. Cancer* **1996**, *68*, 493–500. [CrossRef]
160. Bavaresco, L.; Bernardi, A.; Braganhol, E.; Cappellari, A.R.; Rockenbach, L.; Farias, P.F.; Wink, M.R.; Cañedo, A.D.; Battastini, A.M.O. The role of ecto-5′-nucleotidase in glioma cell line proliferation. *Mol. Cell Biochem.* **2008**, *319*, 61–68. [CrossRef]
161. Wink, M.R.; Lenz, G.; Braganhol, E.; Tamajusuku, A.S.; Schwartsmann, G.; Sarkis, J.J.; Battastini, A.M. Altered extracellular ATP, ADP and AMP catabolism in glioma cell lines. *Cancer Lett.* **2003**, *198*, 211–218. [CrossRef]
162. Toussaint, L.G., 3rd; Nilson, A.E.; Goble, J.M.; Ballman, K.V.; James, C.D.; Lefranc, F.; Kiss, R.; Uhm, J.H. Galectin-1, a gene preferentially expressed at the tumor margin, promotes glioblastoma cell invasion. *Mol. Cancer* **2012**, *11*, 32. [CrossRef]
163. Janes, P.W.; Slape, C.I.; Farnsworth, R.H.; Atapattu, L.; Scott, A.M.; Vail, M.E. EphA3 biology and cancer. *Growth Factors* **2014**, *32*, 176–189. [CrossRef]
164. Kanazawa, T.; Taki, H.; Tanaka, K.; Takashima, Y.; Okada, H. Cell-Penetrating Peptide-Modified Block Copolymer Micelles Promote Direct Brain Delivery via Intranasal Administration. *Pharm. Res.* **2011**, *28*, 2130–2139. [CrossRef]
165. Pescina, S.; Ostacolo, C.; Gomez-Monterrey, I.M.; Sala, M.; Bertamino, A.; Sonvico, F.; Padula, C.; Santi, P.; Bianchera, A.; Nicoli, S. Cell penetrating peptides in ocular delivery: State of the art. *J. Control. Release* **2018**, *284*, 84–102. [CrossRef]
166. Li, F.; Jiang, T.; Li, Q.; Ling, X. Camptothecin (CPT) and its derivatives are known to target topoisomerase I (Top1) as their mechanism of action: Did we miss something in CPT analogue molecular targets for treating human disease such as cancer? *Am. J. Cancer Res.* **2017**, *7*, 2350–2394. [PubMed]
167. Martino, E.; Della Volpe, S.; Terribile, E.; Benetti, E.; Sakaj, M.; Centamore, A.; Sala, A.; Collina, S. The long story of camptothecin: From traditional medicine to drugs. *Bioorgan. Med. Chem. Lett.* **2017**, *27*, 701–707. [CrossRef] [PubMed]
168. Lee, D.H.; Ahn, Y.; Kim, S.U.; Wang, K.C.; Cho, B.K.; Phi, J.H.; Park, I.H.; Black, P.M.; Carroll, R.S.; Lee, J.; et al. Targeting rat brainstem glioma using human neural stem cells and human mesenchymal stem cells. *Clin. Cancer Res.* **2009**, *15*, 4925–4934. [CrossRef]
169. Nakamizo, A.; Marini, F.; Amano, T.; Khan, A.; Studeny, M.; Gumin, J.; Chen, J.; Hentschel, S.; Vecil, G.; Dembinski, J.; et al. Human bone marrow-derived mesenchymal stem cells in the treatment of gliomas. *Cancer Res.* **2005**, *65*, 3307–3318. [CrossRef]

170. Barish, M.E.; Herrmann, K.; Tang, Y.; Herculian, S.A.; Metz, M.; Aramburo, S.; Tirughana, R.; Gutova, M.; Annala, A.; Moats, R.A.; et al. Human neural stem cell biodistribution and predicted tumor coverage by a diffusible therapeutic in a mouse glioma model. *Stem Cells Transl. Med.* **2017**, *6*, 1522–1532. [CrossRef]
171. Gutova, M.; Flores, L.; Adhikarla, V.; Tsaturyan, L.; Tirughana, R.; Aramburo, S.; Metz, M.; Gonzaga, J.; Annala, A.; Synold, T.W.; et al. Quantitative evaluation of intraventricular delivery of therapeutic neural stem cells to orthotopic glioma. *Front. Oncol.* **2019**, *9*, 68. [CrossRef]
172. Klopp, A.H.; Spaeth, E.L.; Dembinski, J.L.; Woodward, W.A.; Munshi, A.; Meyn, R.E.; Cox, J.D.; Andreeff, M.; Marini, F.C. Tumor irradiation increases the recruitment of circulating mesenchymal stem cells into the tumor microenvironment. *Cancer Res.* **2007**, *67*, 11687–11695. [CrossRef]
173. Karp, J.M.; Leng Teo, G.S. Mesenchymal stem cell homing: The devil is in the details. *Cell Stem Cell.* **2009**, *4*, 206–216. [CrossRef]
174. Aboody, K.S.; Najbauer, J.; Metz, M.Z.; D'Apuzzo, M.; Gutova, M.; Annala, A.J.; Synold, T.W.; Couture, L.A.; Blanchard, S.; Moats, R.A.; et al. Neural stem cell-mediated enzyme/prodrug therapy for glioma: Preclinical studies. *Sci. Transl. Med.* **2013**, *5*, 184ra59. [CrossRef] [PubMed]
175. Cao, M.; Mao, J.; Duan, X.; Lu, L.; Zhang, F.; Lin, B.; Chen, M.; Zheng, C.; Zhang, X.; Shen, J. In vivo tracking of the tropism of mesenchymal stem cells to malignant gliomas using reporter gene-based MR imaging. *Int. J. Cancer* **2018**, *142*, 1033–1046. [CrossRef] [PubMed]
176. Li, M.; Sun, S.; Dangelmajer, S.; Zhang, Q.; Wang, J.; Hu, F.; Dong, F.; Kahlert, U.D.; Zhu, M.; Lei, T. Exploiting tumor-intrinsic signals to induce mesenchymal stem cell-mediated suicide gene therapy to fight malignant glioma. *Stem Cell Res. Ther.* **2019**, *10*, 88. [CrossRef] [PubMed]
177. Young, J.S.; Morshed, R.A.; Kim, J.W.; Balyasnikova, I.V.; Ahmed, A.U.; Lesniak, M.S. Advances in stem cells, induced pluripotent stem cells, and engineered cells: Delivery vehicles for anti-glioma therapy. *Expert Opin. Drug Deliv.* **2014**, *11*, 1733–1746. [CrossRef]
178. Bexell, D.; Svensson, A.; Bengzon, J. Stem cell-based therapy for malignant glioma. *Cancer Treat. Rev.* **2013**, *39*, 358–365. [CrossRef]
179. Zhu, Y.; Sun, Z.; Han, Q.; Liao, L.; Wang, J.; Bian, C.; Li, J.; Yan, X.; Liu, Y.; Shao, C.; et al. Human mesenchymal stem cells inhibit cancer cell proliferation by secreting DKK1. *Leukemia* **2009**, *23*, 925–933. [CrossRef]
180. Qiao, L.; Xu, Z.L.; Zhao, T.J.; Ye, L.H.; Zhang, X.D. DKK1 secreted by mesenchymal stem cells inhibits growth of breast cancer cells via depression of Wnt signaling. *Cancer Lett.* **2008**, *269*, 67–77. [CrossRef]
181. Ma, S.; Liang, S.; Jiao, H.; Chi, L.; Shi, X.; Tian, Y.; Yang, B.; Guan, F. Human umbilical cord mesenchymal stem cells inhibit C6 glioma growth via secretion of dickkopf-1 (DKK1). *Mol. Cell Biochem.* **2014**, *385*, 277–286. [CrossRef]
182. An, J.; Yan, H.; Li, X.; Tan, R.; Chen, X.; Zhang, Z.; Liu, Y.; Zhang, P.; Lu, H.; Liu, Y. The inhibiting effect of neural stem cells on proliferation and invasion of glioma cells. *Oncotarget* **2017**, *8*, 76949–76960. [CrossRef]
183. Reitz, M.; Demestre, M.; Sedlacik, J.; Meissner, H.; Fiehler, J.; Kim, S.U.; Westphal, M.; Schmidt, N.O. Intranasal delivery of neural stem/progenitor cells: A noninvasive passage to target intracerebral glioma. *Stem Cells Transl. Med.* **2012**, *1*, 866–873. [CrossRef]
184. Danielyan, L.; Schäfer, R.; von Ameln-Mayerhofer, A.; Buadze, M.; Geisler, J.; Klopfer, T.; Klopfer, T.; Burkhardt, U.; Proksch, B.; Verleysdonk, S.; et al. Intranasal delivery of cells to the brain. *Eur. J. Cell Biol.* **2009**, *88*, 315–324. [CrossRef] [PubMed]
185. Dey, M.; Yu, D.; Kanojia, D.; Li, G.; Sukhanova, M.; Spencer, D.A.; Pituch, K.C.; Zhang, L.; Han, Y.; Ahmed, A.U.; et al. Intranasal oncolytic virotherapy with CXCR4-enhanced stem cells extends survival in mouse model of glioma. *Stem Cell Rep.* **2016**, *7*, 471–482. [CrossRef] [PubMed]
186. Ulasov, I.V.; Zhu, Z.B.; Tyler, M.A.; Han, Y.; Rivera, A.A.; Khramtsov, A.; Curiel, D.T.; Lesniak, M.S. Survivin-driven and fiber-modified oncolytic adenovirus exhibits potent antitumor activity in established intracranial glioma. *Hum. Gene Ther.* **2007**, *18*, 589–602. [CrossRef] [PubMed]
187. Ahmed, A.U.; Tyler, M.A.; Thaci, B.; Alexiades, N.G.; Han, Y.; Ulasov, I.V.; Lesniak, M.S. A comparative study of neural and mesenchymal stem cell-based carriers for oncolytic adenovirus in a model of malignant glioma. *Mol. Pharm.* **2011**, *8*, 1559–1572. [CrossRef]
188. Ahmed, A.U.; Thaci, B.; Tobias, A.L.; Auffinger, B.; Zhang, L.; Cheng, Y.; Kim, C.K.; Yunis, C.; Han, Y.; Alexiades, N.G.; et al. A preclinical evaluation of neural stem cell-based cell carrier for targeted antiglioma oncolytic virotherapy. *J. Natl. Cancer Inst.* **2013**, *105*, 968–977. [CrossRef]

189. Morshed, R.A.; Gutova, M.; Juliano, J.; Barish, M.E.; Hawkins-Daarud, A.; Oganesyan, D.; Vazgen, K.; Yang, T.; Annala, A.; Ahmed, A.U.; et al. Analysis of glioblastoma tumor coverage by oncolytic virus-loaded neural stem cells using MRI based tracking and histological reconstruction. *Cancer Gene Ther.* **2015**, *22*, 55–61. [CrossRef]
190. Balyasnikova, I.V.; Prasol, M.S.; Ferguson, S.D.; Han, Y.; Ahmed, A.U.; Gutova, M.; Tobias, A.L.; Mustafi, D.; Rincón, E.; Zhang, L.; et al. Intranasal delivery of mesenchymal stem cells significantly extends survival of irradiated mice with experimental brain tumors. *Mol. Ther.* **2014**, *22*, 140–148. [CrossRef]

Capítulo 2

Chitosan-Coated Nanoparticles: Effect of Chitosan Molecular Weight on Nasal Transmucosal Delivery

Artigo publicado em 15/02/2019 na revista Pharmaceutics (JCR IF2017=3.746)

Article

Chitosan-coated nanoparticles: effect of chitosan molecular weight on nasal transmucosal delivery

Franciele Aline Bruinsmann [1,2], Stefania Pigana [2], Tanira Aguirre [3], Gabriele Dadalt Souto [1], Gabriela Garrastazu Pereira [1], Annalisa Bianchera [2], Laura Tiozzo Fasiolo [2,4], Gaia Colombo [4], Magno Marques [5], Adriana Raffin Pohlmann [1,6], Silvia Stanisçuaski Guterres [1], and Fabio Sonvico[2,*]

[1] Programa de Pós-Graduação em Ciências Farmacêuticas, Universidade Federal do Rio Grande do Sul, Porto Alegre 90610-000, Brazil; fbruinsmann@gmail.com (F.A.B.); gabrieledadalt@gmail.com (G.D.S.); garrastazugp@gmail.com (G.G.P.); silvia.guterres@ufrgs.br (S.S.G.); adriana.pohlmann@ufrgs.br (A.R.P.);

[2] Food and Drug Department, University of Parma, Parco Area delle Scienze 27/a, 43124 Parma, Italy; stefania.pigana@studenti.unipr.it (S.P.); annalisa.bianchera@unipr.it (A.B.)

[3] Programa de Pós-Graduação em Biociências, Universidade Federal de Ciências da Saúde de Porto Alegre, Porto Alegre, RS 900500-170, Brazil; tanira@ufcspa.edu.br

[4] Department of Life Sciences and Biotechnology, University of Ferrara, Via Fossato di Mortara 17/19, 44121 Ferrara, Italy; laura.tiozzofasiolo@studenti.unipr.it (L.T.F.); clmgai@unife.it (G.C.)

[5] Programa de Pós-Graduação em Ciências Fisiológicas, Universidade Federal do Rio Grande, Rio Grande, RS 96203-000, Brazil; magnomarques@aol.com

[6] Departamento de Química Orgânica, Instituto de Química, Universidade Federal do Rio Grande do Sul, Porto Alegre 91501-970, Brazil

* Correspondence: fabio.sonvico@unipr.it; Tel.: +39-0521-906-282

Abstract: Drug delivery to the brain represents a challenge especially in the therapy of central nervous system malignancies. Simvastatin (SVT), as other statins, has shown potential anticancer properties that are difficult to exploit in the CNS. In the present work the physico-chemical, mucoadhesive and permeability enhancing properties of simvastatin-loaded poly-ε-caprolactone nanocapsules coated with chitosan for nose-to-brain administration were investigated. Lipid-core nanocapsules coated with different molecular weight (MW) chitosans (LNC_{chit}) prepared by a novel one-pot technique were characterized for particle size, surface charge, particle number density, morphology, drug encapsulation efficiency, interaction between surface nanocapsules with mucin, drug release and permeability across two nasal mucosa models. Results show that all formulations present adequate particle size (below 220 nm), positive surface charge, narrow droplet size distribution (PDI<0.2) and high encapsulation efficiency. Nanocapsules presented controlled drug release and mucoadhesive properties dependent on the MW of the coating chitosan. The results of permeation across RPMI 2650 human nasal cell line evidenced that LNC_{chit} increased the permeation of SVT. In particular, the amount of SVT permeated after 4 h for nanocapsules coated with low MW chitosan, high MW chitosan and control SVT was 13.9 ± 0.8 μg, 9.2 ± 1.2 μg and 1.4 ± 0.2 μg respectively. These results were confirmed by the SVT *ex vivo* permeation across rabbit nasal mucosa. This study highlighted the suitability of LNC_{chit} as promising strategy for the administration of simvastatin for a nose-to-brain approach for the therapy of brain tumors.

Keywords: nasal permeability; nose-to-brain; simvastatin; nanocapsules; mucoadhesion; CNS disorders; chitosan

1. Introduction

Statins are potent inhibitors of the hydroxymethyl glutaryl coenzyme A (HMG-CoA) reductase, commonly administered for the treatment of cardiovascular disease [1]. However, in recent years, it has been suggested that the statin therapeutic indications might expand due to their pleiotropic effects [2].

These non-cholesterol related effects include their modulation of immune responses, the enhancement of endothelial function, the reduction oxidative stress and the check of inflammation processes [3,4]. The majority of pleiotropic effects are mediated by preventing the synthesis of isoprenoids and subsequent inhibition of small signaling proteins [5,6]. Among the diseases that could benefit from statins pleiotropic effects are multiple sclerosis, rheumatoid arthritis, systemic lupus erythematosus, chronic obstructive pulmonary disease, neurodegenerative disorders, bacterial infections and cancer [3].

In the field of cancer therapy, statins showed pro-apoptotic effects against various tumor cell lines [7,8] and numerous studies have examined their potential chemopreventive action [9]. Due to the inhibition of the enzyme HMG-CoA reductase, statins decrease the levels of mevalonate, the precursor of dolichol, geranylpyrophosphate (GPP) and farnesyl-pyrophosphate (FPP). Dolichol enhances DNA synthesis and is associated to several proteins found in tumor cells [10]. GPP and FPP are post-translational modifications of intracellular proteins as G-proteins Ras and Rho that regulate the signal transduction of several membrane receptors and are critical for the transcription of genes involved in cell proliferation, differentiation, and apoptosis. Ras and Rho gene mutations are found in a variety of tumor cells [11,7]. Furthermore, statins show apoptotic effect in human glioblastoma cell lines inducing depletion of geranylgeranylated proteins, important for the transition to the cell cycle phases [12]. Statins have also shown to play a role in the prevention of tumor metastases by inhibition of epithelial growth factor–induced tumor cell invasion [13]. Moreover, statins, inducing the inactivation of nuclear factor kB, reduce urokinase and matrix metalloproteinase-9 expression, pivotal for tumor metastatic process [7,14].

In the case of glioma cell lines, simvastatin (SVT) showed suppression of cell proliferation and induction of apoptosis [15,16]. However, when evaluated in an *in vivo* orthotopic model of glioblastoma multiforme model, simvastatin did not show tumor inhibitory effects [17]. As in this experiment, the major factor for failure of chemotherapies against central nervous system (CNS) tumors has been attributed to limited brain-blood barrier (BBB) permeability [18]. In addition, after oral administration statins are extensively metabolized in the liver and their hydrophilic metabolites are prevented from crossing the BBB [19].

Some new strategies have been proposed to deal with such limitations in order to increase distribution of drugs in the CNS, like the use of nose-to-brain route [20,21] and the development of nanocarriers [22, 23, 24]. In recent years, the nose-to-brain delivery has attracted much attention as a mean to deliver drugs more efficiently to the CNS bypassing the BBB. This is because the nasal cavity is anatomically connected to the CNS via the olfactory system [25]. Moreover, it offers advantages such, non-invasiveness, avoidance of hepatic first-pass metabolism, practicality and convenience of administration [26]. However, due to the presence of rapid mucociliary clearance mechanism, nasal delivery application for brain delivery is hindered by the short residence time of conventional formulations. Moreover, the barrier of the nasal epithelium, nasal metabolism and the limited volume of administration are limiting aspects for the development of nose-to-brain drug delivery systems [25,27].

To increase bioavailability after nasal delivery, polymeric nanocapsules have been investigated [28, 29, 30]. These nanocarriers are considered a type of reservoir drug delivery system [31] and can be obtained by interfacial deposition of pre-formed polymers [32]. Their structure is characterized by an oil core surrounded by a polymeric shell stabilized by a surfactant system [31,33]. The lipid-core nanocapsules (LNCs), developed by our research group, are composed by a dispersion of sorbitan monostearate (solid lipid) and medium chain triacylglycerol (liquid lipid) in the core, surrounded by poly(ε-caprolactone), an aliphatic polyester as polymeric wall and polysorbate 80 as stabilizing surfactant [34]. The lipid core dispersion, i.e. sorbitan monostearate dispersed in oil, confers different properties to this system as controlled the drug release and increased the encapsulation efficiency when compared to the core of the conventional nanocapsules containing only liquid lipids [34, 35, 36]. These nanocarriers showed efficient brain delivery of drugs as resveratrol [37] and curcumin [38] when administered orally and intraperitoneally, as well as reduction of side effects of the antipsychotic drug

olanzapine [39]. Furthermore, they demonstrated improved *in vitro* and *in vivo* antitumor effectiveness of resveratrol, methotrexate and acetyleugenol when compared to the free drugs [40, 41, 42].

Bender and co-authors [43], developed a two-step process to obtain modified LNC stabilized simultaneously with polysorbate 80 and lecithin and coated with chitosan. Chitosan is a cationic biopolymer obtained by the partial deacetylation of chitin under alkaline conditions [44]. Chitosan demonstrated several interesting properties for pharmaceutical application, such as biodegradability, biocompatibility, antibacterial activity and controlled release of drugs [45, 46]. Furthermore, chitosan showed mucoadhesive and penetration enhancing properties, particularly desirable for its application in drug nasal delivery [47, 48]. These actions are mediated by structural reorganization of the tight junctions of the nasal epithelium, increasing paracellular transport of drugs [49].

In the present study, LNC stabilized with lecithin and coated with chitosan were obtained by an innovated one-pot technique. Moreover, the pharmaceutical properties of formulations with chitosan of different molecular weight (MW) intended for nose-to-brain delivery of simvastatin were evaluated.

2. Materials and Methods

2.1 Materials

Poly (ε-caprolactone) (PCL) (MW=14,000) and Span 60® (sorbitan monostearate) were purchased from Sigma-Aldrich (Strasbourg, France). Caprylic/capric triglyceride was obtained from Delaware (Porto Alegre, Brazil) and simvastatin (SVT) was purchased from Pharma Nostra (Rio de Janeiro, Brazil). Chitosan low MW (21 kDa - viscosity 9 cP) and high MW (152 kDa - viscosity 114 cP) was provided by Primex (Chitoclear FG, deacetylation degree 95%, Siglufjordur, Iceland). Soybean lecithin (Lipoid S75) was kindly donated by Lipoid AG (Ludwigshafen, Germany). Minimum essential medium (MEM), fetal bovine serum (FBS), phosphate-buffered saline (PBS) and Hank's Balanced Salt Solution (HBSS) were supplied by Gibco (Carlsbad, CA, USA). Transwell® cell culture inserts (1.12 cm^2 surface area, polyester, 0.4 μm pore size) were supplied by Corning Costar (Lowell, MA, USA). All other chemicals and solvents used were of analytical or pharmaceutical grade.

2.2 Preparation of the Lipid-core Nanocapsules Coated using a One-pot Technique

Chitosan-coated simvastatin-loaded lipid-core nanocapsules were prepared according to the interfacial deposition of pre-formed polymer method already reported in literature [35]. An organic phase (25 mL of acetone) containing the polymer (PCL, 0.04 g), sorbitan monostearate (0.016 g) and caprylic/capric triglyceride (0.048 mL) was kept under magnetic stirring at 40°C. After complete dissolution of the components, an ethanolic solution (4 mL) containing lecithin (0.025 g) was added into organic phase and finally, simvastatin (0.010 g) was added and completely dissolved. The aqueous phase (50 mL) contained of 0.1% w/v of chitosan, prepared as a dilution from a 0.5% w/v of chitosan solution in 1% (v/v) acetic acid. The organic phase was injected using a funnel into the aqueous phase under moderate magnetic stirring. The solvents were eliminated at 40°C until the final volume of 10 mL, was obtained by the use of a rotary evaporator Büchi® R-114 (Flawill, Switzerland). The formulations obtained were named $LNC_{SVT\text{-}LMWchit}$ when chitosan low MW (viscosity 9 cP) was used and $LNC_{SVT\text{-}HMWchit}$ when chitosan high MW (viscosity 114cP) was used in alternative. Blank nanocapsules ($LNC_{LMWchit}$ and $LNC_{HMWchit}$) were also prepared, omitting the simvastatin from the organic phase preparation.

2.3 Drug Content and Encapsulation Efficiency

The SVT quantification was carried out by high performance liquid chromatography with detection in the ultraviolet (HPLC-UV), using a previously validated method [30]. The analysis was performed with a Shimadzu HPLC system (Kyoto, Japan) with detection at 238 nm and using a column Phenomenex Lichrosphere® C18 (4.6.x250 mm, 5 μm). The composition of the mobile phase was 65% of

acetonitrile and 35% sodium dihydrogen phosphate buffer (25 mM, pH 4.5), flow rate was 1.0 mL·min^{-1} and injection volume of 100 µL. Calibration curves (n = 3) were prepared to determine linearity (R > 0.99) in the concentration range from 0.1 to 20 µg·mL^{-1}. The drug content in the formulations was determined by diluting a precise volume of nanoparticles suspension (100 µL) in 10 mL of the mobile phase. The samples were then sonicated for 30 min and filtered through a 0.45 µm pore size membrane (Millipore®, Billerica, USA) before being assayed by HPLC-UV. Free simvastatin was determined in the ultrafiltrate after ultrafiltration–centrifugation (Ultrafree-MC, cut-off of 30 kDa, Millipore) at 2688×g (Scilogex D3024, Rocky Hill, CT, USA) for 15 min and quantified by HPLC-UV. Encapsulation efficiency (EE) as percentage was calculated by the difference between the total and free, *i.e.* non-encapsulated, drug amount divided by the total drug amount multiplied by 100. All analyses were performed for triplicate batches (n = 3).

2.4 Physicochemical Characterization

The nanoparticle formulations were characterized with multiple techniques as described below. All analyses, with the exception of the TEM (n = 1), were performed for triplicate batches (n = 3).

2.4.1 Laser Diffraction

The particle size and the size distribution were determined by laser diffraction (Mastersizer® 2000, Malvern Instruments, UK) aiming to spot the eventual presence of micrometric particles or aggregates. The sample was directly added to water in the wet dispersion accessory (Hydro 2000SM - AWM2002, Malvern Instruments, UK) until an obscuration level of 2% was reached. The particle size was then expressed using the volume-weighted mean diameter (D[4,3]), and the diameters calculated at 10, 50 and 90 percentiles [$d_{0.1}$, $d_{0.5}$ and $d_{0.9}$, respectively] of the cumulative size distribution curve by volume (v) and by number (n) of particles. The width of the distribution (Span) was determined according to Eq. 1.

$$Span = \frac{d_{0.9} - d_{0.1}}{d_{0.5}}, \quad (1)$$

2.4.2 Dynamic Light Scattering

The mean particle size (Z-average diameter) and polydispersity index (PDI) of nanocapsules were evaluated by dynamic light scattering (DLS) at 25 °C using a Zetasizer® Nano ZS (Malvern Instruments, UK). After dilution of samples (500×) in purified and filtered (0.45 µm) water, the correlogram was obtained by allowing the instrument software to determine the optimal time of acquisition and the z-average diameter and PDI were calculated by the method of Cumulants with the same software.

2.4.3 *Nanoparticle Tracking Analysis*

The nanoparticles tracking analysis (NTA) method was used to determine the mean diameter and the concentration of nanocapsules per volume, expressed as particle number density (PND) (NanoSight LM10, Malvern Pananalytical, UK). The analysis was carried out diluting the samples in ultrapure water (1000×) and introducing it into the instrument sample chamber cell by a syringe. The chamber is located on an optical microscope that using a laser diode (635 nm) illuminate the particles in suspension. The NTA 3.2 software tracks single particles, which are in Brownian motion, and can relate this particle movement with a sphere equivalent hydrodynamic radius as calculated using the Stokes–Einstein equation (Eq. 2). The samples were evaluated at room temperature for 60 seconds with automatic detection. The results correspond to the arithmetic average of the calculated sizes of all particles analyzed.

$$\overline{(x, y)^2} = \frac{4\,Tk_B}{3\pi\eta d_h}, \quad (2)$$

Where $\boldsymbol{k_B}$ is the Boltzmann constant and $\overline{(\mathbf{x}, \mathbf{y})^2}$ is the mean-squared displacement of a particle during time t at temperature T, in a medium of viscosity η, with a hydrodynamic diameter of $\boldsymbol{d_h}$.

2.4.4 pH and Zeta Potential

The pH values of nanocapsules suspensions were determined using a calibrated potentiometer (DM-22 Digimed, São Paulo, Brazil) via direct measurements of the formulations at 25ºC. The zeta potential values were determined by electrophoretic mobility after the samples were diluted in 10 mM NaCl aqueous solution (500×) previously filtered (0.45 μm, Millipore®, Billerica, USA). The zeta potential of nanoparticles suspensions was also measured at different pH values using the MPT-2 autotitrator for the Zetasizer® Nano ZS (Malvern Instruments, Malvern, UK). The samples (10 mL) were placed in the titration cell and titrated over acidic (0.1 M HCl) towards basic (0.05 M NaOH) pH range at 1.0 pH unit intervals. This combination allowed automated titration over a wide pH range and thus made it possible to determine the isoelectric point (IEP) of nanoparticles.

2.4.5 Morphology

Transmission electron microscopy (TEM) was used to evaluate the morphology of the formulations. TEM samples were diluted in ultrapure water (10×, v/v) and then deposited (10 μL) on specimen grids (Formvar-Carbon support film, Electron Microscopy Sciences, Hatfield, PA, USA) and negatively stained with uranyl acetate solution (2% w/v, Sigma-Aldrich, St.Louis, MO, USA). Analyses were performed using a transmission electron microscope (JEM 2200-FS, Jeol, Tokyo, Japan) operating at 80 kV. The images were processed with Digital Micrograph (Gatan Inc., Pleasanton, CA, USA) software.

2.5 In Vitro Evaluation of the Interaction between Nanocapsules and Mucin

The mucoadhesive properties of the formulations were assessed using mucin from porcine stomach (Type II, Sigma-Aldrich, St. Louis, MO, USA) as previously described [29,50]. The mucin was dispersed in ultrapure water (0.5% w/v) and employing magnetic stirring for 3 h at room temperature. The suspension was centrifuged at 4000×g for 30 min. The supernatant was collected and lyophilized. Then mucin solutions were prepared in simulated nasal electrolytic solution (SNES) [51] at predetermined weight ratios f, determined as:

$$f = \frac{W_{mucin}}{W_{mucin} + WNC}, \quad (3)$$

where W_{mucin} is the mucin mass and WNC is the LNC_{chit} nanocapsules mass.

The Z-average diameter and PDI before and after contact with mucin were measured by DLS as described above after dilution (500×) of the samples in mucin solutions. The mucoadhesive index values (MI) were determined as:

$$MI = \frac{d}{d_0}, \quad (4)$$

Where d and d_0 are the diameter of the LNC_{chit} nanocapsules after and before interaction with mucin, respectively.

Furthermore, changes in the zeta potential were measured after the nanocapsules were diluted (500×) in mucin solutions containing 10 mM NaCl.

2.6 In Vitro Release Study

The *in vitro* release profiles of SVT from formulations were determined using the dialysis bag method. Briefly, 1 mL of each sample was placed in a dialysis bag (14 kDa molecular weight cut-off, Sigma-Aldrich, St. Louis, MO, USA) and suspended into 100 mL of SNES containing 0.5% of polysorbate 80 to improve SVT solubility and to reach the sink conditions. A free drug solution was placed in the dialysis bag in control experiments ($SVT_{solution}$, simvastatin dissolved in 1% ethanol and 0.5% polysorbate 80). The dialysis bags were maintained in the medium under stirring and thermostated in a water bath (37 °C). One milliliter of release medium was collected at predetermined time intervals (from 0.16 to 8h) and filtered (0.45 μm, Millipore®, Billerica, USA). The volume was replaced by adding one milliliter of fresh release medium pre-heated at 37 °C. The samples were analyzed by HPLC-UV, and the cumulative drug release was determined.

2.7 Transport Studies across an in vitro Nasal Epithelial Cell Model

RPMI 2650 human nasal cells (human nasal septum tumor, ECACC, Salisbury, UK) were cultured in MEM media supplemented with 10% (v/v) fetal bovine serum (FBS). Cells were grown at 37°C in an atmosphere of 95% air/5% CO_2. Transwell® cell culture inserts were used to establish an air-liquid interface (ALI) nasal model, as previously reported [52]. Briefly, 200 uL of the cells suspensions ($2.5 \cdot 10^6$ cell/mL) were seeded on Transwell® and after 24 h, the media from apical compartment was removed resulting in ALI culture configuration. After 14 days from seeding the Transwell® were removed and transferred to a 12-well plate containing 1.5 mL of pre-warmed HBSS. Then, 200 μL of $LNC_{SVT\text{-}LMWchit}$, $LNC_{SVT\text{-}HMWchit}$ and SVT were added to the upper compartment and samples of 200 μL were collected from the baso-lateral chamber at pre-determined time points (1, 2, 3 and 4 h) and replaced with the same volume of fresh HBSS buffer. The samples were quantified for simvastatin content using HPLC-UV (n = 4). TEER measurements were performed with a Millicell-ers® (Millipore) at the beginning and at the end of experiment in order to confirm that the integrity of the cell layer was maintained.

2.8 Ex Vivo Transport Experiments across Rabbit Nasal Mucosa

The transport of simvastatin across rabbit nasal tissue was evaluated using Franz type vertical diffusion cells with a receptor volume of 4.5 mL and diffusional area of 0.58 cm^2. On the day of the experiment, nasal mucosae were freshly excised from rabbits obtained from a local slaughterhouse (Pola, Finale Emilia, Italy) and cleaned to remove adhering submucosal tissue [53]. The rabbit nasal mucosa was placed between the donor and the receptor compartment of the diffusion cells. Then, in order to check the mucosa integrity, the donor compartment was filled with medium to confirm that no liquid leaked into the cell receptor compartment. If the nasal mucosa passed this test, the donor compartment received 200 μL one among the three tested preparations, i.e. $LNC_{SVT\text{-}LMWchit}$, $LNC_{SVT\text{-}HMWchit}$ and SVT, equivalent to 200 μg of SVT. Franz cells were maintained at 37 °C under mild magnetic stirring. At predetermined time intervals, 500 μL of the receptor medium, SNES containing 0.5% w/v of polysorbate 80, was withdrawn and the receptor compartment refilled with an equivalent volume of fresh medium. All samples were analyzed by HPLC-UV. In order to evaluate the retention of SVT in the nasal tissue, mucosa samples were placed in a volumetric flask (10 mL) containing a solvent of extraction (acetonitrile) and subjected to vortexing (2 min) and sonication (15 min). The solvent of extraction was then filtered (0.45 μm, Millipore®, Billerica, USA) and simvastatin quantified using HPLC-UV. The experiments were conducted in triplicate for each formulation.

2.9 Preliminary Nasal Toxicity Studies

Nasal toxicity studies were performed using rabbit nasal mucosa in a similar way to *ex vivo* permeation study mentioned above in order to evaluate any damage to the mucosa. Each mucosa piece, of uniform thickness, was treated with $LNC_{SVT\text{-}LMWchit}$, $LNC_{SVT\text{-}HMWchit}$, SVT and PBS pH 6.4 (negative control) by placing 200 µL in the donor compartment of Franz diffusion cells. The acceptor contained 4.5 mL of SNES containing 0.5% w/v of polysorbate 80. After 4 h, for each condition nasal mucosa was washed with PBS, fixed in 10% v/v buffered formalin for 6 h and embedded in histological paraffin. A rotatory microtome was used to perform transverse cuts to obtain sections (5 µm) that were stained with hematoxylin-eosin. Images of mucosa samples were observed using an Olympus BX51 optical microscope with attached camera DP72 (Olympus, Tokyo, Japan) [54].

2.10 Statistical Analysis

Data are presented as mean ± standard deviation (SD) of analysis of at least triplicate batches (n = 3). Statistical analysis was performed using the Student's t-test for two groups or one-way analysis of variance (ANOVA) followed by Tukey's test for multiple groups using GraphPad Prism Software 5.0 (GraphPad Software, Inc., San Diego, CA). Differences were considered significant at $p<0.05$.

3. Results

SVT-nanocapsules were prepared using the interfacial deposition of pre-formed polymer method and coated with chitosan with a one-pot technique. The surface of the NPs was coated with two different chitosan grades, characterized by different molecular weight and hence different viscosities, in order to evaluate the effect of chitosan molecular weight on the mucoadhesive properties and permeability enhancement of the nanocapsules obtained.

3.1. Characterization of nanocapsules

SVT nanocapsules appeared macroscopically like an opalescent white homogeneous dispersion. The total SVT content in the formulations was found to be 0.94 ± 0.04 $mg{\cdot}mL^{-1}$ for $LNC_{SVT\text{-}LMWchit}$ and 0.96 ± 0.02 $mg{\cdot}mL^{-1}$ for $LNC_{SVT\text{-}HMWchit}$. Regarding encapsulation efficiency (EE), SVT was not detected in the ultrafiltrate for both formulations, indicating an almost complete encapsulation. The high EE achieved is probably linked to the high SVT distribution coefficient (log D) of 4.72, which confirms its great affinity for the lipophilic phase and concentration in the core of the nanocapsules [55]. Laser diffraction (LD) analysis showed D[4,3] of 150 ± 7 nm ($LNC_{LMWchit}$), 157 ± 6 nm ($LNC_{HMWchit}$), 163 ± 2 nm ($LNC_{SVT\text{-}LMWchit}$), and 161 ± 3 nm ($LNC_{SVT\text{-}HMWchit}$) with Span values of 1.3 ± 0.1, 1.3 ± 0.1, 1.4 ± 0.03 and 1.2 ± 0.2, respectively. According to the results obtained with this technique, there were no significant difference in terms of particle diameter and polydispersity between the formulations with and without SVT ($p>0.05$). The shape of the curves in the radar chart presented in Figure 1 are fingerprint of the formulations that demonstrate narrow size distributions and confirming the low polydispersity [56]. All the formulations showed similar behaviour and had $d_{0.9}$ calculated both on the cumulative distribution by number and by volume lower than 300 nm (Figure 1).

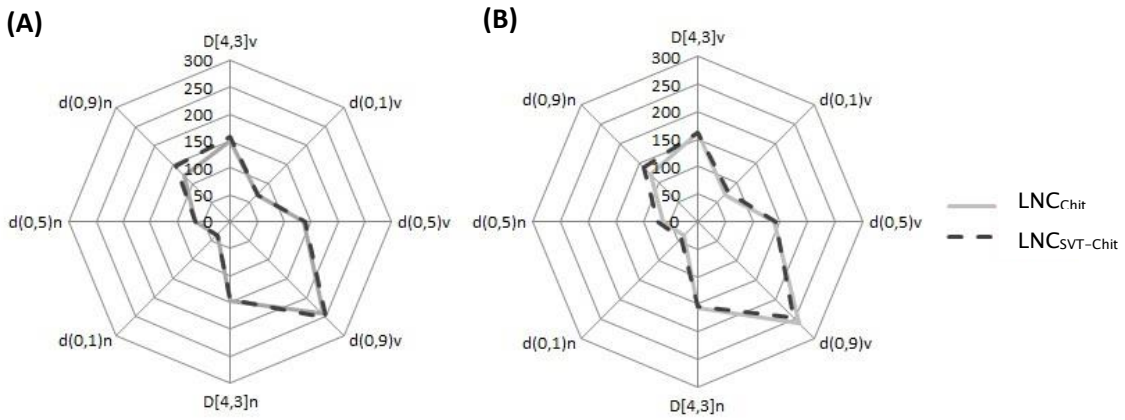

Figure 1. Radar chart presenting the volume-weighted mean diameters (D[4,3]) and the diameters at percentiles 10, 50 and 90 under the size distribution curves by volume and by number of particles. Chitosan-coated simvastatin-loaded lipid-core nanocapsules developed with (a) low MW chitosan and (b) high MW chitosan.

Mean particle size was further confirmed by DLS and NTA analysis as shown in Table 1. DLS analysis showed a narrow particle size distribution for all the formulations (PDI < 0.2). In particular, the encapsulation of SVT did not affect the particle size of nanocapsules coated with low MW chitosan. In fact the diameter of $LNC_{LMWchit}$ and $LNC_{SVT\text{-}LMWchit}$ was not significantly different ($p>0.05$). On the other hand, the presence of SVT led to a significant size increase ($p\leq0.05$) in the case of $LNC_{SVT\text{-}HMWchit}$ (210 ± 10 nm) when compared with blank nanocapsules ($LNC_{HMWchit}$, 188 ± 7 nm) in the case of NTA analysis, but not in the case of DLS data. This difference may be explained with the formation of a small number of particle agglomerates, compared to the formulation prepared without drug. In addition, these agglomerates appeared to be detected more efficiently by the NTA technique compared to DLS. This is supported by the particle number density (PND) also measured by NTA that evidenced upon SVT encapsulation almost an halving of the particle number density (PND), which was 1.1 ± 0.4 × 10^{12} particles/mL for $LNC_{HMWchit}$ and 6.6 ± 0.2 × 10^{11} particles/mL for $LNC_{SVT\text{-}HMWchit}$ (Table 1). Furthermore, in general the nanocapsules coated with HMW chitosan showed a slightly higher mean diameter than those coated with LMW chitosan ($p>0.05$), probably as a consequence of the chitosan higher molecular weight and higher viscosity in the water phase. In general, it has been reported that the higher is the viscosity of the dispersion medium, the higher is the mean diameter of nanoparticles produced [57].

Table 1. Physicochemical characterization of the nanocapsules (n = 3, Mean ± Standard Deviation).

	DLS		NTA			
	Z-average (nm)	PDI	Mean (nm)	PND (particles/mL)	Zeta potential (mV)	pH
$LNC_{LMWchit}$	166 ± 5	0.13 ± 0.02	174 ± 5	1.3 ± 0.3 × 10^{12}	25.4 ± 4.1	4.1 ± 0.01
$LNC_{SVT\text{-}LMWchit}$	168 ± 5	0.12 ± 0.04	166 ± 7	1.2 ± 0.6 × 10^{12}	28.95 ± 2.1	4.1 ± 0.02
$LNC_{HMWchit}$	179 ± 14	0.13 ± 0.02	188 ± 7	1.1 ± 0.4 × 10^{12}	33.6 ± 3.9	4.1 ± 0.03
$LNC_{SVT\text{-}HMWchit}$	185 ± 7	0.16 ± 0.03	210 ± 10	6.6 ± 0.2 × 10^{11}	33.8 ± 5.5	4.4 ± 0.04

Zeta potential represents the surface charge of particles, and, as expected, the formulations produced with chitosan exhibited a positive zeta potential at the pH of the formulations that was between pH 4.0 and 4.5. In fact, the nanocapsules suspensions showed mildly acid pH values, as

expected due to the use of 1% (v/v) acetic acid aqueous solution to dissolve chitosan [43]. The zeta potential of $LNC_{LMWchit}$ and $LNC_{HMWchit}$ were similar to those determined for the SVT-loaded nanocapsules. Therefore, the encapsulation of SVT did not significantly affect this parameter ($p>0.05$). The pH value at which the nanoparticles do not exhibit any net charge is termed isoelectric point (IEP). $LNC_{SVT\text{-}LMWchit}$ and $LNC_{SVT\text{-}HMWchit}$ showed their isoelectric point (IEP) at pH value 7.1 ± 0.2 and 7.2 ± 0.5, respectively. The positive zeta potential obtained for all formulations prepared and the IEP near to IEP of chitosan (IEP=6.8) [58] are good indicatives that the chitosan is present at the external interface of the nanocapsules. $LNC_{SVT\text{-}LMWchit}$ and $LNC_{SVT\text{-}HMWchit}$ were further characterized in terms of the morphology (Figure 2).

Concerning nanocapsules morphology, TEM images clearly display spherical-shaped particles, with a core with low electron density, as expected for lipid nanocapsules. Also form the point of view of particle diameter the images are in good agreement with the mean nanocapsule size determined with DLS, NTA and LD.

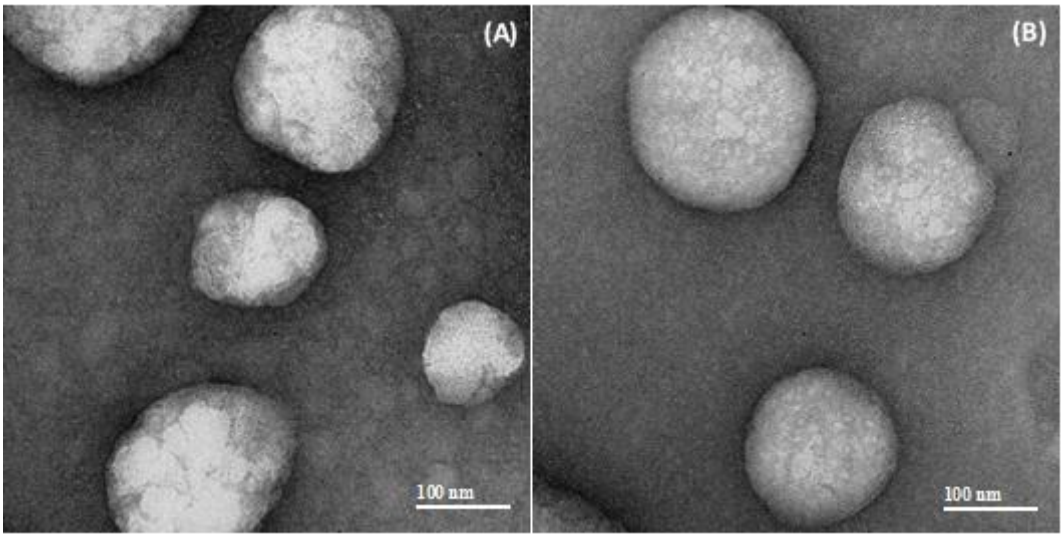

Figure 2. Transmission electron microscopy (TEM) micrographs (magnification 40,000×) of chitosan-coated lipid core nanocapsules: (A) $LNC_{SVT\text{-}LMWchit}$ and (B) $LNC_{SVT\text{-}HMWchit}$.

3.2 Mucoadhesion studies

To investigate the interaction between the formulations and mucin, a mucoadhesion index (MI), the PDI and zeta potential of mixtures between the nanocapsules and mucin were determined for different mucin weight ratios f (Figure 3). For $LNC_{SVT\text{-}LMWchit}$ in the range of f values up to 0.3, particle size and MI values increased to a maximum 474 ± 6 nm and 2.9 ± 0.1 (f = 0.3), respectively. Similarly, $LNC_{SVT\text{-}HMWchit}$ particle size and MI increased in the f range from 0 to 0.55, reaching a maximum of 557 ± 30 nm, 3.0 ± 0.3 (f = 0.55), respectively (Figure 3a). Despite the increase of the fraction by weight of mucin above f values of 0.3, for $LNC_{SVT\text{-}LMWchit}$ particle size and MI decreased to 318 ± 5 nm and 1.9 ± 0.1 for f values of 0.85. It has been hypothesized here, that while at values of f around 0.3 nanocapsules are able to form large agglomerates with mucin chains entangled and linked with more nanoparticles, above this value the mucin is in such a large excess that almost single particles are enrobed with mucins leading to a decrease in the overall mean particle size. In fact, the MI values for f 0.55 and 0.85 do not change significantly. On the other hand, for $LNC_{SVT\text{-}HMWchit}$ this decrease in the MI occurs only for f values above 0.55, with particle size and MI decreasing to 321 ± 7 nm, 1.7 ± 0.1 (f = 0.85). Therefore, the MI maximum was observed at lower f values (0.3) for $LNC_{SVT\text{-}LMWchit}$ and higher f values (0.55) for $LNC_{SVT\text{-}HMWchit}$, indicating a higher capacity to interact with larger quantities of mucin for nanoparticles coated with high MW chitosan, macroscopically translated in a more efficient mucoadhesion.

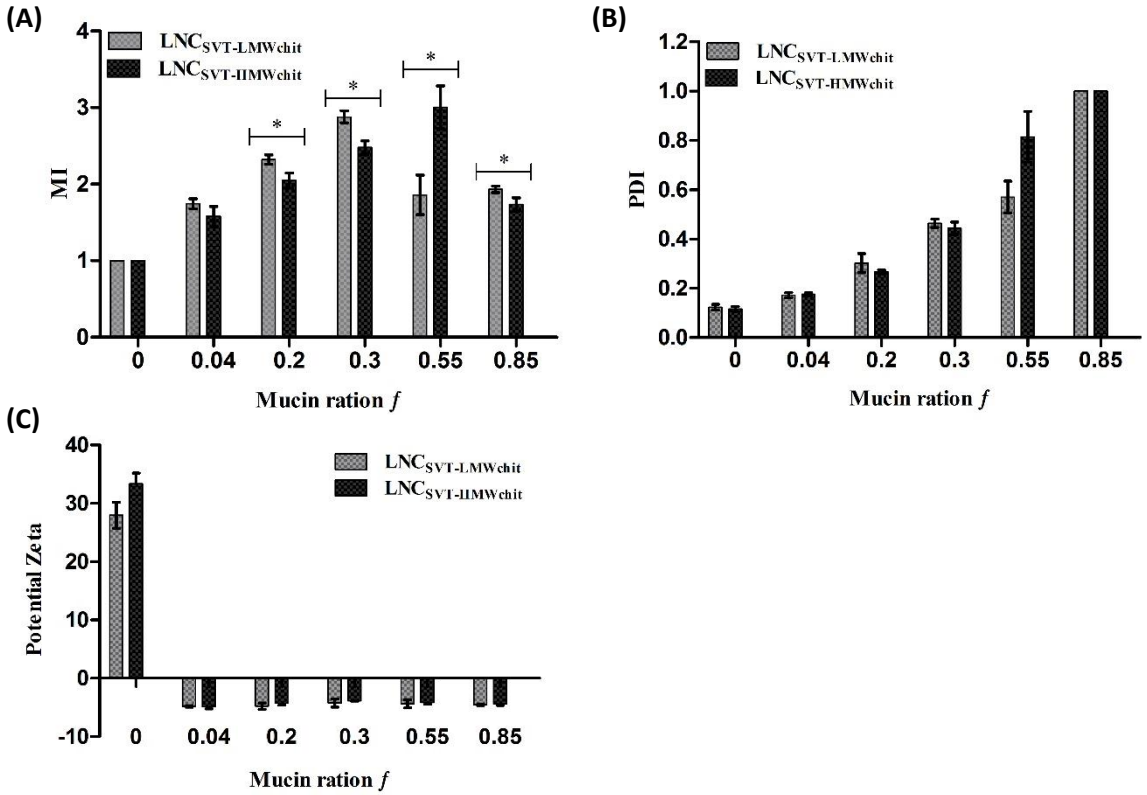

Figure 3. (A) Mucoadhesive index (MI) values, (B) PDI and (C) Zeta potential measured for various mixtures of mucin and nanocapsules. Values of the two formulations were obtained before (f = 0) and after incubation with different mucin weight ratios f.

The polydispersity index (PDI) before nanocapsules interaction with mucin was 0.12 ± 0.01 for $LNC_{SVT\text{-}LMWchit}$ and 0.11 ± 0.01 for $LNC_{SVT\text{-}HMWchit}$. After mixing the nanocapsules with mucin, PDI progressively increased for both formulations up to 1 (f = 0.85), indicating the formation of agglomerates and the switch to highly polydisperse particle size distribution (Figure 3b). The zeta potential of the formulations that was initially positive due to the chitosan coating, immediately after interaction even with the smallest amount of mucin (f = 0.04) became negative for both formulations (-4.8 ± 0.1 mV for $LNC_{SVT\text{-}LMWchit}$ and -4.8 ± 0.7 mV for $LNC_{SVT\text{-}HMWchit}$) and remained roughly constant for both formulations even increasing f values (Figure 3c).

3.3 In Vitro Drug Release

The *in vitro* release profile of simvastatin-loaded chitosan coated lipid core nanocapsules were performed over 8 h (Figure 4). A solution of simvastatin was used as control. It can be observed that 56.3 ± 2.5% of SVT diffused out from the dialysis bag when using the control simvastatin solution within 8 h. On the other hand, the drug released from $LNC_{SVT\text{-}LMWchit}$ and $LNC_{SVT\text{-}HMWchit}$ after 8 h was 37.3 ± 1.5% and 31.0 ± 1.1%, respectively. These results show that nanocapsules provided a controlled release of simvastatin and that the different type of chitosan affected the drug release rate. Indeed, the release of SVT from $LNC_{SVT\text{-}HMWchit}$ was slower in comparison to the $LNC_{SVT\text{-}LMWchit}$.

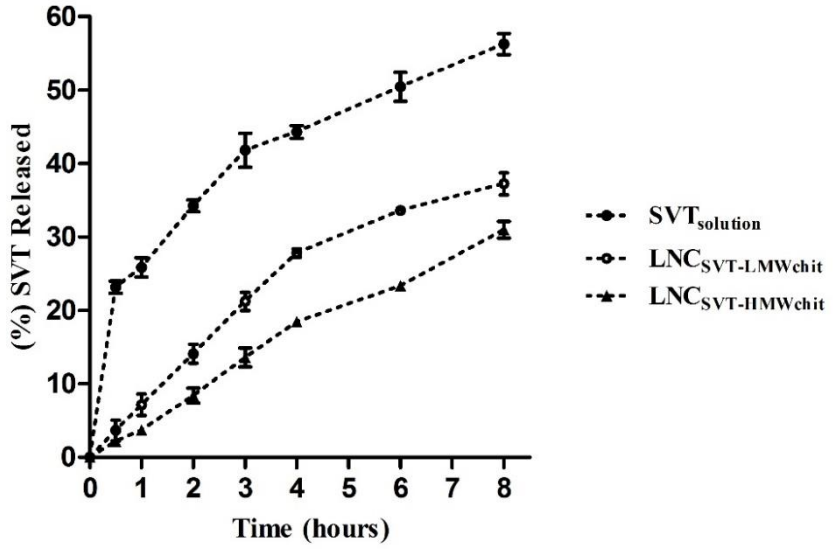

Figure 4. *In vitro* drug release profile from LNCSVT-LMWchit, LNCSVT-HMWchit and from control (SVT solution) using the dialysis bag method at 37 °C (n = 3, ± SD).

3.4 Transport Studies on a Nasal Cell Model

To confirm the potential permeability enhancement effects of the nanocapsules, the total amount of SVT transported across nasal mucosa model was determined using RPMI2650 human nasal epithelial cells [52]. Figure 5 shows the amount of SVT transported using the formulations compared to a suspension of the raw material over 4 h. After 1 h of the experiment, the formulations already showed increased permeation compared to the control. However, no significant differences ($p>0.05$) were observed at 1 h for the SVT permeation between LNCSVT-LMWchit to LNCSVT-HMWchit. After the first hour however, each single time point showed an amount of SVT transported to be statistically different between the formulations ($p < 0.05$) and confirming the greater permeation of LNCSVT-LMWchit.

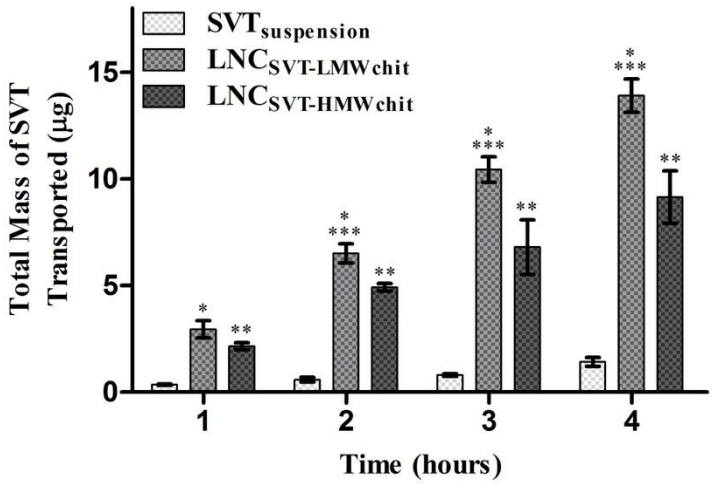

Figure 5. Amount (µg) of SVT transported across RPMI 2650 cells grown under air-liquid interface conditions (n = 4, ± SD). Significant difference ($p<0.05$) is expressed considering the following comparisons: ∗SVT *versus* LNCSVT-LMWchit, ∗∗SVT *versus* LNCSVT-HMWchit *** LNCSVT-LMWchit *versus* LNCSVT-HMWchit.

3.5 Ex vivo Transport Experiments across Rabbit Nasal Mucosa

Figure 6a shows the SVT permeation across excised rabbit nasal mucosa using Franz type vertical diffusion cells. The results of *ex vivo* permeation studies on rabbit nasal mucosa evidenced that the formulations significantly increased the permeation of SVT compared to control. The $LNC_{SVT\text{-}LMWchit}$ showed the highest percent SVT permeation after 4 h (19.2 ± 0.5%·cm^{-2}), followed by $LNC_{SVT\text{-}HMWchit}$ (11.0 ± 0.5%·cm^{-2}), while the control (SVT suspension) showed an extremely low permeation (2.6 ± 0.2%·cm^{-2}). The results indicate that SVT permeation from $LNC_{SVT\text{-}LMWchit}$ was 1.74 and 7.4 times greater than $LNC_{SVT\text{-}HMWchit}$ and SVT control, respectively.

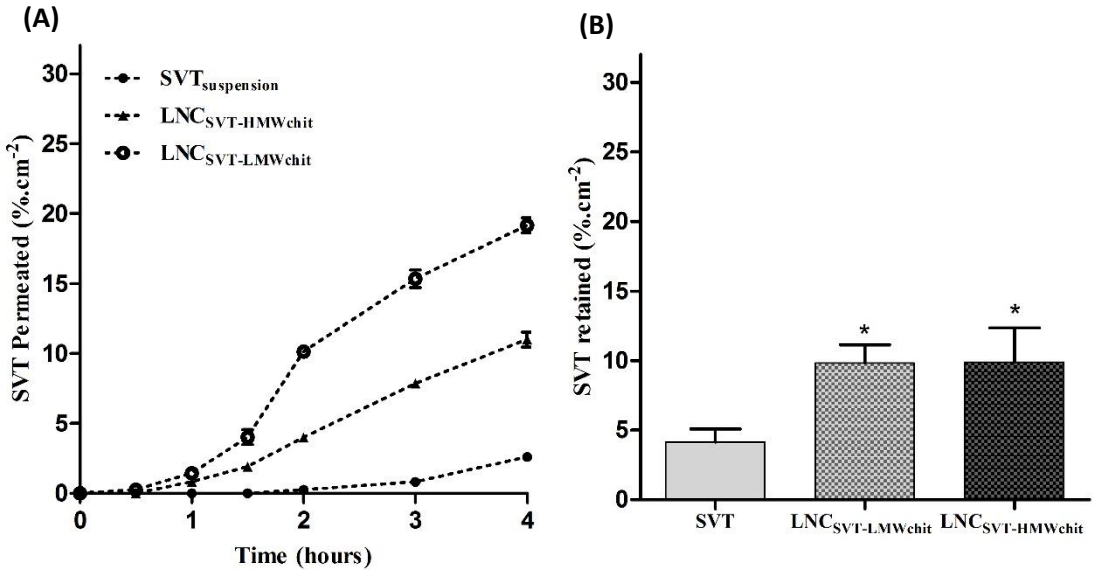

Figure 6. (A) *Ex vivo* SVT permeation across rabbit nasal mucosa until 4 h in simulated nasal electrolytic solution (SNES) containing 0.5% of polysorbate 80 at 37 °C (n = 3, ± SD). (B) Percentage of SVT retained in nasal mucosa after 4 h of permeation test in Franz-type diffusion cell (n = 3, ± SD). Asterisk (*) indicates significant difference between SVT *versus* $LNC_{SVT\text{-}LMWchit}$ and $LNC_{SVT\text{-}HMWchit}$.

The results of SVT retained in the mucosa tissue after 4h of experiment are shown in Figure 6b. It can be seen that there was better retention of both formulations with respect to the control. The SVT fraction found in the tissue for the control was 4.2 ± 0.9%·cm^{-2}, while in the case of $LNC_{SVT\text{-}LMWchit}$ and $LNC_{SVT\text{-}HMWchit}$ the fraction of simvastatin found in the tissue was more than doubled, i.e. 9.8 ± 1.3 and 9.9 ± 2.5%·cm^{-2}, respectively. In this case, the difference between the amount of retained SVT from $LNC_{SVT\text{-}LMWchit}$ and $LNC_{SVT\text{-}HMWchit}$ was not statistically significant.

3.6 Preliminary nasal toxicity studies

Nasal mucosa histopathology studies were performed to assess the integrity of rabbit mucosa after 4h of the permeation test. As shown in Figure 7, the mucosa treated with PBS pH 6.4 (negative control), SVT, $LNC_{SVT\text{-}LMWchit}$ and $LNC_{SVT\text{-}HMWchit}$ did not show any evident structural damage. The results from histological examinations indicate that LNC nanocapsules do not cause any irritation or toxicity and can be considered to be biocompatible for nasal administration.

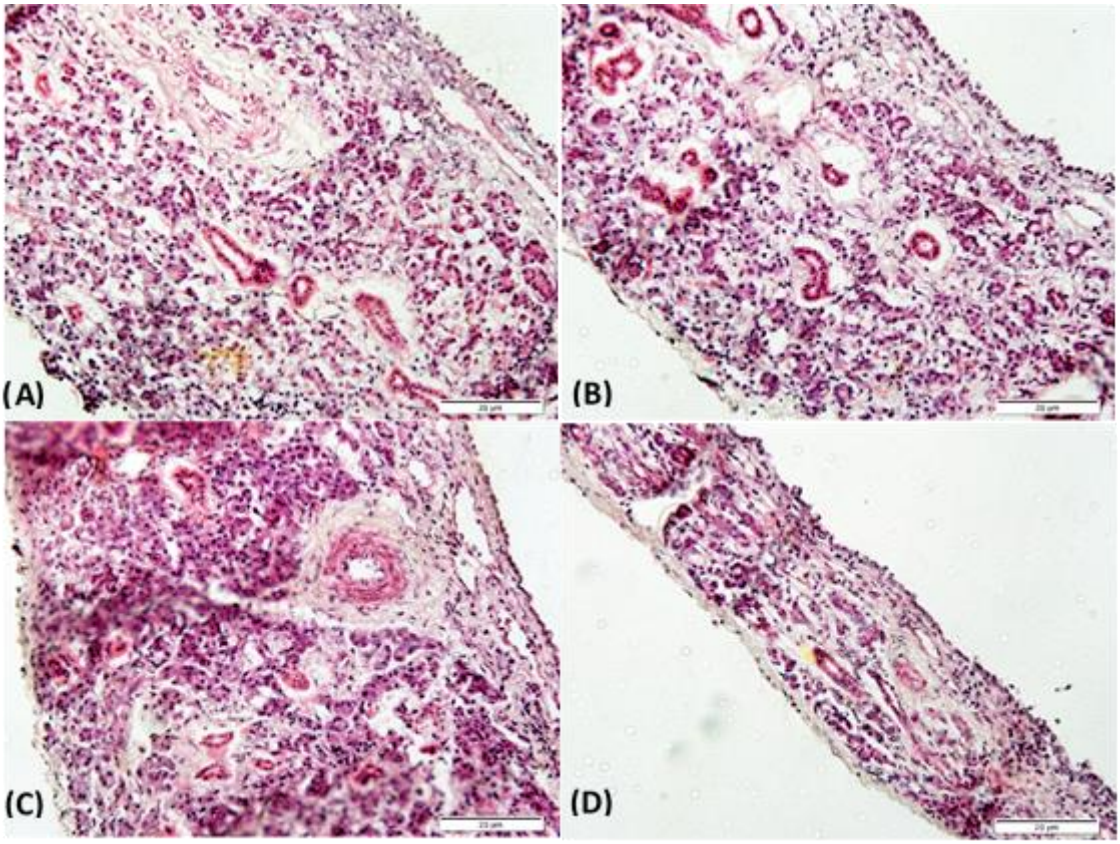

Figure 7. Histopathological sections of rabbit nasal mucosa after 4 h of permeation test in Franz-type diffusion cell treated with (A) PBS pH 6.4 (negative control), (B) SVT, (C) $LNC_{SVT\text{-}LMWchit}$ and (D) $LNC_{SVT\text{-}HMWchit}$. Stained with hematoxylin and eosin.

4. Discussion

Over the past couple of decades pharmaceutical nanotechnology have received considerable attention and demonstrated significant potential for the development of innovative medicinal products both for the therapy and the diagnosis of severe diseases [59]. In this work, we report a new preparation method of lipid-core PCL nanocapsules, optimizing a two-step process (self-assembly step followed by a coating step) into a one-pot technique to develop chitosan-coated nanoparticles. Moreover, we compared the pharmaceutically relevant properties in terms of physicochemical characterization, mucoadhesive properties, drug release and permeability studies of $LNC_{SVT\text{-}LMWchit}$ and $LNC_{SVT\text{-}HMWchit}$ coated by chitosan with low MW and high MW in view of a nose-to-brain administration.

Polymeric nanocapsules containing poly(ε-caprolactone), capric/caprylic triglyceride, and sorbitan monostearate, and coated with chitosan, were developed. This formulation has the advantage of efficiently encapsulating lipophilic drugs such as simvastatin [34,35]. The production of positively-coated lipid-core nanocapsules in one step, avoiding the use of non-ionic surfactants in the aqueous phase, is the main novelty of this approach. Previously, we developed mucoadhesive amphiphilic nanocapsules based on a blend of PCL and poly(methyl methacrylate-b-2-(dimethylamino)ethyl methacrylate) for the nose-to-brain delivery of olanzapine. Nevertheless, the self-assembly of the nanocapsules by using this block copolymer (positive surface) avoids the use of sorbitan monostearate in the formulation. Indeed, the cores of those nanocapsules are composed exclusively of medium-chain triglycerides [29]. Sorbitan monostearate dispersed in core of the lipid-core nanocapsules has been demonstrated to provide an addition diffusional barrier to control the drug release, and an increase of the rigidity of the nanocapsules polymer wall [34,36]. Furthermore, a comparative study conducted with polymeric nanocapsules demonstrated that the presence of sorbitan monostearate instead of sorbitan monooleate in the core improved the anti-apoptotic and antioxidant effects of melatonin during bovine embryo development [60]. In the present development, it was possible to obtain in a one-step process,

lipid-core nanocapsules incorporating sorbitan monostearate in the oily core, and decorated on the surface with chitosan, providing mucoadhesion and penetration-enhancing properties that appear to be fundamental for nose-to-brain delivery [21].

The combination between the composition and the interfacial deposition of pre-formed polymer method produced nanocapsules with adequate particle size and narrow size distributions as was confirmed by complementary techniques such as laser diffraction, DLS and NTA. Besides that, coating the nanocapsules with chitosan with different molecular weight (21 kDa and 152 kDa) influenced their pharmaceutical properties. For example, chitosan molecular weight and viscosity in water affected the size of the nanoparticles. In fact, particle size could be reduced by using lower molecular weight chitosan [61,62]. Actually, $LNC_{SVT\text{-}HMWchit}$ higher mean particle hydrodynamic diameter could be attributed to the length chains of chitosan present on the particle surface, possibly expanding the water hydration shell of the nanoparticle. In addition, chitosan low MW has been reported to have higher aqueous solubility and this together with shorter polymer chains contributed to forming smaller particles compared to chitosan high MW [63]. The positive zeta potential obtained for all formulations is an evidence of the polysaccharide coating. Furthermore, using different chitosan did not cause significant changes in zeta potential of both formulations, probably due of a similar degree of deacetylation (95%) [64]. Mucoadhesive polymers such as chitosan represent a significant strategy to overcome the nasal drug delivery limits as low membrane permeability, short residence time and mucociliary clearance. The polysaccharide presence on nanocapsules surface is expected to prolong permanence of the formulation in the nasal cavity, open the tight junctions between nasal epithelial cells and promote the drug permeation through the biological barriers granting access to the CNS [65,66,67]. For these reasons, the evaluation of the ability of nanocapsules to interact with mucin is of great interest for nasal administration. Mucous membranes internally delimiting the body cavities (stomach, esophagus, cornea, oral cavity, reproductive and respiratory tracts) and are characterized by a superficial mucus layer with protective and lubricating function [68]. The mucus is composed of water (approximately 95%), lipids, inorganic salts and mucin, a glycoprotein composed by N-acetylgalactosamine, N-acetylglucosamine, fucose, galactose, and sialic acid, responsible for the adhesive properties and the viscosity of the mucus [66]. Lipophilic drugs show an affinity for mucus glycoproteins reducing the adsorption and the bioavailability. This issue, together with the drug poor aqueous solubility, are limiting factor for the nose-to-brain delivery of lipophilic drugs. To improve the transport of SVT through this barrier we used nanoparticles as a drug delivery system [69].

Our results showed how, for both formulations, particle size and MI increased with the increase in the mucin weight ratio until a critical point. A previous study [50] has led to the conclusion that the nanoparticles in mucin solution form agglomerates in which the nanoparticles are the points of contact between negatively charged mucin chains. Beyond the critical value of the mucin ratio the repulsive forces among the mucin chains break these agglomerates. Our results support this theory, nevertheless it has to be stressed that the decrease of MI observed for high mucin weight ratio does not indicate a decrease in the mucoadhesive capacity of the formulations [50]. However, the results indicate how in mucin excess, the smaller aggregates are formed in order to minimize the repulsive forces between the chains of the mucin and maximize the points of contact between the positive charges of chitosan and the negative mucin chains. Moreover, it was noticed that the critical point of the formulations was different for the nanocapsules coated with chitosan with different characteristics ($LNC_{SVT\text{-}LMWchit}$ $f = 0.3$ and for $LNC_{SVT\text{-}HMWchit}$ $f = 0.55$). This difference could be attributed to the different chain lengths of the two chitosan batches [63]. Indeed, in a previous study conducted with a different method Menchicchi and co-authors proposed that mucin interact mostly with high molecular weight chitosan [70]. On the other hand, the results presented in this paper compared to similar uncoated LNC demonstrate a large increase in the mucoadhesive capacity due to the presence of chitosan. The uncoated LNC showed values of MI = 1.4, PDI = 0.51 and zeta potential of -9.5 mV after contact with the maximum concentration of mucin (0.5% w/v) [71]. The PDI increase with the increase in the f mucin ratio corroborates the above-mentioned explanation. In fact, PDI results indicated that the heterogeneity of the distribution of the particle size in solution increased along with the mucin weight ratio because of the formation of

aggregates of different sizes. The oligosaccharide chains of mucin glycoproteins present terminal sialic acid residues confer negative charge to the molecule, therefore the variation of the particle zeta potential from positive to negative values demonstrates how the mucin enrobes nanocapsules interacting with their surface layer of chitosan. This suggests that the mucoadhesion mechanism are driven by electrostatic interaction of positively charged amine groups of D-glucosamine molecules of chitosan with negatively charged sialic acid residues of mucin [72].

SVT-loaded lipid core nanocapsules formulation was able to control the drug release due the two diffusional barriers: the PCL polymer wall and the lipid dispersion present in the nanocapsule core. The nanoencapsulation reduced the diffusion rate of SVT across a dialysis membrane, confirming data frequently described in the literature as a property of polymeric nanoparticles [33]. Regarding the comparison between the two formulations, $LNC_{SVT\text{-}HMWchit}$ afforded better control of drug release. In order to explain the different release profile, we evaluated the differences in terms of physicochemical properties. Firstly, this can be explained due to the higher viscosity of the chitosan used to develop the $LNC_{SVT\text{-}HMWchit}$. Previous studies demonstrated that the viscosity of the chitosan is an important factor for modulating the release control [73]. Moreover, nanoparticle size can influence in the release profile, which increases with decreasing particle size. Indeed, $LNC_{SVT\text{-}LMWchit}$ had lower mean particle diameter than $LNC_{SVT\text{-}HMWchit}$, that could contribute to explain the different release profile between them because of the greater available surface area [74,75].

The permeation across RPMI 2650 human nasal cell line showed that the SVT transported across the nasal cell model by $LNC_{SVT\text{-}LMWchit}$ and $LNC_{SVT\text{-}HMWchit}$ can enhance the drug transport across a cell pseudo-monolayer that also secrete mucin on its apical surface. The increase of SVT permeation across the human nasal cell layer can be explained by different mechanisms. In literature, chitosan is associated with an opening of tight junctions that increase cell layers permeability. However, this mechanism is generally favoring the permeation of water-soluble drugs and it has been evidenced that is slightly less efficient for chitosan bound to nanoparticles compared to simple polysaccharide solutions [76]. More recently, it has been demonstrated that the biodegradation of nanocapsules by enzymes in the mucus barrier or intracellularly could be pivotal in enhancing transcellular transport of lipophilic drugs [77]. The results of the *ex vivo* permeation studies on rabbit nasal mucosa confirmed and further added evidence of the fact that the nanoencapsulation of SVT significantly increased its permeation across excised nasal mucosa. In this case, the higher permeation evidenced for $LNC_{SVT\text{-}LMWchit}$ could be explained by a combination of factors. The smaller particle size of nanocapsules coated with low molecular weight chitosan could have facilitated the absorption to the mucosal tissue as reported before [78]. Moreover, an important factor is the bioadhesion of the nanostructures, as previously explained given by the particles shell of chitosan that interacts by electrostatic forces with the anionic sites of the nasal mucus [65]. However, from the mucoadhesion data a better interaction with mucus could be expected from nanocapsules coated with the high molecular weight chitosan. However, the slower release kinetics evidenced for these particles have probably contributed to limit the amount of drug permeated, especially considering that drug accumulation into the tissue is superimposable for the two nanocapsules formulations.

Previous findings [79,80], agreed that chitosan coated nanoparticles increased the drug permeation across the nasal mucosa compared to the free drug control. This controlled SVT permeation, together with mucoadhesion effect, may be an important strategy to prolong the effect of the drug when administered via the nasal route.

5. Conclusions

In the present investigation, the coating process of lipid-core nanocapsules using a one-pot technique approach was presented. Furthermore, two chitosan-coated simvastatin-loaded lipid core nanocapsules suitable for nasal administration were successfully developed. Both the nanoparticles produced with different chitosan were designed to have adequate physicochemical and mucoadhesive properties for a potential nose-to-brain application. The formulations prepared combine a controlled release of simvastatin and mucoadhesion properties able to increase the drug permeation across the

nasal mucosa, as demonstrated using two different model of nasal epithelium. In summary, simvastatin-loaded chitosan-coated lipid core nanocapsules seems to be a promising mucoadhesive system for nose-to-brain delivery of poorly soluble anticancer drugs. The follow up studies will focus on the investigation of the potential of these nanoparticles for the treatment of brain tumors involving studies with glioma cells and an orthotopic intracranial tumor model in mice.

Author Contributions: Conceptualization, A.R.P. S.S.G., and F.S.; Methodology, F.A.B., S.P., T.A., G.D.S., G.G.P., M.M., L.T.F.; Investigation, F.A.B., S.P.; Resources, A.R.P., S.S.G.; Writing-Original Draft Preparation, F.A.B., S.P.; Writing-Review & Editing, F.A.B., F.S.; Supervision, A.B., G.C., F.S.

Acknowledgments: Franciele Aline Bruinsmann, Fabio Sonvico, Adriana Raffin Pohlmann, and Silvia Stanisçuaski Guterres would like to acknowledge the Brazilian government as recipients of CNPq grants in the programs "Ciências sem Fronteiras" (BOLSA PESQUISADOR VISITANTE ESPECIAL—PVE 401196/2014-3) and "Produtividade em Pesquisa". This study was financed in part by the Coordenação de Aperfeiçoamento de Pessoal de Nível Superior – Brasil (CAPES) – Finance Code 001.

Conflicts of Interest: The authors declare no conflict of interest.

References

1. Chiang, K.H.; Cheng, W.L.; Shih, C.M.; Lin, Y.W.; Tsao, N.W.; Kao, Y.T.; Lin, C.T.; Wu, S.C.; Huang, C.Y.; Lin, F.Y. Statins, HMG-CoA Reductase Inhibitors, Improve Neovascularization by Increasing the Expression Density of CXCR4 in Endothelial Progenitor Cells. *PLoS One* **2015**, 10(8), e0136405.
2. Liao, J.K.; Ulrich, L. Pleiotropic effects of statins. Annu. *Rev. Pharmacol. Toxicol*. **2005**, 45, 89-118.
3. Davies, J.T.; Delfino, S.F.; Feinberg, C.E.; Johnson, M.F.; Nappi, V.L.; Olinger, J.T.; Schwab, A.P.; Swanson, H.I. Current and Emerging Uses of Statins in Clinical Therapeutics: A Review. *Lipid Insights* **2016**, 9, 13-29.
4. Jain, M.K.; Ridker, P.M. Anti-inflammatory effects of statins: clinical evidence and basic mechanisms. *Nat. Rev. Drug Discov*. **2005**, 4, 977-987.
5. Liao, K.J. Isoprenoids as mediators of the biological effects of statins. *J. Clin. Invest*. **2002**, 110, 285–288.
6. Tanaka, S.; Fukumoto, Y.; Nochioka, K.; Minami, T.; Kudo, S.; Shiba, N.; Shimokawa, H. Statins exert the pleiotropic effects through small GTP-binding protein dissociation stimulator upregulation with a resultant Rac1 degradation. *Arter. Thromb. Vasc. Biol*. **2013**, 33, 1591-1600.
7. Hindler, K.; Cleeland, C.S.; Rivera, E.; Collard, C.D. The role of statins in cancer therapy. *Oncologist.* **2006**, 11, 306-315.
8. Altwairgi, A.K. Statins are potential anticancerous agents (Review). *Oncol. Rep.* **2015**, 33, 1019-1039.
9. Gazzerro, P.; Proto, M.C.; Gangemi, G.; Malfitano, A.M.; Ciaglia, E.; Pisanti, S.; Santoro, A.; Laezza, C.; Bifulco, M. Pharmacological actions of statins: a critical appraisal in the management of cancer. *Pharmacol. Rev.* **2012**, 64, 102-146.
10. Wejde J., Hjertman, M.; Carlberg, M.; Egestad, B.; Griffiths, W.J.; Sjövall, J.; Larsson, O. Dolichol-like lipids with stimulatory effect on DNA synthesis: substrates for protein dolichylation. *J. Cell Biochem*. **1998**, 71, 502-514.
11. Bifulco, M. Therapeutic potential of statins in thyroid proliferative disease. *Nat. Clin Pract. Endocrinol. Metab.* **2008**, 4, 242-243.
12. Chan, K.K.; Oza, A.M.; Siu, L.L. The statins as anticancer agents. *Clin. Cancer Res*. **2003**, 9, 10-19.
13. Frick, M.; Dulak, J.; Cisowski, J.; Jozkowicz, A.; Zwick, R.; Alber, H.; Dichtl, W.; Schwarzacher, S.P.; Pachinger, O.; Weidinger, F. Statins differentially regulate vascular endothelial growth factor synthesis in endothelial and vascular smooth muscle cells. *Atherosclerosis* **2003**, 170, 229-236.
14. Denoyelle, C.; Vasse, M.; Körner, M.; Mishal, Z.; Ganné, F.; Vannier, J.P.; Soria, J.; Soria, C. Cerivastatin, an inhibitor of HMG-CoA reductase, inhibits the signaling pathways involved in the invasiveness and metastatic properties of highly invasive breast cancer cell lines: an in vitro study. *Carcinogenesis* **2001**, 1139-1148.
15. Yanae, M.; Tsubaki, M.; Satou, T.; Itoh, T.; Imano, M.; Yamazoe, Y.; Nishida, S. Statin-induced apoptosis via the suppression of ERK1/2 and Akt activation by inhibition of the geranylgeranyl-pyrophosphate biosynthesis in glioblastoma. *J. Exp. Clin. Cancer Res.* **2011**, 30, 74.
16. Wu, H.; Jiang, H.; Lu, D.; Xiong, Y.; Qu, C.; Zhou, D.; Mahmood, A.; Chopp, M. Effect of simvastatin on glioma cell proliferation, migration, and apoptosis. *Neurosurgery* **2009**, 65, 1087-1096.

17. Bababeygy, S.R.; Polevaya, N.V.; Youssef, S.; Sun, A.; Xiong, A.; Prugpichailers, T.; Veeravagu, A.; Hou, L.C.; Steinman, L.; Tse, V. HMG-CoA Reductase Inhibition Causes Increased Necrosis and Apoptosis in an In Vivo Mouse Glioblastoma Multiforme Model. *Anticancer Res.* **2009**, 29, 4901-4908.
18. Parrish, K.E.; Sarkaria, J.N.; Elmquist, W.F. Improving drug delivery to primary and metastatic brain tumors: strategies to overcome the blood-brain barrier. *Clin. Pharmacol. Ther*. **2015**, 97, 336-346.
19. Romana, B.; Batger, M.; Prestidge, C.A.; Colombo, G.; Sonvico, F. Expanding the therapeutic potential of statins by means of nanotechnology enabled drug delivery systems. *Curr. Top Med. Chem*. **2014**, 14, 1182-1193.
20. Mittal, D.; Ali, A.; Md, S.; Baboota, S.; Sahni, J.K.; Ali, J. Insights into direct nose to brain delivery: current status and future perspective. *Drug Deliv*. **2014**, 21, 75-86.
21. Sonvico, F.; Clementino, A.; Buttini, F.; Colombo, G.; Pescina, S.; Guterres, S.S.; Pohlmann, A.R.; Nicoli, S. Surface-Modified Nanocarriers for Nose-to-Brain Delivery: From Bioadhesion to Targeting. *Pharmaceutics* **2018**, 10, 34.
22. Bernardi A.; Braganhol, E.; Jäger, E.; Figueiró, F.; Edelweiss, M.I.; Pohlmann, A.R.; Guterres, S.S.; Battastini, A.M. Indomethacin-loaded nanocapsules treatment reduces in vivo glioblastoma growth in a rat glioma model. *Cancer Lett*. **2009**, 281, 53-63.
23. Patel, T.; Zhou, J.; Piepmeier, J.M.; Saltzman. W.M. Polymeric Nanoparticles for Drug Delivery to the Central Nervous System. *Adv. Drug Deliv. Rev*. **2012**, 64, 701-705.
24. Rodrigues, S.F.; Fiel, L.A.; Shimada, A.L.; Pereira, N.R.; Guterres, S.S.; Pohlmann, A.R.; Farsky, S.H. Lipid-Core Nanocapsules Act as a Drug Shuttle Through the Blood Brain Barrier and Reduce Glioblastoma After Intravenous or Oral Administration. *J. Biomed. Nanotechnol*. **2016**, 12, 986-1000.
25. Bahadur, S.; Pathak, K. Physicochemical and physiological considerations for efficient nose-to-brain targeting. *Expert Opin. Drug Deliv*. **2012**, 9, 19-31.
26. Comfort, C.; Garrastazu, G.; Pozzoli, M.; Sonvico, F. Opportunities and challenges for the nasal administration of nanoemulsions. *Curr. Top Med. Chem*. **2015**, 15, 356-368.
27. Illum, L. Nasal drug delivery-possibilities, problems and solutions. *J. Control. Release* **2003**, 87, 187-198.
28. Prego, C.; Torres, D.; Alonso, M.J. Chitosan nanocapsules: a new carrier for nasal peptide delivery. *J. Nanosci. Nanotechnol*. **2006**, 6, 2921-2928.
29. Fonseca, F.N.; Betti, A.H.; Carvalho, F.C.; Gremião, M.P.; Dimer, F.A.; Guterres, S.S.; Tebaldi, M.L.; Rates, S.M.; Pohlmann, A.R. Mucoadhesive Amphiphilic Methacrylic Copolymer-Functionalized Poly(ε-caprolactone) Nanocapsules for Nose-to-Brain Delivery of Olanzapine. *Biomed Nanotechnol.* **2015**, 11, 1472-1481.
30. Clementino, A.; Batger, M.; Garrastazu, G.; Pozzoli, M.; Del Favero, E.; Rondelli, V.; Gutfilen, B.; Barboza, T.; Sukkar, M.B.; Souza, S.A.; Cantù. L.; Sonvico, F. The nasal delivery of nanoencapsulated statins – an approach for brain delivery. *Int J Nanomedicine* **2016**, 11, 6575–6590.
31. Couvreur, P.; Barratt, G.; Fattal, E.; Vauthier, C. Nanocapsule Technology: A Review. *Crit. Rev. Ther. Drug Carrier Syst*. **2002**, 19, 99-134.
32. Mora-Huertas, C.E.; Fessi, H.; Elaissari, A. Polymer-based nanocapsules for drug delivery. *Int. J. Pharm*. **2010**, 385, 113-142.
33. Pohlmann, A.R.; Fonseca, F.N.; Paese, K.; Detoni, C.B.; Coradini, K.; Beck, R.C.; Guterres, S.S. Poly (e-caprolactone) microcapsules and nanocapsules in drug delivery. *Expert Opin. Drug Deliv*. **2013**, 10, 623-638.
34. Jäger, E.; Venturini, C.G.; Poletto, F.S.; Colomé, L.M.; Pohlmann, J.P.; Bernardi, A.; Battastini, A.M.; Guterres, S.S.; Pohlmann, A.R.. Sustained release from lipid-core nanocapsules by varying the core viscosity and the particle surface area. *J. Biomed. Nanotechnol*. **2009**, 5, 130-140.
35. Venturini, C.G.; Jäger, E.; Oliveira, C.P.; Bernardi, A.; Battastini, A.M.O.; Guterres, S.S.; Pohlmann, A.R. Formulation of lipid core nanocapsules. *Colloids Surf. A. Physicochem. Eng. Asp*. **2011**, 375, 200-208.
36. Fiel, L.A.; Rebêlo, L.M.; Santiago, T.M.; Adorne, M.D.; Guterres, S.S.; Sousa, J.S.; Pohlmann, A.R. Diverse Deformation Properties of Polymeric Nanocapsules and Lipid-Core Nanocapsules. *Soft Matter* **2011**, 7, 7240-7247.
37. Frozza, R.L.; Bernardi, A.; Paese, K.; Hoppe, J.B.; da Silva, T.; Battastini, A.M.; Pohlmann, A.R.; Guterres, S.S.; Salbego, C. Characterization of trans-resveratrol-loaded lipid-core nanocapsules and tissue distribution studies in rats. *J. Biomed. Nanotechnol*. **2010**, 6, 694-703.
38. Zanotto-Filho A.; Coradini, K.; Braganhol, E.; Schröder, R.; de Oliveira, C.M.; Simões-Pires, A.; Battastini, A.M.; Pohlmann, A.R.; Guterres, S.S.; Forcelini, C.M.; Beck, R.C.; Moreira, J,C. Curcumin-loaded lipid-core

nanocapsules as a strategy to improve pharmacological efficacy of curcumin in glioma treatment. *Eur. J. Pharm. Biopharm*. **2013**, 83, 156-167.

39. Dimer, F.A.; Ortiz, M.; Pase, C.S.; Roversi, K.; Friedrich, R.B.; Pohlmann, A.R.; Burger, M.E.; Guterres, S.S. Nanoencapsulation of Olanzapine Increases Its Efficacy in Antipsychotic Treatment and Reduces Adverse Effects. *J. Biomed. Nanotechnol*. **2014**, 10, 1137-1145.
40. Figueiró, F.; Bernardi, A.; Frozza, R.L.; Terroso, T.; Zanotto-Filho, A.; Jandrey, E.H.; Moreira, J.C.; Salbego, C.G.; Edelweiss, M.I.; Pohlmann, A.R.; Guterres, S.S.; Battastini, A.M. Resveratrol-loaded lipid-core nanocapsules treatment reduces in vitro and in vivo glioma growth. *J. Biomed. Nanotechnol*. **2013**, 9, 516-526.
41. Figueiró, F.; de Oliveira, C.P.; Rockenbach, L.; Mendes, F.B.; Bergamin, L.S.; Jandrey, E.H.; Edelweiss, M.I.; Guterres, S.S.; Pohlmann, A.R.; Battastini, A.M. Pharmacological Improvement and Preclinical Evaluation of Methotrexate-Loaded Lipid-Core Nanocapsules in a Glioblastoma Model. *J. Biomed. Nanotechnol*. **2015**, 11, 1808-1818.
42. Drewes, C.C.; Fiel, L.A.; Bexiga, C.G.; Asbahr, A.C.; Uchiyama, M.K.; Cogliati, B.; Araki, K.; Guterres, S.S.; Pohlmann, A.R.; Farsky, S.P. Novel therapeutic mechanisms determine the effectiveness of lipid-core nanocapsules on melanoma models. *Int. J. Nanomedicine* **2016**, 11, 1261-1279.
43. Bender, E.A.; Adorne, M.D.; Colomé, L.M.; Abdalla, D.S.P.; Guterres, S.S.; Pohlmann, A.R. Hemocompatibility of poly(epsilon-caprolactone) lipid-core nanocapsules stabilized with polysorbate 80-lecithin and uncoated or coated with chitosan. *Int. J. Pharm.* **2012**, 426, 271-279.
44. Muxika, A.; Etxabide, A.; Uranga, J.; Guerrero, P.; De la Caba, K. Chitosan as a bioactive polymer: Processing, properties and applications. *Int. J. Biol. Macromol*. **2017**, 105, 1358-1368.
45. Kim, I.Y.; Seo, S.J.; Moon, H.S.; Yoo, M.K.; Park, I.Y.; Kim, B.C.; Cho, C.S. Chitosan and its derivatives for tissue engineering applications. *Biotechnol. Adv*. **2008**, 26, 1-21.
46. Rodrigues, S.; Dionísio, M.; López, C.R.; Grenha, A. Biocompatibility of Chitosan Carriers with Application in Drug Delivery. *J. Funct. Biomater*. **2012**, 3, 615-641.
47. Ways, T.M.M; Lau, W.M.; Khutoryanskiy, V.V. Chitosan and Its Derivatives for Application in Mucoadhesive Drug Delivery Systems. *Polymers* **2018**, 10, 267.
48. Ali, A.; Ahmed, S. A review on chitosan and its nanocomposites in drug delivery. *Int. J. Biol. Macromol*. **2018**, 109, 273-286.
49. Bernkop-Schnürch, A.; Dünnhaupt, S. Chitosan-based drug delivery systems. *Eur. J. Pharm. Biopharm.* **2012**, 81. 463-469.
50. Eliyahu, S.; Aharon, A.; Bianco-Peled, H. Acrylated Chitosan Nanoparticles with Enhanced Mucoadhesion. *Polymers* **2018**, 10, 106.
51. Castile, J.; Cheng, Y.H.; Simmons, B.; Perelman, M.; Smith, A.; Watts, P. Development of in vitro models to demonstrate the ability of PecSys®, an in situ nasal gelling technology, to reduce nasal run-off and drip. *Drug Dev. Ind. Pharm*. **2013**, 39, 816-824.
52. Pozzoli, M.; Ong, H.X.; Morgan, L.; Sukkar, M.; Traini, D.; Young, P.M.; Sonvico, F. Application of RPMI 2650 nasal cell model to a 3D printed apparatus for the testing of drug deposition and permeation of nasal products. *Eur. J. Pharm. Biopharm*. **2016**, 107, 223-233.
53. Bortolotti, F.; Balducci, A.G.; Sonvico, F.; Russo, P.; Colombo, G. In vitro permeation of desmopressin across rabbit nasal mucosa from liquid nasal sprays: the enhancing effect of potassium sorbate. *Eur. J. Pharm. Sci*. **2009**, 37, 36-42.
54. Vaz, G.R.; Hädrich, G.; Bidone, J.; Rodrigues, J.L.; Falkembach, M.C.; Putaux, J.L.; Hort M.A.; Monserrat, J.M.; Varela Junior, A.S.; Teixeira, H.F.; Muccillo-Baisch, A.L.; Horn, A.P.; Dora, C.L. Development of Nasal Lipid Nanocarriers Containing Curcumin for Brain Targeting. *J. Alzheimers Dis*. **2017**, 59, 961-974.
55. Oliveira, P.; Venturini, C.G.; Donida, B.; Poletto, F.S.; Guterres, S.S.; Pohlmann, A.R. An algorithm to determine the mechanism of drug distribution in lipid-core nanocapsule formulations. *Soft Matter*, **2013**, 9, 1141-1150.
56. Bianchin, M.D.; Külkamp-Guerreiro, I.C.; Oliveira, C.P.; Contri, R.V.; Guterres, S.S.; Pohlmann, A.R. Radar charts based on particle sizing as an approach to establish the fingerprints of polymeric nanoparticles in aqueous formulations. *J. Drug Deliv. Sci. Technol.* **2016**, 30, 180-189.
57. Frank, L.A.; Chaves, P.S.; D'Amore, C.M.; Contri, R.V.; Frank, A.G.; Beck, R.C.; Pohlmann, A.R.; Buffon, A.; Guterres, S.S. The use of chitosan as cationic coating or gel vehicle for polymeric nanocapsules: Increasing penetration and adhesion of imiquimod in vaginal tissue. *Eur. J. Pharm. Biopharm*. **2017,** 114, 202-212.

58. Gouda, M.; Elayaan, U.; Youssef, M.M. Synthesis and Biological Activity of Drug Delivery System Based on Chitosan Nanocapsules. *Adv. Nanoparticles*, **2014**, 3, 148-158.
59. Mir, M.; Ishtiaq, S.; Rabia, S.; Khatoon, M.; Zeb, A.; Khan, G.M.; Ur Rehman, A.; Ud Din, F. Nanotechnology: from In Vivo Imaging System to Controlled Drug Delivery. *Nanoscale Res. Lett.* **2017**, 12, 500.
60. Komninou, E.R.; Remião, M.H.; Lucas, C.G.; Domingues, W.B.; Basso, A.C.; Jornada, D.S.; Deschamps, J.C.; Beck, R.C.; Pohlmann, A.R.; Bordignon, V.; Seixas, FK.; Campos, V.F.; Guterres, S.S.;Collares, T. Effects of Two Types of Melatonin-Loaded Nanocapsules with Distinct Supramolecular Structures: Polymeric (NC) and Lipid-Core Nanocapsules (LNC) on Bovine Embryo Culture Model. *PLoS One* **2016**, 11(6), e0157561.
61. Haliza, K.; Alpar, H.O. Development and characterization of chitosan nanoparticles for siRNA delivery. *J. Control. Release* **2006**, 115, 216–225.
62. Sonvico, F.; Cagnani, A.; Rossi, A.; Motta, S.; Di Bari, M.T.; Cavatorta. F.; Alonso, M.J.; Deriu, A.; Colombo, P. Formation of self-organized nanoparticles by lecithin/chitosan ionic interaction. *Int J Pharm*. **2006,** 324, 67-73.
63. Zaki, S.S.O.; Ibrahim, M.N.; Katas, H. Particle Size Affects Concentration-Dependent Cytotoxicity of Chitosan Nanoparticles towards Mouse Hematopoietic Stem Cells. *J. Nanotechnol.* **2015**, 15, 1-5.
64. Huang, M.; Khor, E.; Lim, L.Y. Uptake and cytotoxicity of chitosan molecules and nanoparticles: effects of molecular weight and degree of deacetylation. *Pharm. Res*. **2004**, 21, 344-353.
65. Casettari, L.; Illum, L. Chitosan in nasal delivery systems for therapeutic drugs. *J. Control. Release* **2014**, 190, 189-200.
66. Mazzarino, L.; Coche-Guérente, L.; Labbé, P.; Lemos-Senna, E.; Borsali, R. On the mucoadhesive properties of chitosan-coated polycaprolactone nanoparticles loaded with curcumin using quartz crystal microbalance with dissipation monitoring. *J. Biomed. Nanotechnol*. **2014**, 10, 787-794.
67. Mistry, A.; Stolnik, S.; Illum, L. Nanoparticles for direct nose-to-brain delivery of drugs. *Int. J. Pharm*. **2009**, 379, 146-157.
68. Sosnik, A.J.; Neves, J.; Sarmento, B. Mucoadhesive polymers in the design of nano-drug delivery systems for administration by non-parenteral routes: A review. *Prog. Polym. Sci*. **2014**, 39, 2030-2075.
69. Sigurdsson, H.H.; Kirch, J.; Lehr, C.M. Mucus as a barrier to lipophilic drugs. *Int. J. Pharm.* **2013**, 453, 56-64.
70. Menchicchi, B.; Fuenzalida, J.P.; Bobbili, K.B.; Hensel, A.; Swamy, M.J.; Goycoolea, F.M. Structure of chitosan determines its interactions with mucin. *Biomacromol.* **2014**, 15, 3550-3558.
71. Chaves, P.D.; Ourique, A.F.; Frank, L.A.; Pohlmann, A.R.; Guterres, S.S.; Beck, R.C. Carvedilol-loaded nanocapsules: Mucoadhesive properties and permeability across the sublingual mucosa. *Eur. J. Pharm. Biopharm*. **2017**, 114, 88-95.
72. Singh, I.; Rana, V. Enhancement of Mucoadhesive Property of Polymers for Drug Delivery Applications: A Critical Review. *Rev. Adhesion Adhesives* **2013**, 1, 271-290.
73. Chiou, S.H.; Wu, W.T.; Huang, Y.Y.; Chung, T.W. Effects of the characteristics of chitosan on controlling drug release of chitosan coated PLLA microspheres. *J. Microencapsul*. **2001**, 18, 613-25.
74. Trotta, M.; Cavalli, R.; Chirio, D. Griseofulvin nanosuspension from triacetin-in-water emulsions. *S.T.P. Pharma Sci*. **2003**, 13, 423-426.
75. Zili, Z.; Sfar, S.; Fessi, H. Preparation and characterization of poly-e-caprolactone nanoparticles containing griseofulvin. *Int. J. Pharm*. **2005**, 294, 261-267.
76. Vllasaliu, D.; Exposito-Harris, R.; Heras A.; Casettari, L.; Garnett, M.; Illum, L.; Stolnik S. Tight junction modulation by chitosan nanoparticles: comparison with chitosan solution. *Int. J. Pharm*. **2010**, 15, 183-93.
77. Barbieri,S.; Sonvico, F.; Como, C.; Colombo, G.; Zani, F.; Buttini, F.; Bettini, R.; Rossi, A.; Colombo, P. Lecithin/chitosan controlled release nanopreparations of tamoxifen citrate: loading, enzyme-trigger release and cell uptake. *J Control Release*. **2013**, 167, 276-283.
78. Ahmad, J.; Singhal, M.; Amin, S.; Rizwanullah, M.; Akhter, S.; Kamal, M.A.; Haider, N.; Midoux, P.; Pichon,C. Bile salt stabilized vesicles (Bilosomes): a novel nano-pharmaceutical design for oral delivery of proteins and peptides. *Curr. Pharm. Des*. **2017**, 23, 1575-1588.
79. Colombo, M.; Figueiró, F.; de Fraga Dias, A.; Teixeira, H.F.; Battastini, A.M.O.; Koester, L.S. Kaempferol-loaded mucoadhesive nanoemulsion for intranasal administration reduces glioma growth in vitro. *Int. J. Pharm*. **2018**, 543, 214-223.

80. Khan, A.; Aqil, M.; Imam, S.S.; Ahad, A.; Sultana, Y.; Ali, A.; Khan, K. Temozolomide loaded nano lipid based chitosan hydrogel for nose to brain delivery: Characterization, nasal absorption, histopathology and cell line study. *Int. J. Biol. Macromol*. **2018**, 116, 1260-1267.

Capítulo 3

Nose-to-brain delivery of simvastatin mediated by chitosan-coated lipid-core nanocapsules for the treatment of glioblastoma

Artigo a ser submetido a periódico científico

O texto completo do capítulo 3, que no texto completo da tese defendida ocupa o intervalo de páginas compreendido entre as páginas 97 – 129, foi suprimido por tratar-se de manuscrito em preparação para publicação em periódico científico. Consta da descrição do potencial antitumoral de nanocápsulas revestidas por quitosana contento sinvastatina administradas pela via nasal no tratamento de ratos portadores de glioblastoma.

DISCUSSÃO GERAL

Nas últimas três décadas, a nanotecnologia farmacêutica recebeu considerável atenção e demonstrou um potencial significativo para o desenvolvimento de formulações inovadoras, tanto para a terapia quanto para o diagnóstico de doenças graves (MIR *et al*., 2017). Dentre as áreas mais estudadas, destaca-se a terapia do câncer.

O glioblastoma é uma neoplasia do SNC altamente letal, apresentando uma sobrevida média do paciente extremamente baixa (OZDEMIR-KAYNAK *et al*., 2018). Isso decorre de uma série de fatores, como: alto grau de invasividade e recorrência do tumor, heterogeneidade celular, presença da BHE e, consequentemente, baixa disponibilidade dos fármacos no tecido tumoral (SHERGALIS *et al*., 2018). Além disso, os agentes quimioterápicos disponíveis, até o momento, apresentam eficácia clínica limitada. A temozolomida (Temodal®) é o tratamento quimioterápico de escolha, no entanto, a sua administração aumenta a sobrevida média dos pacientes em, apenas, dois meses (STUPP *et al*., 2005). Assim, diversos estudos vem se concentrando em encontrar novas abordagens terapêuticas para o tratamento do glioblastoma. Destaca-se o uso de abordagens que visam aumentar a biodisponibilidade de fármacos no SNC, dentre elas o emprego da nanotecnologia e da via de administração nasal.

O interesse pela administração intranasal de fármacos com propriedades antitumorais nanoencapsulados para a entrega no SNC é recente e está em crescimento, sendo exemplos os estudos com temozolomida (CHU *et a*l., 2018), bevacizumab (SOUSA *et al*., 2019), carboplatina (ALEX *et al*., 2016), metotrexato (JAIN *et al*., 2016), camptotecina (TAKI *et al*., 2012; KANAZAWA *et al*., 2014), kaempferol (COLOMBO *et al*., 2018) e curcumina (MADANE *et al*., 2016; SHINDE and DEVARAJAN, 2017).

Essa via de administração elimina a necessidade do fármaco ultrapassar a BHE, pois, uma vez na cavidade nasal, o fármaco pode seguir pelo bulbo olfatório ou trigêmeo e, assim, acessar diretamente o cérebro (SONVICO *et al*., 2018). Além disso, outras vantagens dessa via residem na ausência de interferência do metabolismo de primeira passagem, ser uma via indolor e não-invasiva. Portanto, é uma via considerada confortável para o paciente (COMFORT *et al*., 2015). Por outro lado, uma limitação dessa via é a presença do mecanismo de depuração mucociliar, que pode remover imediatamente a formulação da cavidade nasal (ILLUM, 2003). Uma estratégia para

superar essa limitação é o emprego de sistemas nanoestruturados associados a polímeros mucoadesivos, que podem aumentar o contato entre a formulação e os locais de absorção na cavidade nasal. Assim, aumentando a permeação e absorção do fármaco (ILLUM, 2003; UGWOKE *et al*., 2005). Os sistemas poliméricos nanoestruturados têm atraído atenção em virtude do direcionamento do fármaco para alvos específicos, controle de liberação, aumento da eficiência e/ou biodisponibilidade, da sua versatilidade, segurança e biocompatibilidade (POHLMANN *et al*., 2013; FRANK *et al*., 2015). Além disso, o emprego de polímeros mucoadesivos vem sendo utilizado para preparar nanocápsulas para diversos fins, desde a administração oral (VERAGTEN *et al*., 2020), vaginal (FRANK *et al*., 2017) e sublingual (CHAVES *et al*., 2017) até a entrega cerebral (FONSECA *et al*., 2015).

O capítulo 1 da presente tese apresenta um artigo científico de revisão de literatura sobre a utilização da administração intranasal como uma estratégia para o tratamento do glioblastoma. Neste contexto, recentemente, várias formulações foram desenvolvidas visando aumentar a entrega de fármacos no cérebro, principalmente, utilizando sistemas nanoestruturados.

A sinvastatina, um fármaco que atua na inibição da síntese do colesterol, vem emergindo como um agente potencial para o tratamento do glioblastoma e de outros tipos de câncer. No entanto, seus mecanismos em oncologia ainda não estão completamente elucidados (Di BELLO *et al*., 2020). O glioblastoma, assim como outros tumores cerebrais malignos, apresenta elevadas taxas de síntese de colesterol e atividade da enzima HMG-CoA redutase aumentada (GRIEB *et al*., 1999). O colesterol é um componente indispensável das membranas celulares e sua biossíntese é controlada pela via do mevalonato, que controla a geranilação e farnesilação de proteínas. Essas modificações pós-traducionais são críticas para a isoprenilação das proteínas G (Ras, Rho ou Rac), que estão envolvidas na proliferação, progressão e sobrevivência de células tumorais (RIKITAKE e LIAO, 2005; ALTWAIRGI, 2015).

In vitro, a sinvastatina induz apoptose por meio da via de sinalização PI3K/Akt/caspase-3 (Wu *et al*., 2009). Além disso, apresenta propriedades anti-inflamatórias, que podem ser particularmente interessantes, visto que glioblastoma está normalmente associado à presença de um microambiente inflamatório (WATERS *et al*.,

2019). Contudo, o extenso metabolismo hepático da sinvastatina dificulta a sua aplicação no tratamento do glioblastoma, uma vez que é necessário que o fármaco atinja o SNC em altas concentrações (ROMANA *et al*., 2014). Até o momento, não existem estudos descritos na literatura que avaliem a liberação da sinvastatina pela via intranasal para tratamento do glioblastoma, seja na sua forma livre ou em nanosistemas.

Neste contexto, aliando as vantagens que a nanobiotecnologia e a administração intranasal podem oferecer, a nossa hipótese de trabalho considera que a nanoencapsulação da sinvastatina combinada ao revestimento com um polímero mucoadesivo podem promover uma maior concentração do fármaco no tecido cerebral. Consequentemente, há um aumento na eficácia terapêutica quando comparado com o fármaco não nanoencapsulado.

O capítulo 2 do presente trabalho apresentou o desenvolvimento de nanocápsulas revestidas com quitosana pela técnica inovadora *one-pot* e avaliou as suas propriedades mucoadesivas e de permeação/retenção pela mucosa nasal *in vitro*. O revestimento em uma única etapa (*one-pot)* otimizou o processo de revestimento previamente descrito por Bender e colaboradores (2012). Essa técnica consistia em um processo de duas etapas, sendo a primeira a produção das LNCs e após, em um segundo momento, a realização do revestimento das nanocápsulas (Bender *et al*., 2012). Além disso, comparamos as propriedades farmacêuticas relevantes em termos de caracterização físico-química, propriedades mucoadesivas, liberação e permeabilidade das formulações revestidas por quitosana com dois diferentes pesos moleculares (MW).

As nanocápsulas poliméricas foram produzidas com poly(ε-caprolactona), triglicerídeos de cadeia média, monoestearato de sorbitano, sendo estabilizadas e revestidas com lecitina e quitosana. Essa formulação apresenta a vantagem de encapsular eficientemente fármacos lipofílicos como a sinvastatina (JÄGER *et al*., 2009; VENTURINI *et al*., 2011). A associação, entre a composição e o método de obtenção das LNCs empregado, produziu nanocápsulas com tamanho de partícula adequado e distribuição estreita, como confirmado por técnicas complementares como difração de laser, espalhamento de luz dinâmico e análise de rastreamento de nanopartículas. Além disso, observamos que o revestimento das nanocápsulas com quitosana de diferentes MW (21 kDa e 152 kDa) influenciou suas propriedades físico-químicas. Obtivemos

nanopartículas com tamanho menores quanto foi utilizada a quitosana de menor MW, conforme já descrito para outros tipos de partículas (SONVICO *et a*l., 2006; HALIZA *et al*., 2006).

O emprego da quitosana, um biopolímero catiônico, representa uma estratégia interessante para superar as limitações de fármacos com baixa permeabilidade nasal. A interação eletrostática da partícula carregada positivamente com os sítios aniônicos do muco proporciona que essa partícula permaneça mais tempo em contato com a mucosa, assim potencializando a absorção de fármacos (MAZZARINO *et al*., 2014; SOSNIK *et al*., 2014). A mucosa nasal possui características aniônicas devido a presença de moléculas de mucina, que é uma glicoproteína presente no muco (SINGH e RANA, 2013).

Em seguida, avaliamos o comportamento adesivo das formulações quando colocadas em contato com diferentes concentrações de mucina (Capítulo 2, Figura 3). Os resultados de diâmetro de partícula e potencial zeta, após o contato com a mucina, evidenciaram uma grande interação das nanocápsulas com essa glicoproteína. Além disso, a formulação revestida com a quitosana com MW maior, apresentou maior índice de mucoadesividade, provavelmente, devido a sua maior cadeia polimérica apresentar mais sítios disponíveis de interação com a mucina.

A liberação do fármaco a partir das nanocápsulas foi mais lenta quando comparada a solução controle devido, principalmente, às duas barreiras de difusão: a dispersão lipídica presente no núcleo da nanocápsulas e a parede polimérica de PCL (Capítulo 2, Figura 4). Além disso, estudos anteriores demonstraram que a viscosidade da quitosana utilizada no desenvolvimento de formulações é um fator importante para modular o controle de liberação de fármacos (CHIOU *et al*., 2001). Outro fator que pode influenciar no perfil de liberação é o tamanho das nanopartículas. De fato, a formulação produzida com quitosana de maior MW e maior diâmetro de partícula proporcionou melhor controle de liberação do fármaco (TROTTA *et al*., 2003; ZILI *et al*.; 2005).

A avaliação da permeabilidade das formulações na mucosa nasal foi realizada por dois modelos distintos. Primeiramente, pelo modelo *in vitro* utilizando células nasais humanas da linhagem RPMI 2650 (Capítulo 2, Figura 5). Nesse caso, as células foram cultivadas sob placas Transwells®, ocorrendo a formação de uma monocamada celular

que também tem capacidade de secretar muco em sua superfície apical (POZZOLI *et al*., 2016). A quantificação da fração permeada foi realizada com cromatografia líquida de alta eficiência. Os resultados demonstraram que as nanocápsulas aumentaram significativamente a quantidade de sinvastatina permeada pela monocamada celular em comparação a sinvastatina livre.

No caso do segundo modelo utilizado, os resultados dos estudos de permeação/retenção *ex vivo* na mucosa nasal de coelho confirmaram e adicionaram mais evidências que a nanoencapsulação da SVT aumentou significativamente sua permeação na mucosa nasal (Capítulo 2, Figura 6). Além disso, a retenção do fármaco na mucosa nasal foi maior quando nanoencapsulado, porém não apresentou diferença significativa entre as duas formulações avaliadas (p>0.05). Também observamos, em ambos modelos estudados, uma menor permeação do fármaco para a formulação revestida com a quitosana de maior MW. Esse resulado pode ser explicado pela cinética de liberação mais lenta evidenciada para essa formulação e que, provavelmente, contribuiu para limitar a quantidade de fármaco permeado. E, também, devido ao seu maior tamanho de partícula, que pode ter dificultado sua absorção pela mucosa, conforme já estudado anteriormente (AHMAD *et al*., 2017). Estudos anteriores demonstraram que a biodegradação das nanopartículas por enzimas na barreira mucosa ou intracelularmente pode ser essencial para melhorar o transporte transcelular de fármacos lipofílicos (BARBIERI *et al*., 2013).

Um estudo paralelo de permeação *ex vivo* foi realizado para avaliar possíveis alterações histológicas causadas pelas formulações na mucosa nasal de coelho (Capítulo 2, Figura 7). Contudo, nesse estudo preliminar de toxicidade não foram evidenciadas alterações histológicas na mucosa, indicando a viabilidade das formulações na administração intranasal.

No capítulo 3, avaliamos a citotoxicidade *in vitro* da suspensão de nanocápsulas (revestida com a quitosana de baixo MW) e da sinvastatina livre em duas linhagens tumorais de glioma (Capítulo 3, Figura 2 e Tabela 3). Os resultados obtidos demonstraram que na linhagem C6 (rato), nos diferentes tempo de tratamento (24, 48 e 72 h), os valores de IC_{50} da SVT livre e do fármaco nanoencapsulado foram equivalentes. Na linhagem U-138 MG (humana), em 24 h e 48 os valores de IC_{50}

também foram equivalente para os 2 tratamentos. Por outro lado, após 72 h de tratamento, a sinvastatina livre apresentou IC_{50} de 2.05 ± 0.13 µM, enquanto a $LNC_{SVT\text{-}chit}$ apresentou IC_{50} de 1.18 ± 0.09, evidenciando uma redução significativa ($p < 0.05$). Esse achado demonstra a necessidade de um tempo maior de incubação para a internalização e atividade citotóxica da $LNC_{SVT\text{-}chit}$.

Comparando os valores de IC_{50} entre as duas linhagens celulares estudas, a linhagem U-138 MG apresentou maior resistência ao tratamento com a sinvastatina, corroborando com dados da literatura que demonstraram ser necessário doses maiores de tratamento para a linhagem U-138 MG (ZANOTTO-FILHO *et al*., 2012; SILVA *et al*., 2016). A diferença na sensibilidade das células de glioma pode ser devido ao perfil de mutações genéticas, potencial endocítico e permeabilidade de membrana (ZANOTTO-FILHO *et al*., 2013).

Após a realização dos experimentos iniciais *in vitro*, seguimos os estudos avaliando a distribuição cerebral da sinvastatina após a administração intranasal *in vivo* da nanoformulação e da sua forma livre (Capítulo 3, Figura 3). Observou-se um aumento significativo ($p < 0,001$) do teor de fármaco no cérebro dos animais que receberam a nanoformulação. Esse incremento foi de, aproximadamente, 2,4 vezes em relação ao fármaco livre. Esse fato não é atribuído apenas à rápida depuração mucociliar e drenagem nasal do fármaco livre, mas também a sua baixa solubilidade em meio aquoso, que é um fator que limita a sua absorção (SONVICO *et al*., 2018; UPADHAYA *et al*., 2020). Além disso, este achado corrobora e confirma os resultados de permeação/retenção do capítulo 2, em que a nanoformulação apresentou uma maior permeação em relação ao fármaco livre.

A administração intranasal de nanopartículas poliméricas visando facilitar o acesso de fármacos no cérebro vem sendo amplamente estudada (FONSECA *et al*., 2015; ALEX *et al*., 2016; DE OLIVEIRA JUNIOR *et al*., 2019; SOUSA *et al*., 2019). O maior transporte de fármacos da cavidade nasal para o cérebro quanto nanoencapsulado pode também estar relacionado ao seu pequeno tamanho (100-400 nm), o que permite maior capacidade de penetrar no muco nasal e, em seguida, o fármaco ser transportada através do nervo olfatório e trigêmeo para o cérebro (MISTRY *et al*., 2009). Além disso, estudos anteriores (COLOMBO *et al*., 2018; KHAN *et al*.,

2018) demonstraram que nanopartículas revestidas com quitosana aumentam a permeação de fármacos através da mucosa nasal, em comparação com o fármaco livre e nanopartículas não revestidas usadas como controle.

Com base nesse achado, foi avaliado o efeito do tratamento com a sinvastatina administrada intranasalmente em modelo *in vivo* de gliomas implantados unilateralmente em cérebros de ratos. Após 5 dias do implante do tumor, os animais foram tratados por 14 dias consecutivos com salina, nanocápsulas brancas, sinvastatina livre e com as nanocápsulas mucoadesivas contendo sinvastatina. As análises histopatológicas das lâminas de H&E demonstraram que os animais tratados com a nanoformulação apresentaram uma redução significativa no volume do tumor (78%) após 14 dias de tratamento (Capítulo 3, Figura 4). Ressalta-se que o tratamento com a $LNC_{SVT\text{-}chit}$, além de reduzir o tamanho do tumor, foi capaz de reduzir algumas características histopatológicas de malignidade dos tumores como hemorragia, necrose e pseudopaliçada periférica (Capítulo 3, Tabela 4 e Figura 5).

Esses resultados foram observados somente nos animais tratados com a sinvastatina nanoencapsulada, portanto, fármaco na forma livre não apresentou redução significativa no tamanho tumoral quando comparado com os controles. Esse resultado pode ser atribuído emprego de sistemas nanoestruturados associados a um polímero mucoadesivo. A presença da quitosana na superfície das nanocápsulas pode prolongar a permanência da formulação na cavidade nasal, além de abir as *tight junctions* entre as células epiteliais nasais, assim promovendo a permeação do fármaco pelas barreiras biológicas e conferindo maior absorção cerebral da SVT (MISTRY et al., 2009; VLLASALIU et al., 2010; CASETTARI e ILLUM, 2014).

As análises bioquímicas do soro do animais demonstraram que o tratamento com $LNC_{SVT\text{-}chit}$ não alterou os marcadores bioquímicos de toxicidade renal e hepáticos (Capítulo 3, Tabela 5). Além disso, o tratamento não afetou o ganho de peso dos animais. Por outro lado, o tratamento com $LNC_{SVT\text{-}chit}$ reduziu o nível sérico de colesterol total. Esse fato, pode ser explicado devido ao mecanismo indireto de absorção de fármacos administrados pela via nasal. Neste caso, o fármaco, é primeiramente absorvido na circulação sistêmica e, subsequentemente, acessa o SNC após cruzar a BHE (SONVICO *et al*., 2018). Assim, ao entrar na circulação a sinvastatina pode desempenhar seu efeito

de reduzir os níveis de colesterol. Esta redução não foi observada para o fármaco livre, corroborando com os demais achados e evidenciando a maior absorção da sinvastatina pela mucosa nasal quando nanoencapsulada. Apesar da suspensão de nanocápsulas branca (LNC_{chit}) apresentar uma pequena redução da viabilidade celular após 72 h de tratamento nas duas linhagens estudadas ($p<0,05$), no estudo *in vivo*, não foi evidenciado alterações nos marcadores bioquímicos avaliados bem como alteração no ganho de peso dos animais.

Previamente, nosso grupo mostrou que nanocápsulas de núcleo lipídico foram mais eficientes em carrear indometacina e *trans*-resveratrol para o cérebro de ratos após administração intraperitoneal quando comparado com o fármaco livre. E, portanto, apresentaram maior atividade antitumoral *in vivo* (BERNARDI *et al*., 2009b; FROZZA *et al*., 2010; FIGUEIRÓ *et al*., 2013). Além disso, Fonseca e colaboradores (2015) prepararam nanocápsulas poliméricas mucoadesivas com uma de blenda PCL e um copolímero anfifílico em bloco [Poli(MMA-b-DMAEMA)], e avaliam a liberação cerebral da olanzapina pela via nasal. Na avaliação *in vivo* das nanocápsulas, foi demonstrado que a administração intranasal da formulação em ratos aumentou o teor de fármaco no cérebro, o que acarretou maior efeito antipsicótico no modelo animal de esquizofrenia (FONSECA *et al*., 2015).

Várias evidências científicas demonstram que as estatinas também apresentam papel terapêutico na Doença de Alzheimer (FONSECA *et al*., 2010). Recentemente, Lorenzoni e colaboradores (2020) demonstraram que a administração oral de nanocápsulas de núcleo lipídico contendo sinvastatina foi capaz de reverter o dano cognitivo induzido por obesidade e hipercolesterolemia em ratos (LORENZONI *et al*., 2020). Os níveis elevados de colesterol é um fator de riscos para o desenvolvimento da Doença de Alzheimer. A hipercolesterolemia está associados com a produção do peptídeo β-amilóide insolúvel que se deposita no cérebro de pacientes acometidos por essa doença (SPARKS *et al*., 1990).

Embora a sinvastatina não seja um fármaco utilizado no tratamento do glioblastoma, nossos resultados sugerem que a sinvastatina, quando nanoencapsulada, pode ser considerada uma alternativa promissora no tratamento do glioblastoma por meio de uma administração minimamente invasiva. Portanto, de forma inédita, pode-se

considerar que, nesta tese, foram desenvolvidas nanocápsulas de núcleo lipídico revestidas por quitosana contendo sinvastatina por um método inovador e com resultados *in vivo* promissores.

CONCLUSÕES GERAIS

Este trabalho demonstrou a viabilidade tecnológica na obtenção de nanocápsulas de núcleo lipídico revestidas com quitosana contendo sinvastatina. As formulações obtidas pela técnica de revestimento *one-pot* apresentaram características físico-químicas adequadas e a incorporação do fármaco não influenciou nas suas propriedades. As formulações combinam uma liberação controlada de sinvastatina e propriedades de mucoadesão que são capazes de aumentar a permeação/retenção do fármaco na mucosa nasal. Esses resultados foram demonstrados utilizando dois modelos diferentes de epitélio nasal. O tratamento com formulação desenvolvida demonstrou citotoxicidade frente à duas linhagens celulares de glioma *in vitro*. Além disso, administração intranasal da nanoformulação aumentou o teor de sinvastatina no cérebro de ratos Wistar quando comparado com o fármaco na sua forma livre. Consequentemente, a nanoencapsulação da sinvastatina também aumentou seu efeito antitumoral *in vivo* após administração intranasal. Portanto, o conjunto dos resultados obtidos ao longo dessa tese demonstram, de forma inédita, as potencialidades do uso de nanocápsulas mucoadesivas contento sinvastatina para administração por via nasal com vistas para a terapia do glioblastoma.

REFERÊNCIAS

AHMAD, J.; SINGHAL, M.; AMIN, S.; RIZWANULLAH, M.; AKHTER, S.; KAMAL, M.A.; HAIDER, N.; MIDOUX, P.; PICHON, C. Bile salt stabilized vesicles (Bilosomes): a novel nano-pharmaceutical design for oral delivery of proteins and peptides. **Current Pharmaceutical Design**, v. 23, n. 11, p. 1575–1588, 2017.

ALAM, M.I.; BEG, S.; SAMAD, A. BABOOTA, S.; KOHLI, K.; ALI, J.; AHUJA, A.; AKBAR, M. Strategy for effective brain drug delivery. **European Journal of Pharmaceutical Sciences**, v. 40, p. 385–403, 2010.

ALEX, A.T.; JOSEPH, A.; SHAVI, G.; RAO, J.V.; UDUPA, N. Development and evaluation of carboplatin-loaded 1148 PCL nanoparticles for intranasal delivery. **Drug Delivery**, v. 23, p. 2144-2153, 2016.

ALI, A.; AHMED, S. A review on chitosan and its nanocomposites in drug delivery. **International Journal of Biological Macromolecules**, v. 109, p. 273–286, 2008.

ALIZADEH, J.; ZEKI, A.A.; MIRZAEI, N.; TEWARY, S.; REZAEI MOGHADAM, A.; GLOGOWSKA, A.; NAGAKANNAN, P.; EFTEKHARPOUR, E.; WIECHEC, E.; GORDON, J.W.; XU, F.Y.; FIELD, J.T.; YONEDA, K.Y.; KENYON, N.J.; HASHEMI, M.; HATCH, G.M.; HOMBACH-KLONISCH, S.; KLONISCH, T.; GHAVAMI, S. Mevalonate cascade inhibition by simvastatin induces the intrinsic apoptosis pathway via depletion of isoprenoids in tumor cells. **Scientific Reports**, v. 7, p. 44841, 2017.

ALTWAIRGI, A.K. Statins are potential anticancerous agents (review). O**ncology reports**, v. 33, n. 3, p. 1019-39, 2015.

AMERICAN CANCER SOCIETY. **Cancer facts & figures 2019**. Atlanta: American Cancer Society, 2019

ARMITAGE, J. The safety of statins in clinical practice. **The Lancet**, v. B370, n. 9601, p. 1781-1790, 2007.

BABABEYGY, S.R.; POLEVAYA, N.V.; YOUSSEF, S.; SUN, A.; XIONG, A.; PRUGPICHAILERS, T.; VEERAVAGU, A.; HOU, L.C.; STEINMAN, L.; TSE, V. HMG-CoA Reductase Inhibition Causes Increased Necrosis and Apoptosis in an In Vivo Mouse Glioblastoma Multiforme Model. **Anticancer Research**, v. 29, n. 12, p. 4901–4908, 2009.

BAGRI, A.; KOUROS-MEHR, H.; LEONG, K.G.; PLOWMAN, G.D. Use of anti-VEGF adjuvant therapy in cancer: challenges and rationale. **Trends in Molecular Medicine**, v.16, n.3, p.122-132, 2010.

BARBIERI, S.; SONVICO, F.; COMO, C.; COLOMBO, G.; ZANI, F.; BUTTINI, F.; BETTINI, R.; ROSSI, A.; COLOMBO, P. Lecithin/chitosan controlled release nanopreparations of tamoxifen citrate: loading, enzyme-trigger release and cell uptake. **Journal Controlled Release**, v. 167, n. 3, p. 276–83, 2013.

BELLOSTA, S.; PAOLETTI, R.; CORSINI, A. Safety of statins: focus on clinical pharmacokinetics and drug interactions. **Circulation**, v. 109, n. (23 Suppl 1), p.III50-7, 2004.

BENDER, E.A.; ADORNE, M.D.; COLOMÉ, L.M.; ABDALLA, D.S.P.; GUTERRES, S.S.; POHLMANN, A.R. Hemocompatibility of poly(epsilon-caprolactone) lipid-core nanocapsules stabilized with polysorbate 80-lecithin and uncoated or coated with chitosan. **International Journal of Pharmaceutics**, v. 426, n. (1-2), p. 271–279, 2012.

BERNARDI, A.; FROZZA, R,L.; JÄGER, E.; FIGUEIRO, F.; BAVARESCO, L.; SALBEGO, C.; POHLMANN, A.R.; GUTERRES, S.S ; BATTASTINI, A.M. Selective cytotoxicity of indomethacin and indomethacin ethyl ester-loaded nanocapsules against

glioma cell lines: an in vitro study. **European Journal of Pharmacology**, v. 586, n. 1-3, p. 24-34, 2008.

BERNARDI, A.; ZILBERSTEIN, A.C.; JAGER, E.; CAMPOS, M.M.; MORRONE, F.B.; CALIXTO, J.B.; POHLMANN, A.R.; GUTERRES, S.S.; BATTASTINI, A.M.O. Effects of indomethacin-loaded nanocapsules in experimental models of inflammation in rats. **British Journal of Pharmacology**, v. 158, v. 4, p. 1104-1111, 2009a.

BERNARDI, A.; BRAGANHOL, E.; JÄGER, E.; FIGUEIRÓ, F.; EDELWEISS, M.I.; POHLMANN, A.R.; GUTERRES, S. S.; BATTASTINI, A.M.O. Indomethacinloaded nanocapsules treatment reduces in vivo glioblastoma growth in a rat glioma model. **Cancer Letters**, v. 281, n. 1, p. 53–63, 2009b.

BIFULCO, M. Therapeutic potential of statins in thyroid proliferative disease. **Nature clinical practice. Endocrinology & metabolism**, v. 4, n. 5, p. 242–243, 2008.

BERNKOP-SCHNÜRCH, A.; DÜNNHAUPT, S. Chitosan-based drug delivery systems. **European Journal of Pharmaceutics and Biopharmaceutics**, v. 81, n. 3, p. 463–9, 2012.

BRASIL. Instituto Nacional de Câncer José Alencar Gomes da Silva (INCA). Estimativa 2020: incidência de câncer no Brasil. Rio de Janeiro: INCA, 2020. 106 p.

BRUINSMANN, F.A.; RICHTER, V.G.; DE CRISTO SOARES ALVE, A, AGUIRRE T.; RAFFIN, A.R; GUTERRES, S.S.; SONVICO, F. Nasal Drug Delivery of Anticancer Drugs for the Treatment of Glioblastoma: Preclinical and Clinical Trials. **Molecules**, v. 24, n. 23, p.pii: E4312, 2019.

BULCAO, R.P.; FREITAS, F.A.; VENTURINI, C.G; DALLEGRAVE, E.; DURGANTE, J.; GOETHEL, G.; CERSKI, C.T.; ZIELINSKY, P.; POHLMANN, A.R.; GUTERRES, S.S.; GARCIA, S.C. Acute and subchronic toxicity evaluation of

poly(epsilon-caprolactone) lipid-core nanocapsules in rats. **Toxicological Sciences**, v. 132, n. 1, p. 162-176, 2012.

CAGEL, M.; GROTZ, E.; BERNABEU, E.; MORETTON, M.A.; CHIAPPETTA, D.A. Doxorubicin: nanotechnological overviews from bench to bedside. **Drug Discovery Today**, v. 22, n. 2, p. 270-281, 2017.

CAMPBELL, M.J.; ESSERMAN, L.J.; ZHOU, Y.; SHOEMAKER, M.; LOBO, M.; BORMAN, E.; BAEHNER, F.; KUMAR, A.S.; ADDUCI, K.; MARX, C.; PETRICOIN, E.F.; LIOTTA, L.A.; WINTERS, M.; BENZ, S.; BENZ, C.C. Breast cancer growth prevention by statins. **Cancer Research**, v. 66, n. 17, p. 8707-14, 2006.

CASETTARI, L.; ILLUM, L. Chitosan in nasal delivery systems for therapeutic drugs. J. **Control. Release**, 190, 189–200, 2014.

CHAN, K.K.; OZA, A.M.; SIU, L.L. The statins as anticancer agents. **Clinical Cancer Research**, v. 9, n. 1, p. 10–19, 2003.

CHAPMAN, C.D.; FREY, W.H.; CRAFT, S.; DANIELYAN, L.; HALLSCHMID, M.; SCHIÖTH, H.B.; BENEDICT, C. Intranasal treatment of central nervous system dysfunction in humans. **Pharmaceutical Research**, v. 30, n. 10, p. 2475–84, 2013.

CHAVES, P.D.; OURIQUE, A.F.; FRANK, L.A.; POHLMANN, A.R.; GUTERRES, S.S.; BECK. R.C. Carvedilol-loaded nanocapsules: Mucoadhesive properties and permeability across the sublingual mucosa. **European Journal of Pharmaceutics and Biopharmaceutics**, v. 114, p. 88-95, 2017.

CHIANG, K.H,; CHENG, W.L; SHIH, C.M; LIN, Y.W; TSAO, N.W; KAO, YT; LIN, C.T; WU, S.C; HUANG, C.Y; LIN, F.Y. Statins, HMG-CoA Reductase Inhibitors, Improve Neovascularization by Increasing the Expression Density of CXCR4 in Endothelial Progenitor Cells. **Plos one**, v. 26, p. 10(8):e013640, 2015.

CHINOT, O.L.; WICK, W.; MASON, W.; HENRIKSSON, R.; SARAN, F.; NISHIKAWA, R.; CARPENTIER, A.F.; HOANG-XUAN, K.; KAVAN, P.; CERNEA, D. Bevacizumab plus radiotherapy-temozolomide for newly diagnosed glioblastoma. **New England Journal of Medicine**, v. 370, p. 709–722, 2014.

CHIOU, S.H.; WU, W.T.; HUANG, Y.Y.; CHUNG, T.W. Effects of the characteristics of chitosan on controlling drug release of chitosan coated PLLA microspheres. **Journal of Microencapsulation**, v. 18, n. 5, 613–625, 2001.

CHO, S.J.; KIM, J.S.; KIM, J.M.; LEE, J.Y.; JUNG, H.C.; SONG, I.S. Simvastatin induces apoptosis in human colon cancer cells and in tumor xenografts, and attenuates colitis-associated colon cancer in mice. **International Journal of Cancer**, v. 123, n. 4, p. 951-7, 2008.

CHU, L.; AIPING, W.; NI, L.; YAN, X.; SONG, Y.; ZHAO, M.; , SUN, K.; MU, H.; LIU, S.; WU, Z.; ZHANG, C. Nose-to-brain delivery of temozolomide-loaded PLGA nanoparticles functionalized with anti-EPHA3 1124 for glioblastoma targeting. **Drug Delivery**, v. 25, p. 1634-1641, 2018.

COLOMBO, M.; FIGUEIRÓ, F.; DE FRAGA DIAS, A.; TEIXEIRA, H.F.; BATTASTINI, A.M.O.; KOESTER, LS. Kaempferol-loaded mucoadhesive nanoemulsion for intranasal administration reduces glioma growth in vitro. **International Journal of Pharmaceutics**, v. 543, n. (1-2), p. 214-223, 2018.

COMFORT, C.; GARRASTAZU, G.; POZZOLI, M.; SONVICO, F. Opportunities and challenges for the nasal administration of nanoemulsions. **Current Topics in Medicinal Chemistry**, v. 15, n. 4, p. 356-68, 2015.

DAVIES, J.T.; DELFINO, S.F.; FEINBERG, C.E.; JOHNSON, M.F.; NAPPI, V.L.; OLINGER, J.T.; SCHWAB, A.P.; SWANSON, H.I. Current and Emerging Uses of Statins in Clinical Therapeutics: A Review. **Lipid Insights**, v. 14, n. 9, p. 13-29, 2016.

DAVIS, M.W. “Glioblastoma: Overview of Disease and Treatment”. **Clinical journal of oncology nursing**, v. 20, n. 5, p. S2-8, 2016.

DE OLIVEIRA JUNIOR, E.R.; NASCIMENTO, T.L.; SALOMÃO, M.A.; DA SILVA, A.C.G.; VALADARES, M.C.; LIMA, E.M. Increased Nose-to-Brain Delivery of Melatonin Mediated by Polycaprolactone Nanoparticles for the Treatment of Glioblastoma. **Pharmaceutical Research**, v. 36, p. 131, 2019.

DENG, J.L.; ZHANG, R.; ZENG, Y.; ZHU, Y.S.; WANG, G. Statins induce cell apoptosis through a modulation of AKT/FOXO1 pathway in prostate cancer cells. **Cancer Management and Research**, v. 11, p. 7231-7242, 2019.

DHURIA, S.V.; HANSON, L.R.; FREY, W.H. Intranasal delivery to the central nervous system: mechanisms and experimental considerations. **Journal of pharmaceutical sciences**, v. 99, n. 4, p. 1654–73, 2010.

DI BELLO, E.; ZWERGEL, C.; MAI, A.; VALENTE, S. The Innovative Potential of Statins in Cancer: New Targets for New Therapies. **Frontiers in Chemistry**, v. 8, n. 516, 2020.

DIMER, F.A.; ORTIZ, M.; PASE, C.S.; ROVERSI, K.; FRIEDRICH, R.B.; POHLMANN, A.R.; BURGER, M.E.; GUTERRES, S.S. Nanoencapsulation of Olanzapine Increases Its Efficacy in Antipsychotic Treatment and Reduces Adverse Effects. **Journal of Biomedical Nanotechnology**, v. 10, n. 6, p. 1137-1145, 2014.

DJUPESLAND, P.G. Nasal drug delivery devices: characteristics and performance in a clinical perspective-a review. **Drug Delivery and Translational Research**, v. 3, n. 1, p. 42–62, 2013.

DREWES, C.C,; FIEL, L.A.; BEXIGA, C.G.; ASBAHR, A.C.; UCHIYAMA, M.K.; COGLIATI, B.; ARAKI, K.; GUTERRES, S.S.; POHLMANN, A.R.; FARSKY, S.P.

Novel therapeutic mechanisms determine the effectiveness of lipid-core nanocapsules on melanoma models. **International Journal of Nanomedicine**, v. 11, p. 1261-79, 2016.

FERRIS, J.S.; MCCOY, L.; NEUGUT, A.I.; WRENSCH, M.; LAI, R.; HMG CoA reductase inhibitors, NSAIDs and risk of glioma. **International Journal of Cancer**, v. 131, n. 6, 2012

FESSI, H.; PUISIEUX, F.; DEVISSAGUET, J. P.; AMOURY, N.; BENITA, S. Nanocapsules formation by interfacial polymer deposition following solvent displacement. **International Journal of Pharmaceutics**, v. 113, p. 1-4, 1989.

FIEL, L.A.; REBÊLO, L.M.; SANTIAGO, T.M.; ADORNE, M.D.; GUTERRES, S.S.; SOUSA, J.S.; POHLMANN, A.R. Diverse deformation properties of polymeric nanocapsules and lipid-core nanocapsules. **Soft Matter**, v. 7, n. 16, p. 7240 – 7247, 2011.

FIEL, L.A.; ADORNE, M.D.; GUTERRES, S.S.; NETZ, P.A.; POHLMANN, A.R. Variable temperature multiple light scattering analysis to determine the enthalpic term of a reversible agglomeration in submicrometric colloidal formulations: A quick quantitative comparison of the relative physical stability. **Colloids and Surfaces A: Physicochemical and Engineering Aspects**, v. 431. p. 93-104, 2013.

FIGUEIRÓ, F.; BERNARDI, A.; FROZZA, R.L.; TERROSO, T.; ZANOTTOFILHO, A.; JANDREY, E.H.F.; MOREIRA, J.C.F.; SALBEGO, C.G.; EDELWEISS, M.I.; POHLMANN, A.R.; GUTERRES, S.S.; BATTASTINI, A.M.O. Resveratrol-Loaded Lipid-Core Nanocapsules Treatment Reduces In Vitro and In Vivo Glioma Growth. **Journal of Biomedical Nanotechnology**, v. 9, n. 3, p. 1–11, 2012.

FIGUEIRÓ, F.; OLIVEIRA, C.P.; MENDES, F.B.; BERGAMIN, L.; ROCKENBACH, L.; JANDREY, E.H.F.; Edelweiss, M.I; GUTERRES, S.S.; POHLMANN, A.R.;

BATTASTINI, A.M . Pharmacological Improvement and Preclinical Evaluation of Methotrexate-Loaded Lipid-Core Nanocapsules in a Glioblastoma Model. **Journal of Biomedical Nanotechnology**, v. 11, n. 10, p. 1808-1818, 2015.

FONSECA, A.C.; RESENDE, R.; OLIVEIRA, C.R.; PEREIRA, C.M. Cholesterol and statins in Alzheimer's disease: Current controversies. **Experimental Neurology**, v. 223, p. 282-293, 2010.

FONSECA, F.N.; BETTI, A.H.; CARVALHO, F.C.; GREMIÃO, M.P.; DIMER, F.A.; GUTERRES, S.S.; TEBALDI, M.L.; RATES, S.M.; POHLMANN, A.R. Mucoadhesive Amphiphilic Methacrylic Copolymer-Functionalized Poly(ε-caprolactone) Nanocapsules for Nose-to-Brain Delivery of Olanzapine. **Journal of Biomedical Nanotechnology**, v. 11, n. 8, p. 1472-81, 2015.

FONTANA, M.C.; CORADINI, K.; POHLMANN, A.R.; GUTERRES, S.S.; BECK, R.C. Nanocapsules prepared from amorphous polyesters: Effect on the physiochemical characteristics, drug release, and photostability. **Journal of Nanoscience and Nanotechnology**, v. 10, n. 5, p. 3091-3099, 2010.

FRANK, L.A.; CONTRI, R.V.; BECK, R.C.; POHLMANN, A.R.; GUTERRES, S.S. Improving drug biological effects by encapsulation into polymeric nanocapsules. **Wiley Interdisciplinary Rev Nanomed Nanobiotechnology**, v. 7, n. 5, p. 623-39, 2015.

FRANK, L.A.; CHAVES, P.S.; D'AMORE, C.M.; CONTRI, R.V.; FRANK, A.G.; BECK, R.C.; POHLMANN, A.R.; BUFFON, A.; GUTERRES, SS. The use of chitosan as cationic coating or gel vehicle for polymeric nanocapsules: Increasing penetration and adhesion of imiquimod in vaginal tissue. **European Journal of Pharmaceutics and Biopharmaceutics**, v. 114, p. 202-212, 2017.

FROZZA, R.L.; BERNARDI, A.; PAESE, K.; HOPPE, J.B.; SILVA, T.; BATTASTINI, A.M.O.; POHLMANN, A.R.; GUTERRES, S.S.; SALBEGO, C.

Characterization oftrans-Resveratrol-Loaded Lipid-Core Nanocapsules and Tissue Distribution Studies in Rats. **Journal of Biomedical Nanotechnology**, v. 6, p. 1–10, 2010.

GAIST, D.; ANDERSEN, L.; HALLAS, J.; SØRENSEN, H.T.; SCHRØDER, H.D.; FRIIS, S. Use of statins and risk of glioma: a nationwide case-control study in Denmark. **British Journal of Cancer**, v. 108, n. 3, p. 715-20, 2013

GANIPINENI, L.P.; UCAKAR, B.; JOUDIOU, N.; RIVA, R.; JÉRÔME, C.; GALLEZ, B.; DANHIER, F.; PRÉAT, V.Paclitaxel-loaded multifunctional nanoparticles for the targeted treatment of glioblastoma. **Journal of Drug Targeting**, v. 27, n. 5-6, p. 614-623, 2019.

GILBERT, M.R.; DIGNAM, J.J.; ARMSTRONG, T.S.; WEFEL, J.S.; BLUMENTHAL, D.T.; VOGELBAUM, M.A.; COLMAN, H.; CHAKRAVARTI, A.; PUGH, S.; WON, M.; et al. A randomized trial of bevacizumab for newly diagnosed glioblastoma. **New England Journal of Medicine**, v. 370, p. 699–708, 2014.

GIZURARSON, S. Anatomical and Histological Factors Affecting Intranasal Drug and Vaccine Delivery. **Current Drug Delivery**, v. 9, n. 5, p 566-582, 2012.

GLOBOCAN/IARC. Global Cancer Observatory: Cancer Today. Lyon, France: International Agency for Research on Cancer (2018). Disponível em <https://gco.iarc.fr/today/home> Acesso em maio de 2020.

GOC, A.; KOCHUPARAMBIL, S.T.; AL-HUSEIN, B.; AL-AZAYZIH, A.; MOHAMMAD, S.; SOMANATH, P.R. Simultaneous modulation of the intrinsic and extrinsic pathways by simvastatin in mediating prostate cancer cell apoptosis. **BMC Cancer**, v. 12, n. 1, p. 409, 2012.

GRIEB, P.; RYBA, M.S, JAGIELSKI, J.; GACKOWSKI, W.; PACZKOWSKI, P.; CHRAPUSTA, S.J. Serum cholesterol in cerebral malignancies. **Journal of Neuro-Oncology**, v. 41, n. 2, p. 175-80, 1999.

HALIZA, K.; ALPAR, H.O. Development and characterization of chitosan nanoparticles for siRNA delivery. **Journal Control. Release**, v. 115, n. 2, p. 216–225, 2006.

HAN, S.J.; ENGLOT, D.J.; BIRK, H.; MOLINARO, A.M.; CHANG, S.M.; CLARKE, J.L.; PRADOS, M.D.; TAYLOR, J.W.; BERGER, M.S.; BUTOWSKI, N.A Impact of Timing of Concurrent Chemoradiation for Newly Diagnosed Glioblastoma: A Critical Review of Current Evidence. **Neurosurgery**, v. 62, n. 1, p. 160-5, 2015.

HARDER, B.G.; BLOMQUIST, M. R.; WANG, J.; KIM, A.J.; WOODWORTH, G.F.; WINKLES, J.A.; LOFTUS, J.C.; TRAN, N.L. Developments in Blood-Brain Barrier Penetrance and Drug Repurposing for Improved Treatment of Glioblastoma. **Frontiers in oncology**, v. 8, 462, 2018.

HE, X.; ZHU, Y.; WANG, M.; JING, G.; ZHU, R.; WANG, S. Antidepressant effects of curcumin and HU-211 coencapsulated solid lipid nanoparticles against corticosterone-induced cellular and animal models of major depression. **International Journal of Nanomedicine**, n. 3, v. 11, p. 4975-4990, 2016.

HÖGLUND, K.; BLENNOW, K. Effect of HMG-CoA reductase inhibitors on beta-amyloid peptide levels: implications for Alzheimer's disease. **CNS Drugs**, n. 21, v. 6, p. 449-62, 2007.

HU, K.; SHI, Y.; JIANG, W.; HAN, J.; HUANG, S.; JIANG, X. Lactoferrin conjugated PEG-PLGA nanoparticles for brain delivery: preparation, characterization and efficacy in Parkinson's disease. **International Journal of Pharmaceutics**, v. 415, n. (1-2), p. 273-83, 2011.

HUTTNER, A. Overview of primary brain tumors: pathologic classification, epidemiology, molecular biology, and prognostic markers. **Hematology/Oncology Clinics of North America**, v. 26, n. 4, p.715-732, 2012.

ILLUM, L. Transport of drugs from the nasal cavity to the central nervous system. **European Journal of Pharmaceutical Sciences**, v. 11, n. 1, p. 1–18, 2000.

ILLUM, L. Nasal drug delivery – possibilities, problems and solutions. **Journal of Controlled Release**, v. 87, p. 187-198, 2003.

ILLUM, L. Nanoparticulate Systems for Nasal Delivery of Drugs: A Real Improvement over Simple Systems?. **Journal of Pharmaceutical Sciences**, v. 96, p. 473-483, 2006.

INCA. Instituto Nacional de Câncer. Ministério da Saúde. Disponível em <http://www.inca.gov.br/> Acesso em maio de 2020.

JÄGER, A.; STEFANI, V.; GUTERRES, S.S.; POHLMANN, A.R.; Physico-chemical characterization of nanocapsule polymeric wall using fluorescent benzazole probes. **International Journal of Pharmaceutics,** v. 338, n. 1-2, p. 297-305, 2007.

JÄGER, E.; VENTURINI, C.G.; POLETTO, F.; COLOME, L.M.; BERNARDI, A.; BATTASTINI, A.M.O.; GUTERRES, S.S.; POHLMANN, A.R.; Sustained release from lipid-core nanocapsules by varying the core viscosity and the particle surface area. **Journal of Biomedical Nanotechnology**, v. 5, n. 1, p. 130-140, 2009.

JAIN, D.S.; BAJAJ, A.N.; ATHAWALE, R.B.; SHIKHANDE, S.S.; PANDEY, A.; GOEL, P.N.; GUDE, R.P.; PATIL, S.; RAUT, P. Thermosensitive PLA based nanodispersion for targeting brain tumor via intranasal route. **Materials Science and Engineering: C**, v. 63, p. 411-21, 2016.

JAKOBISIAK, M.; Golab, J. Potential antitumor effects of statins (Review). **International Journal of Oncology**, v. 23, n. 4, p. 1055-69, 2003.

JONES, N. The nose and paranasal sinuses physiology and anatomy. **Advanced Drug Delivery Reviews**, v. 51, n. 1-3, p. 5–19, 2001.

KANAZAWA, T.; MORISAKI, K.; SUZUKI, S.; TAKASHIMA, Y. Prolongation of life in rats with malignant glioma by intranasal siRNA/drug codelivery to the brain with cell-penetrating peptide-modified micelles. **Molecular Pharmaceutics**, v. 11, n. 5, p. 1471-8, 2014.

KHAN, A.; AQIL, M.; IMAM, S.S.; AHAD, A.; SULTANA, Y.; ALI, A.; KHAN, K. Temozolomide loaded nano lipid based chitosan hydrogel for nose to brain delivery: Characterization, nasal absorption, histopathology and cell line study. **International Journal of Biological Macromolecules**, v. 116, p. 1260–1267, 2018.

KIM, I.Y.; SEO, S.J.; MOON, H.S.; YOO, M.K.; PARK, I.Y.; KIM, B.C.; CHO, C.S. Chitosan and its derivatives for tissue engineering applications. **Biotechnology Advances**, v. 26, n. 1, p. 1–21, 2008.

KOTAMRAJU, S.; WILLAMS, C.L.; KALYANARAMAN, B. Statin-induced breast cancer cell death: role of inducible nitric oxide and arginase-dependent pathways. **Cancer Research**, v. 67, n. 15, p. 7386–94, 2007.

KOYUTURK, M.; ERSOZ, M.; ALTIOK, N. Simvastatin induces proliferation inhibition and apoptosis in C6 glioma cells via c-jun N-terminal kinase. **Neuroscience letters,** v. 370, n. 2-3, p. 212-7, 2004.

KULKAMP, I.C.; PAESE, K.; POHLMANN, A.R.; GUTERRES, S.S. ESTABILIZAÇÃO DO ÁCIDO LIPÓICO VIA ENCAPSULAÇÃO EM

NANOCÁPSULAS POLIMÉRICAS PLANEJADAS PARA APLICAÇÃO CUTÂNEA. **Química Nova**, v. 32, p. 2078-2084, 2009.

LAIZURE, S.C.; HERRING, V.; HU, Z.; WITBRODT, K.; PARKER, R.B. The role of human carboxylesterases in drug metabolism: have we overlooked their importance?. **Pharmacotherapy**, v. 33, n. 2, p. 210-22, 2013.

LEECE, R.; XU, J.; OSTROM, Q.T.; CHEN, Y.; KRUCHKO, C.; BARNHOLTZ-SLOAN, J.S. Global incidence of malignant brain and other central nervous system tumors by histology, 2003–2007**. Neuro Oncology**, v. 19, p. 1553–1564, 2017.

LI, Y.; WEI, X.; WANG, Q.; LI, W.; YANG, T. Inverse screening of Simvastatin kinase targets from glioblastoma druggable kinome. **Computational Biology and Chemistry**, v. 86, 07243, 2020.

LI, Y.M.; SUKI, D.; HESS, K.; SAWAYA, R.; The influence of maximum safe resection of glioblastoma on survival in 1229 patients: Can we do better than gross-total resection?. **Journal of Neurosurgery**, v. 124, n. 4, p. 977-88, 2016.

LIAO, J.K; ULRICH, L. Pleiotropic effects of statins. **Annual review of pharmacology and toxicology**, v. 45, p. 89-118, 2005.

LIM, M.; JACKSON, C.M. Fire in the Smoke: Battling Brain Tumors. **Cerebrum**, v. 2018, n. cer-07-18, 2018

LINDNER, G.R.; BONFANTI S.D.; COLLE, D.; GASNHAR MOREIRA, E.L.; DANIEL PREDIGER, R.; FARINA, M.; KHALIL, N.M.; MARA MAINARDES, R. Improved neuroprotective effects of resveratrol-loaded polysorbate 80-coated poly(lactide) nanoparticles in MPTP-induced Parkinsonism. **Nanomedicine (Lond)**, v. 10, n.7, p. 1127–1138, 2015.

LORENZONI, R.; DAVIES, S.; CORDENONSI, L.M.; VIÇOSA, J.A.D.S.; MEZZOMO, N.J.; DE OLIVEIRA, A.L.; CARMO, G.M.D.; RAFFIN, R.P.; ALVES, O.L.; VAUCHER, R.A.; RECH, V.C. Lipid-core nanocapsules containing simvastatin improve the cognitive impairment induced by obesity and hypercholesterolemia in adult rats. **European Journal of Pharmaceutical Sciences**, v. 151, n. 105397, 2020.

MADANE, R.G.; MAHAJAN, H.S. Curcumin-loaded nanostructured lipid carriers (NLCs) for nasal administration: design, characterization, and in vivo study. **Drug Delivery**, v. 23, n. 4, p. 1326-34, 2016.

MAZZARINO, L.; COCHE-GUÉRENTE, L.; LABBÉ, P.; LEMOS-SENNA, E.; BORSALI, R. On the mucoadhesive properties of chitosan-coated polycaprolactone nanoparticles loaded with curcumin using quartz crystal microbalance with dissipation monitoring. **Journal of Biomedical Nanotechnology**, v. 10, n. 5, p. 787–794, 2014.

MIR, M.; ISHTIAQ, S.; RABIA, S.; KHATOON, M.; ZEB, A.; KHAN, G.M.; UR REHMAN, A.; UD DIN, F. Nanotechnology: from In Vivo Imaging System to Controlled Drug Delivery. **Nanoscale Research Letters**, v. 12, n. 1, p. 500, 2017.

MISIRKIC, M.; JANJETOVIC, K.; Vucicevic, L.; Tovilovic, G.; Ristic, B.; Vilimanovich, U.; Harhaji-Trajkovic, L.; Sumarac-Dumanovic, M.; Micic, D.; Bumbasirevic, V.; Trajkovic, V. Inhibition of AMPK-dependent autophagy enhances in vitro antiglioma effect of simvastatin. **Pharmacological Research**, v. 65, n. 1, p. 111-9, 2012.

MISTRY, A.; STOLNIK, S.; ILLUM, L. Nanoparticles for direct nose-to-brain delivery of drugs. **International Journal of Pharmaceutics**, v. 379, n. 1, p. 146–157, 2009.

MORA-HUERTAS, C. E.; FESSI, H.; ELAISSARI, A. Polymer-based nanocapsules for drug delivery. **International Journal of Pharmaceutics**, v. 385, n. 1-2, p. 113–142, 2010.

MORSY, A.A,; NG, W.H. Re-do craniotomy for recurrent glioblastoma. **CNS oncology**, v. 4, n. 2, p. 55–57, 2016.

MUXIKA, A.; ETXABIDE, A.; URANGA, J.; GUERRERO, P.; DE LA CABA, K. Chitosan as a bioactive polymer: Processing, properties and applications. **International Journal of Biological Macromolecules**, v. 105, p. 1358–1368, 2017.

OHGAKI, H.; KLEIHUES, P. The Definition of Primary and Secondary Glioblastoma. **Clinical Cancer Research**, v. 19, n. 4, p. 764-72, 2013.

OSTROM, Q.T.; GITTLEMAN, H.; TRUITT, G.; BOSCIA, A.; KRUCHKO, C.; BARNHOLTZ-SLOAN, J.S. CBTRUS Statistical Report: Primary Brain and Other Central Nervous System Tumors Diagnosed in the United States in 2011-2015**. Neuro-Oncology**, v. 20, n. suppl_4, p. iv1-iv86, 2018.

OURIQUE, A.F.; MELERO, A.; SILVA, C.B.; SCHAEFER, U. F.; POHLMANN, A.R.; GUTERRES, S.S.; LEHR, C.M.; KOSTKA, K.H.; BECK, R.C.R. Improved photostability and reduced skin permeation of tretinoin: Development of a semisolid nanomedicine. **European Journal of Pharmaceutics and Biopharmaceutics**, v. 79, n. 1, p. 95-101, 2011.

OZDEMIR-KAYNAK, E.; QUTUB, A.A.; YESIL-CELIKTAS, O. Advances in glioblastoma multiforme treatment: new models for nanoparticle therapy. **Frontiers in Physiology**, v. 9, 170, 2018.

PATEL, Y.T.; JACUS, M.O.; Davis, A.D.; BOULOS, N.; TURNER, D.C.; VUPPALA, P.K.; FREEMAN, B.B.; GILBERTSON, R.J.; STEWART, C.F. Simvastatin Hydroxy Acid Fails to Attain Sufficient Central Nervous System Tumor Exposure to Achieve a Cytotoxic Effect: Results of a Preclinical Cerebral Microdialysis Study. **Drug Metabolism and Disposition**, v. 44, n. 4, p. 591-4, 2016.

PAUN, J. S.; BAGADA, A A; RAVAL, M. K. Nasal drug delivery – As an effective tool for brain targeting - A Review. **International Journal of Pharmaceutical and Applied Sciences**, v. 1, n. 2, p. 43–55, 2010.

PIRES, A.; FORTUNA, A.; ALVES, G,.; FALCÃO, A. Intranasal drug delivery: how, why and what for?. **Journal of Pharmacy and Pharmaceutical Sciences**, v. 12, n. 3, p. 288–311, 2009.

PIRZKALL, A.; MCGUE, C.; SARASWATHY, S.; CHA, S.; LIU, R.; VANDENBERG, S.; LAMBORN, K.R.; BERGER,M.S.; CHANG, S.M.; NELSON, S.J. Tumor regrowth between surgery and initiation of adjuvant therapy in patients with newly diagnosed glioblastoma. **Neuro-oncology**, v. 11, n. 6, p. 842-52, 2009.

PLATZ, E.A.; LEITZMANN, M.F.; VISVANATHAN, K.; RIMM, E.B.; STAMPFER, M.J.; WILLETT, W.C.; GIOVANNUCCI, E. Statin drugs and risk of advanced prostate cancer**. Journal of the National Cancer Institute**, v. 98, p. 1819–1825, 2006.

POHLMANN, A.R.; FONSECA, F.N.; PAESE, K.; DETONI, C.B.; CORADINI, K.; BECK, R.C.; GUTERRES, SS. Poly(ε-caprolactone) microcapsules and nanocapsules in drug delivery. **Expert Opinion on Drug Delivery**, v.10, n.5, 623-638, 2013.

POHLMANN, A.R.; CRUZ, L.; MEZZALIRA, G.; SOARES, L.U.; SILVEIRA, N.P.; GUTERRES, S.S. Structural model of polymeric nanospheres containing indomethacin ethyl ester and in vivo antiedematogenic activity. **International Journal of Nanotechnology**, v.4, p.454-467, 2007.

POYNTER, J.N.; GRUBER, S.B.; HIGGINS, P.D.; ALMOG, R.; BONNER, J.D.; RENNERT, H.S.; LOW, M.; GREENSON, J.K.; RENNERT, G. Statins and the risk of colorectal cancer. **New England Journal of Medicine**, v. 352, p. 2184–2192, 2005.

POZZOLI, M.; ONG, H.X.; MORGAN, L.; SUKKAR, M.; TRAINI, D.; YOUNG, P.M.; SONVICO, F. Application of RPMI 2650 nasal cell model to a 3D printed apparatus for the testing of drug deposition and permeation of nasal products. **European Journal of Pharmaceutics and Biopharmaceutics**, 107, 223–233, 2016.

QI, X.F.; ZHENG, L.; LEE, K.J.; KIM, D.H.; KIM , C.S.; CAI, D.Q.; WU, Z.; QIN, J.W.; YU, Y.H.; KIM, S.K. HMG-CoA reductase inhibitors induce apoptosis of lymphoma cells by promoting ROS generation and regulating Akt, Erk and p38 signals via suppression of mevalonate pathway. **Cell Death & Disease**, v.4, p. e518, 2013.

REZENDE, L.F.M.; LEE, D. H.; LOUZADA, M.L.C.; SONG, M.; GIOVANNUCCI, E.; ELUF-NETO, J. Proportion of cancer cases and deaths attributable to lifestyle risk factors in Brazil**. Cancer Epidemiology**, v.59, p. 148-157, 2019.

ROMANA, B.; BATGER, M.; PRESTIDGE, C.A.; COLOMBO, G.; SONVICO, F. Expanding the therapeutic potential of statins by means of nanotechnology enabled drug delivery systems. **Current Topics in Medicinal Chemistry**, v. 14, n. 9, p. 1182–1193, 2014.

RIKITAKE, Y.; LIAO, J.K. Rho GTPases, statins, and nitric oxide. **Circulation Research**, v. 97, n. 12, p. 1232-5, 2005.

SADEEGH, M.S.; AZADI, A.; IZADI, Z.; KURD, M.; DARA, T.; DIBAEI, M.; SHARIF, Z.M.; AKBARI, J.H., HAMIDI, M. Brain Delivery of Curcumin Using Solid Lipid Nanoparticles and Nanostructured Lipid Carriers: Preparation, Optimization, and Pharmacokinetic Evaluation. **ACS Chemical Neuroscience**, v. 10, n. 1, p. 728–739, 2018.

SAITO, A.; SAITO, N.; MOL, W.; FURUKAWA, H.; TSUTSUMIDA, A.; OYAMA, A.; SEKIDO, M.; SASAKI, S.; YAMAMOTO, Y. Simvastatin inhibits growth via

apoptosis and the induction of cell cycle arrest in human melanoma cells. **Melanoma Research**, v. 18, n. 2, p. 85-94, 2008.

SCHAFFAZICK, S. R.; GUTERRES, S. S.; FREITAS, L. L.; POHLMANN, A. R. Caracterização e estabilidade físico-química de sistemas poliméricos nanoparticulados para administração de fármacos. **Química Nova**, v. 26, p. 726-737, 2003.

SELVARAJ, K.; GOWTHAMARAJAN, K.; KARRI, V.V.S.R. Nose to brain transport pathways an overview: potential of nanostructured lipid carriers in nose to brain targeting. **Artificial Cells, Nanomedicine, and Biotechnology**, v. 46, n.8, p.2088-2095, 2018.

SHAH, L., YADAV, S. & AMIJI, M. Nanotechnology for CNS delivery of bio-therapeutic agents. **Drug Delivery and Translational Research**, v.3, p.336–351, 2013.

SHELLMAN, Y.G.; RIBBLE, D.; MILLER, L.; GENDALL, J.; VANBUSKIRK, K.; KELLY, D. Lovastatin-induced apoptosis in human melanoma cell lines. **Melanoma Research**, v. 15, n. 2. p. 83-9, 2005.

SHEN, Y.Y.; YUAN, Y.; DU, Y.Y.; PAN, Y.Y. Molecular mechanism underlying the anticancer effect of simvastatin on MDA-MB-231 human breast cancer cells. **Molecular Medicine Reports**, v. 12, n. 1, p.623-30, 2015.

SHERGALIS, A.; BANKHEAD, A.; LUESAKUL, U.; MUANGSIN, N.; NEAMATI, N. Current Challenges and Opportunities in Treating Glioblastoma. **Pharmacological Reviews**, v. 70, n. 3, p. 412-445, 2018.

SHINDE, R.L.; DEVARAJAN, P.V. Docosahexaenoic acid-mediated, targeted and sustained brain delivery of curcumin microemulsion. **Drug Delivery**, v. 24, n. 1, p. 152-161, 2017.

SIGURDSSON, H.H.; KIRCH, J.; LEHR, C.M. Mucus as a barrier to lipophilic drugs. **International Journal of Pharmaceutics**, v. 453, n. 1, p. 56–64, 2013.

SILVA, A.O.; DALSIN, E.; ONZI, G.R.; FILIPPI-CHIELA, E.C.; LENZ, G. The regrowth kinetic of the surviving population is independent of acute and chronic responses to temozolomide in glioblastoma cell lines. **Experimental Cell Research**, v. 348, n. 2, p. 177-183, 2016.

SINGH, I.; RANA, V. Enhancement of Mucoadhesive Property of Polymers for Drug Delivery Applications: A Critical Review. Rev. **Adhesion Adhesives**, n. 2, p. 271–290, 2013.

SLEIJFER, S.; VAN DER GAAST, A.; PLANTING, A.S.; STOTER, G.; VERWEIJ, J. The potential of statins as part of anti-cancer treatment. **European Journal of Cancer**, v. 41, n. 4, p. 516-22, 2005.

SONG, W.; RUDER, A.M.; HU, L.; LI, Y.; NI. R.; SHAO, W.; KASLOW, RA.; BUTLER, M.; TANG, J. Genetic epidemiology of glioblastoma multiforme: confirmatory and new findings from analyses of human leukocyte antigen alleles and motifs. **PLoS One**, v. 4, n. 9, p. e7157, 2009.

SONVICO, F.; CAGNANI, A.; ROSSI, A.; MOTTA, S.; DI BARI, M.T.; CAVATORTA, F.; ALONSO, M.J.; DERIU, A.; COLOMBO, P. Formation of self-organized nanoparticles by lecithin/chitosan ionic interaction. **International Journal of Pharmaceutics**, v. 324, n. 1, p. 67–73, 2006.

SONVICO, F.; CLEMENTINO, A.; BUTTINI, F.; COLOMBO, G.; PESCINA, S.; GUTERRES, S.S.; POHLMANN, A.A.; NICOLI, S. Surface-Modified Nanocarriers for Nose-to-Brain Delivery:From Bioadhesion to Targeting. **Pharmaceutics**, v. 10, n. 1, 2018.

SOSNIK, A.J.; NEVES, J.; SARMENTO, B. Mucoadhesive polymers in the design of nano-drug delivery systems for administration by non-parenteral routes: A review. **Progress in Polymer Science**, v. 39, n. 12, p. 2030–2075, 2014.

SOUSA, F.; DHALIWAL, H.K.; GATTACCECA, F.; SARMENTO, B.; AMIJI, M.M. Enhanced anti-angiogenic effects of bevacizumab in glioblastoma treatment upon intranasal administration in polymeric nanoparticles. **Journal of Controlled Release**, v. 309, p. 37–47, 2019.

SPARKS, D.L.; HUNSAKER, J.C.3RD.; SCHEFF, S.W.; KRYSCIO, R.J.; HENSON, J.L.; MARKESBERY, W.R. Cortical senile plaques in coronary artery disease, aging and Alzheimer's disease. **Neurobiology of Aging**, v. 11, n. 6, p. 601-7, 1990

STUPP, R.; MASON, W.P.; VAN DEN BENT, M.J.; WELLER, M.; FISHER, B.; TAPHOORN, M.J.; BELANGER, K.; BRANDES, A.A.; MAROSI, C.; BOGDAHN, U.; CURSCHMANN, J.; JANZER, R.C.; LUDWIN, S.K.; GORLIA, T.; ALLGEIER, A.; LACOMBE, D.; CAIRNCROSS, J.G.; EISENHAUER, E.; MIRIMANOFF, R.O.; Radiotherapy plus concomitant and adjuvante temozolomide for glioblastoma. **New England Journal of Medicine**, v. 352, p. 987–96, 2005.

SUMAN, J.D. Current understanding of nasal morphology and physiology as a drug delivery target. **Drug Delivery and Translational Research**, v. 3, n. 1, p. 4–15, 2013.

SZAKÁCS, G.; PATERSON, J.K.; LUDWIG, J.A.; BOOTH-GENTHE, C.; GOTTESMAN, M.M. Targeting multidrug resistance in cancer. **Nature Reviews Drug Discovery**, v. 5, n. 3, p. 219-34, 2006.

TAKI, H.; KANAZAWA, T.; AKIYAMA, F.; TAKASHIMA, Y.; OKADA, H. Intranasal delivery of camptothecin-loaded Tat-modified nanomicells for treatment of intracranial brain tumors. **Pharmaceuticals**, v. 5, n. 10, p. 1092-102, 2012.

TANAKA, S., FUKUMOTO, Y., NOCHIOKA, K., MINAMI, T., KUDO, S., SHIBA, N., SHIMOKAWA, H. Statins Exert the Pleiotropic Effects Through Small GTP-Binding Protein Dissociation Stimulator Upregulation With a Resultant Rac1 Degradation. **Arteriosclerosis, Thrombosis, and Vascular Biology**, v. 33, n. 7, p. 1591-600, 2013.

TAN, Q.; LIU, X.; FU, X.; LI, Q.; DOU, J.; ZHAI, G. Current development in nanoformulations of docetaxel. **Expert Opin Drug Delivery**, v. 9, n. 8, p. 975-90, 2012.

TATARANU, L.G. Current Trends in Glioblastoma Treatment. Brain Tumors – An Update. 2018.

THAKKAR, J.P.; DOLECEK, T.A.; HORBINSKI, C.; OSTROM, Q.T.; LIGHTNER, D.D.; BARNHOLTZ-SLOAN, J.S.; VILLANO, J.L. Epidemiologic and molecular prognostic review of glioblastoma. **Cancer Epidemiology, Biomarkers & Prevention**, v. 23, n. 10, p. 1985–96, 2014.

TIEK, D.M.; RONE, J.D.; GRAHAM, G.T.; PANNKUK, E.L.; HADDAD, B.R.; RIGGINS, R.B. Alterations in Cell Motility, Proliferation, and Metabolism in Novel Models of Acquired Temozolomide Resistant Glioblastoma. **Scientific reports**, v. 8, n. 1, p. 7222, 2018.

TODD, P.A.; GOA, K.L. Simvastatin. A review of its pharmacological properties and therapeutic potential in hypercholesterolaemia. **Drugs**, v. 40, n. 4, p. 583-607, 1990.

TROTTA, M.; CAVALLI, R.; CHIRIO, D. Griseofulvin nanosuspension from triacetin-in-water emulsions. **S.T.P. Pharma Sciences**, v. 13, p. 423-426, 2003.

UGWOKE, M. I.; AGU, R. U.; VERBEKE, N.; KINGET, R. Nasal mucoadhesive drug delivery: Background, applications, trends and future perspectives. **Advanced Drug Delivery Reviews**, v. 57, p. 1640-1665, 2005.

UPADHAYA, P.G.; PULAKKAT, S.; PATRAVALE, V.B. Nose-to-brain delivery: exploring newer domains for glioblastoma multiforme management. **Drug Delivery and Translational Research**, v. 10, n. 4, p. 1044-1056, 2020

VENTURINI, C.G.; JÄGER, E.; OLIVEIRA, C.P.; BERNARDI, A.; BATTASTINI, A. M.O.; GUTERRES, S.S.; POHLMANN, A.R. Formulation of lipid core nanocapsules. **Colloids and Surfaces A: Physicochemical and Engineering Aspects**, v. 375, p. 200-208, 2011.

VERAGTEN, A.; CONTRI, R.V.; BETTI, A.H.; HERZFELDT, V.; FRANK, L.A.; POHLMANN, A.R.; RATES, S.M.K.; GUTERRES, S.S. Chitosan-coated nanocapsules ameliorates the effect of olanzapine in prepulse inhibition of startle response (PPI) in rats following oral administration. **Reactive and Functional Polymers**, v. 148; n. 1044932, 2020.

VLLASALIU, D.; EXPOSITO-HARRIS, R.; HERAS, A.; CASETTARI, L.; GARNETT, M.; ILLUM, L.; STOLNIK, S. Tight junction modulation by chitosan nanoparticles: comparison with chitosan solution. **International Journal of Pharmaceutics**, v. 400, n. (1-2), p. 183–193, 2010.

WANG, D.; ZOU, L.; JIN, Q.; HOU, J.; GE, G.; YANG, L. Human carboxylesterases: a comprehensive review. **Acta Pharmaceutica Sinica**, v. 8, n. 5, p. 699-712, 2018.

WATERS, M.R.; GUPTA, A.S.; MOCKENHAUPT, K.; BROWN, L.N.; BISWAS, D.D.; KORDULA, T. RelB acts as a molecular switch driving chronic inflammation in glioblastoma multiforme. **Oncogenesis**, v. 8, n. 6, p. 37, 2019.

WAYS, T.M.M; LAU, W.M.; KHUTORYANSKIY, V.V. Chitosan and Its Derivatives for Application in Mucoadhesive Drug Delivery Systems**. Polymers**, v. 10, n. 3, p. 267, 2018.

WHO. World Health Organization. Disponível em <http://www.who.int/en/> Acesso em maio de 2020.

WILLRICH, M.A.; HIRATA, M.H.; HIRATA, R.D. Statin regulation of CYP3A4 and CYP3A5 expression. **Pharmacogenomics**, v. 10, n. 6, p. 1017-24, 2009.

WOHLFART, S.; GELPERINA, S.; KREUTER, J. Transport of drugs across the blood-brain barrier by nanoparticles. **Journal Control Release**, v. 161, n. 2, p. 264–73, 2012.

WU, H.; JIANG, H.; LU, D.; XIONG, Y.; QU, C.; ZHOU, D.; MAHMOOD, A.; CHOPP, M. Effect of simvastatin on glioma cell proliferation, migration, and apoptosis. **Neurosurgery**, v. 65, n. 6, p. 1087–1096, 2009.

XU, W.; LI, T.; GAO, L.; ZHENG, J.; SHAO, A.; ZHANG, J. Efficacy and safety of long-term therapy for high-grade glioma with temozolomide: A meta-analysis. **Oncotarget**, v. 8, n. 31, p. 51758-51765, 2017.

YANAE, M.; TSUBAKI, M.; SATOU, T.; ITOH, T.; IMANO, M.; YAMAZOE, Y.; NISHIDA, S. Statin-induced apoptosis via the suppression of ERK1/2 and Akt activation by inhibition of the geranylgeranyl-pyrophosphate biosynthesis in glioblastoma. **Journal of Experimental & Clinical Cancer Research**, v. 30, n. 1, p. 74, 2011.

YANG, T.; YAO, H.; HE, G.; SONG, L.; LIU, N.; WANG, Y.; YANG, Y.; KELLER, T.E.; DENG, X. Effects of lovastatin on MDA-MB-231 breast cancer cells: an antibody microarray analysis. **Journal of Cancer**, v. 7, n. 2, p. 192–9, 2016.

YU, X.; PAN, Y.; MA, H.; LI, W. Simvastatin inhibits proliferation and induces apoptosis in human lung cancer cells. **Oncology Research**, v. 20, n. 8, p. 351-7, 2013.

ZANOTTO-FILHO, A.; BRAGANHOL, E.; EDELWEISS, M.I.; BEHR, G.A.; ZANIN, R.; SCHRÖDER, R.; SIMÕES-PIRES, A.; BATTASTINI, A.M.; MOREIRA, J.C. The curry spice curcumin selectively inhibits cancer cells growth in vitro and in preclinical model of glioblastoma. **Journal of Nutritional Biochemistry**, v. 23, n. 6, p. 591-601, 2012.

ZANOTTO-FILHO, A.; CORADINI, K.; BRAGANHOL, E.; SCHRÖDER, R.; OLIVEIRA, C.M.; SIMÕES-PIRES, A.; BATTASTINI, A.M.O.; POHLMANN, A.R.; GUTERRES, S.S.; FORCELINI, C.M.; BECK, R.C.R.; MOREIRA, J.C.F. Curcumin-loaded lipid-core nanocapsules as a strategy to improve pharmacological efficacy of curcumin in glioma treatment. **European Journal of Pharmaceutics and Biopharmaceutics**, v. 83, n. 2, p. 156-167, 2013.

ZAORSKY, N.G.; CHURILLA, T.M.; EGLESTON, B.L.; FISHER, S.G.; RIDGE, J.A.; HORWITZ, E.M.; MEYER, J.E. Causes of death among cancer patients. **Annals of oncology**, v. 28, n. 2, p. 400-407, 2017.

ZARA, G.P.; CAVALLI, R.B.; BARGONI, A.C.; FUNDARO, A.A.; VIGHETTO, D.A, GASCO, M.R Intravenous administration to rabbits of non-stealth and stealth doxorubicin-loaded solid lipid nanoparticles at increasing concentrations of stealth agent: pharmacokinetics and distribution of doxorubicin in brain and other tissues. **Journal of Drug Targeting**, v. 10, n. 4, p. 327-335, 2002.

ZHAN, C.; GU, B.; XIE, C.; LI, J.; LIU, Y.; LU, W. Cyclic RGD conjugated poly(ethylene glycol)-co-poly(lactic acid) micelle enhances paclitaxel anti-glioblastoma effect. **Journal of Controlled Release**, v. 143, n. 1, p. 136–142, 2010.

ZHANG, C.; WAN, X.; ZHENG, X.; SHAO, X.; LIU, Q.; ZHANG, Q.; QIAN, Y. Dual-functional nanoparticles targeting amyloid plaques in the brains of Alzheimer's disease mice. **Biomaterials**, v. 35, n. 1, p. 456-65, 2014.

ZILI, Z.; SFAR, S.; FESSI, H. Preparation and characterization of poly-e-caprolactone nanoparticles containing griseofulvin. **International Journal of Pharmaceutics**, v. 294, p. 261-267, 2005.